Philippine Journal of Science
128 (4): 353 - 356, December 1999
ISSN 0031 - 7683

An Optical Sensor for Lead Based on Immobilized Dithizone

Edna C. Quinto[1]* and Nena V. Rodriguez[2]

[1]Research Center for the Natural Sciences, University of Santo Tomas, Manila, Philippines
[2]Department of Chemistry, University of San Carlos, Cebu City, Philippines

An optical sensor for lead based on dithizone immobilized in plasticized polyvinyl chloride (PVC) was studied. The sensing material is composed of dithizone (0.0031%) dissolved in a mixture of PVC in tetrahydrofuran (THF, 92.25%) and 2-nitrophenyl octyl ether (4.45%). The solution is spin coated on an acetate film and stored in 0.1M HCl solution. The sensor is housed in a flow cell to which the analyte is injected by a peristaltic pump at a rate of about 1.9 μL/s. Readings were taken kinetically using a UV-VIS spectrophotometer at 620 nm and the film was regenerated by brief exposure to 0.01M HCl. Response time is about 10 minutes and calibration gives a slope of 0.001635 for a range of 1-18 ppm concentration of lead (II) ion. Reproducibility evaluation for a 16 ppm standard solution gave a relative standard deviation 12.78% for 5 samples. This simple set-up may find application in sensing lead in environmental waters in real time.

Key words: environmental monitoring, chemical sensor, lead sensor, intelligent membrane

The Environmental Protection Agency (EPA) limits lead in air to 1.5 μg/m³ averaged over 3 months (Agency for Toxic Substances and Disease Registry 1993). Measurements show that an increase in airborne lead concentration of 1μg/m³ results to an increase of 1-2 μg/dL in blood levels (Masters 1991). Lead monitoring therefore finds a wide application in the environment.

Conventionally, lead may be determined by spectrophotometry and amperometry (Christian 1994). These methods, however, cannot give results in real time. A method for determination of chemical composition or quantity that has an advantage over the conventional methods for continuous monitoring done in real time is chemical sensing (Jiri 1989). The sensing material is made available at any time by immobilization of the reagent on a surface or in a bulk material. There are different ways of immobilizing reagents (Mosbach and Danielsson 1987) but the most critical concern is keeping the reagent active. The sensing material attached to a surface or bulk material can be exposed to the analyte in a flow cell or it can take the form of an electrode. Among the sensing devices, optical-based sensors have been observed to be simple, inexpensive and reliable. These sensors use optical fibers, which are very flexible and they can be configured to reach inaccessible areas. Furthermore they are hardly affected by electrical disturbances and they have minimal losses in terms of data transmissions. Among the work done for lead sensing were those of Trutneva et al (1989), Czolk et al

---

*Corresponding author: edna.qui@ustcc.ust.edu.ph

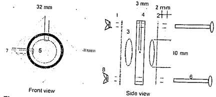

Figure 1. Fabricated flow-through cell (Frame, 1; Cover film, 2; O-rings, 3; Middle frame, 4; OSM, 5; Screws, 6; Analyte entry and exit points, 7; Winged nut, 8).

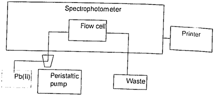

Figure 2. Instrumentation system.

(1992), Lerchi, M. et al (1992), and Narayanaswamy & De Oliveira (1992), which illustrated the capabilities of some lead sensors.

This study aims to develop a sensor for lead using immobilized reagents. Earlier works have used immobilized xylenol orange (Trutneva et al. 1992) and dithizone (Narayanaswamy & De Oliveira 1992). This paper presents the report of an optical sensing membrane (OSM) for lead, based on dithizone immobilized in polymeric membrane. This work particularly differs from Narayanswamy's work as it uses a film as a solid support.

Methods

Reagents

All reagents are of analytical reagent grade supplied mostly by Sigma-Aldrich, Ajax Chemicals or T.J. Baker Inc.

Instrumentation system

The instrumentation system consists of a peristaltic pump (Ismatech MPC Model 78002 Cole Parmer Instruments Co.) to inject the analyte into a flow-through cell where the optical sensing membrane is attached. Fig. 1 shows the diagram of the fabricated flow-through cell. The cell is housed in a Perkin Elmer Lambda 2 UV-VIS spectrophotometer equipped with an Epson EX 1000 printer. Fig. 2 shows the schematic diagram of the instrumentation system.

Immobilization of sensing membranes

Initially studies were conducted to find a suitable reagent for lead. Tetrahydroxy benzoquinone (THQ) and dithizone (DZ) were considered based on their capacity to detect the presence of lead at considerably low concentrations (Feigl et al. 1972).

The reagents were immobilized in some polymers and tested for stability and response to low levels of lead ion. Analytical grade ethyl cellulose (EC), non-ionic resin XAD2, hydrophilic polymers of Tyndale Plains Hunter, Ltd such as D4 and D7, and polyvinyl chloride (PVC) were tried using different solvents such as toluene-methanol mixtures for EC, ethanol-isopropanol mixture for D4 and D7 and tetrahydrofuran (THF) for PVC to adsorb the reagents. For the non-polar membranes some amount of plasticizers have to be added to allow the analyte to penetrate the membrane.

Optical sensing membrane

The optimum sensing material consisted of dithizone (0.30 wt %) dissolved in a mixture of 1:19 PVC in THF (95.25 wt %) and 2-nitrophenyl octyl ether (4.45 wt%). The cocktail solution was thoroughly mixed and spin coated on an acetate film or a glass slide. The resulting OSM was stored in a 0.1M HCl solution contained in an amber bottle. Qualitative tests were done to determine the characteristics of the optical sensing membrane.

Measurement procedure

For analysis, the OSM was sized to fit into the window of the flow-through cell fitted on to the base plate of the UV-VIS spectrophotometer. The analyte was injected in the cell at a flow rate maintained by peristaltic pump at 1.9 µL/s. The spectra of OSM at different lead concentrations were scanned in the visible region. A wavelength that showed the largest spectral change wa chosen for further characterization

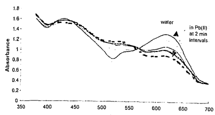

Figure 3. Spectra of the OSM to varied Pb(II) concentrations

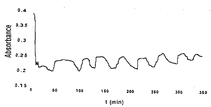

Figure 4. Reproducibility Evaluation of the film to 16 ppm Pb(II)

of the sensor.

Results and Discussion

Immobilization studies

The polar membranes EC, D4 and D7 showed a visible response in 30 seconds after they were exposed to the analyte. However the sensing material in the membrane leached out as the analyte flowed. This was considered useless for a flow-through system.

For the non-polar membrane, tests showed that a 7% plasticizer produces an equally good response but it leached the reagent. On the other hand a 3% plasticizer did not leach the reagent but it required at least 35 minutes for visible color change. Tests were done by varying the amount of plasticizer between 7% and 3% and taking the time required to show a visible color change. These showed that the optimum composition was 4.45 wt% plasticizer (2-nitrophenyl octyl ether). The overall optimum composition was found to be 0.30 wt% dithizone dissolved in a mixture of 1:19 PVC in a cocktail consisting of 95.25 wt % THF and 4.45 wt% plasticizer.

Absorption spectrum of sensing reagent

The green colored membrane with optimized composition was stored in an amber bottle in HCl solution due to its sensitivity to light. This membrane was tested for lead reactions at low concentrations. The membrane turned red in about 2 seconds on a drop of the lead(II) solution. To confirm this observation water was injected into the flow cell and the membrane was scanned, after which lead was injected. Fig. 3 showed the response with and without lead(II). The spectra generated without lead (II) showed maximum peaks at about 420 and 620 nm wavelength. When lead (II) was injected the maximum peak at 620 nm began to decrease while that of 450 nm showed little change hence all readings were done at 620 nm.

The stability of the sensor was determined by exposing the film to visible radiation at a 620 nm wavelength; an absorbance of 0.82 was observed for about six hours. Hence the color change was due to lead and not due to the degradation of the reagent. This result agreed with the findings of Narayanaswamy (1992). The above observations indicated no leaching of the reagent from the support.

Sensor response

Response time. Based on Fig. 4 on pumping lead (II) solution into the flow cell, it took more than 20 minutes to achieve steady-state readings. Injecting a 0.01M HCl solution regenerated the film; and brought back the absorbance to the base line.

Reproducibility. To test for the reproducibility of the reagent, a 16 ppm standard solution of lead (II) was injected followed by the HCl solution to regenerate the film and bring it to the base line. This was done repeatedly for 5 trials. Fig. 4 showed the result of the reproducibility evaluation. The result gave a relative standard deviation of 12.78% for 5 samples. There was a slight increase in the base line towards the end of the evaluation. Further tests rendered the film poorly responsive.

Variation of response with lead concentrations

Solutions ranging from 1 to 18 ppm Pb(II) were

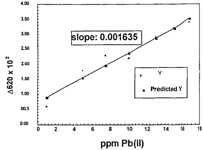

Figure 5. Absorbance vs ppm Pb(II)

freshly prepared from a 100 ppm stock solution of lead (II). The different solutions were pumped into the cell. A kinetic approach was used to gather response data (i.e., lead standards were injected and time drive data was gathered.) Absorbance readings were taken 10 min after injection time. The relative change in absorbance was related to the concentration of the lead (II) standard injected. The plot of change in absorbance, Δ620 versus the concentration in ppm is shown in Fig. 5. The calibration showed a sensitivity of 0.00164 change in absorbance/ppm. The linear coefficient was 0.9839. Based on the formula: $R_{LOD} = R_{BLK} + 3S_{BLK}$ the limit of detection was estimated to be 3.2 ppm.

Conclusion

The study presents the development of an optical sensor for lead (II) ion. The sensor was tested using standards prepared in the laboratory and showed promising characteristics such as stability of film, a sensitivity of 0.00164 change in response/ppm concentration of lead (II), and reproducibility data with a relative standard deviation of 12.78%. The set up is relatively simple and finds application for environmental on-line monitoring. For further studies it is recommended that the OSM be improved to give lower limits of detection and increase the lifetime of the film.

Acknowledgments

We are grateful to the Funds for Assistance to Private Education (FAPE) for funding this research project.

References

Agency for Toxic Substances and Disease Registry (ATSDR). 1993. Toxicological profile for lead. Atlanta: U.S. Department of Health and Human Services, Public Health Service.

Christian GD. 1994. Analytical chemistry. John Wiley & Sons. NY p. 721 & 726

Czolk R, Reichert J & Ache H. 1992. J. Sensors and Actuators B-Chemical, 7(1-3): 540-543.

Feigl F, Anger V & Pesler R. 1972. Spot tests in inorganic analysis, 6th ed.. Elsevier Publishing Co. Amsterdam. pp. 282 - 287

Janata J. 1989. Principles of chemicals sensors. Plenum Press, NY. p. 1

Lerchi M, Bakker E, Rusterholz G & Simon W. 1992. Anal. Chem. 64(14): 1534-1540.

Masters G. M. 1991. Introduction to environmental engineering and science. Prentice Hall, NJ. p. 300

Mosbach K & Danielsson B (eds). 1987. Immobilization of proteins. In: Methods in Enzymol. Vols. 135 & 136. Academic Pres, FL.

Narayanaswamy R & De Oliveira W. 1992. A flow-cell photosensor for lead based on immobilized dithizone. Talanta. 39(11): 1500.

Trutneva LM, Shvoeva OP & Savvin SB. 1989. Immobilized xylenol orange as a sensor for fiberoptic determination of thorium(IV) and lead (II). J. Anal. Chem. of the USSR. 44(10): 1430-1433.

Philippine Journal of Science
128 (4): 357 - 365, December 1999
ISSN 0031 - 7683

Integrating Biotechnology in the National Rice R&D Agenda

A Feauture on Philippine Rice Research Institute

Leocadio S. Sebastian* and Santiago R. Obien
Philippine Rice Research Institute (PhilRice)
Maligaya, Muñoz, Nueva Ecija

Rice self-sufficiency is one of the main concerns of Philippine agriculture today. Projections on yield and production, along with the constraints and problems suggest that the country may not be able to satisfy the growing demand. One strategy to strengthen the country's efforts to attain rice self-sufficiency is the use of biotechnology in rice R&D. At the Philippine Rice Research Institute (PhilRice), biotechnology is integrated in the new R&D programs to make sure that it responds to the immediate problems and issues of the country's rice industry. This enables researches to come up with more location-specific technologies. Biotechnology is mainly applied to develop varieties that are of good eating quality, high-yielding, and resistant to pests and diseases. To attain its maximum potential and benefits, it can be combined with other methods or tools. Biotechnology research at PhilRice is supported by the Philippine government, the Rockefeller Foundation (RF), Asian Rice Biotechnology Network (ARBN), and the Japan International Cooperating Agency (JICA).

The current level of total rice production *vis-a-vis* an annual population growth rate of about 2.3% suggests that the country may forever depend on imported rice to satisfy the demand. One way to avert this situation is to employ modern science tools such as biotechnology to increase production way beyond current yield levels.

The application of biotechnology in agriculture is starting the so-called "Gene Revolution" that may lead to higher agricultural productivity. Biotechnology is enabling researchers to manipulate the genomes of organisms allowing their improvement in ways not attainable using conventional tools.

The potentials of biotechnology can best be attained when combined with other tools. It can be used to enhance conventional methods or complement advances in other fields. However, the cost of applying it in agriculture is prohibitive for many developing countries like the Philippines.

Application of biotechnology needs to be prioritized and integrated in the holistic approach to tackling agricultural productivity problems, many of which can still be solved using cheaper and more practical approaches. Interdisciplinary collaboration among researchers can produce more appropriate technologies for local application.

In the Philippines, biotechnology research is primarily undertaken to address food security, particularly rice. It is an integral part of the breeding program of PhilRice, the Philippines' lead agency for rice research. Financial support comes from the Rockefeller Foundation (RF), Japan International Cooperation Agency (JICA), Asian Rice Biotechnology Network (ARBN), and the Philippine government.

The use of biotechnology is integrated in PhilRice's Research & Development (R&D) thrusts, which also form the National Rice R&D Agenda. Biotechnology is mainly used to speed up the development of rice varieties that are high-yielding, pest-resistant, tolerant to environmental stresses, and of good eating quality.

---

*Corresponding author: genetics@mozcom.com

Table 1. Philippine palay production, area harvested, and yield by ecosystem.

Item	Year								
	1970	1975	1980	1985	1990	1995	1996	1997	1998
Production (mt)									
All	5.32	6.38	7.65	8.80	9.32	10.54	11.28	11.27	8.55
Irrigated	2.95	3.45	4.51	5.82	6.60	7.60	8.23	8.48	
Rainfed	2.01	2.60	2.89	2.83	2.59	2.76	2.82	2.59	
Upland	0.36	0.34	0.26	0.15	0.12	0.19	0.23	0.20	
Area Harvested (ha)									
All	3.10	3.63	3.47	3.31	3.32	3.76	3.95	3.84	3.17
Irrigated	14.32	1.49	1.61	1.84	2.01	2.33	2.48	2.50	
Rainfed	1.29	1.74	1.60	1.33	1.21	1.30	1.30	1.21	
Upland	0.38	0.39	0.27	0.14	0.10	0.12	0.16	0.14	
Yield (mt/ha)									
All	1.71	1.76	2.20	2.66	2.81	2.80	2.86	2.93	2.70
Irrigated	2.06	2.31	2.80	3.17	3.29	3.26	3.31	3.39	
Rainfed	1.56	1.49	1.80	2.12	2.13	2.11	2.16	2.14	
Upland	0.94	0.86	0.98	1.12	1.31	1.54	1.43	1.50	

The Philippine Rice Industry

Issues and constraints

One must fully understand the issues and constraints stifling rice production in the Philippines to adequately address them. Among these are numerous problems on land, water, infrastructure, socio-economic and policy situations which are worsened by the ever-increasing national population.

For the past four decades, palay production more than doubled from 5.3 M mt in 1970 to 11.8 M mt in 1999 at an average annual growth rate of 3% (Table 1). Consequently, area harvested also increased through the years from 2.1 M ha in 1970 to 3.8 M ha in 1997, with an average growth of 0.89% per year. In 1997, the national average yield per hectare was 2.9 mt/ha. The irrigated areas produced the highest average yield with 3.4 mt/ha, followed by the rainfed ecosystem at 2.1 mt/ha, and upland areas at 1.5 mt/ha.

The growth in output from 1970-1977 was mainly attributed to the expansion of area devoted to rice production, increase in areas covered by irrigation, technologies developed during the green revolution, and the farm support program *Masagana* 99. This resulted in rice surplus in the late 1970s and early 1980s.

The growth rate in yield, however, declined from 5% in the 1970s to less than 1% in the late 1980s. Production has not been enough to feed the burgeoning population thereby resulting in rice deficits. The country only attained rice self-sufficiency in 9 out of 29 years (1970-1999) and imported rice to cover the deficit for the other years. The biggest rice importation was recorded in 1998 amounting to 2.1 M mt, which is primarily due to the adverse effects of *El Niño* on production (Table 2).

Issues and constraints in rice production can be discussed under three broad components: supply, market/policy, and demand.

1. Supply

High cost of production. The high cost of seeds, fertilizers, and labor demands more capital from farmers. Because small farmers can hardly afford these inputs, their usage is far below what is required to attain target yields. Farmers' lack of knowledge on the rate and proper timing of fertilizer application makes them less efficient.

Water in many irrigable areas is barely available because of poor irrigation facilities. The lack of water impounding infrastructure such as large reservoirs results in wasted water which could irrigate rice fields.

Pieces of farm equipment are usually accessed by small farmers through cooperatives. Since only ten

Table 2. Philippine rice imports

Year	Volume (mt)	Year	Volume (mt)
1980	0	1990	620795
1981	0	1991	0
1982	0	1992	0
1983	0	1993	209
1984	191020	1994	0
1985	540927	1995	198864
1986	5979	1996	no data
1987	0	1997	no data
1988	180076	1998	2100000
1989	219929	1999	

Source: National Food Authority (NFA)
Note: Importation is specifically high in 1998 because of low production brought about by El Niño

cooperatives have enough funds to loan for equipment, farmers resort to manual labor from which, by and large, increase costs and losses during harvest and postharvest processing.

High risk in production. The *El Niño* phenomenon that hit the country latest in 1998 brought about tremendous reduction in rice production, translating to a steep decline from 11.3 M mt in 1997 to only 8.6 M mt in 1998. Because of the severe drought, many farmers did not grow rice during the regular planting season. Farmers also incur heavy losses during severe pest outbreaks. This is worsened by their lack of knowledge on the pest management options.

High quality seeds are available but farmers either lack understanding and knowledge on their importance or could hardly afford them. Hybrid rice seed production technologies have yet to be fully adopted by seed growers. This technology, if properly managed, can increase farmers' production by 15% or more.

2. Market and Policy

The country has not been able to maintain enough buffer stock and has not come up with effective buffer stocking methods. In addition, realistic projections on the supply and demand for rice could not be made because the networking of information is still relatively slow.

Poor or lack of farm-to-market roads and trading facilities provides more problems in marketing. Irrigation systems are primarily constrained by: (1) substantial and increasing costs for irrigation development; (2) management problems for large scale irrigation projects; (3) growing concern for negative environmental effects such as reduction of fish habitat; (4) depletion of groundwater; and, (5) increased water logging.

3. Demand

Local production can not always support the population. Although there have been campaigns to promote population control measures, our population growth rate continues to be comparatively high. Studies project that there will be about 90 M Filipinos by 2010 and 100 M by 2020.

Modernizing Agriculture in the Philippines

The growing competition in the world market and the expected weakening of all forms of protection in national trade by year 2004, such as the reduction of tariffs on agricultural products, suggest that the country must look for opportunities and resources to be self-sufficient.

The current administration pursues the *Agrikulturang MakaMASA* which reflects the country's strategy for poverty alleviation, and food security anchored on rice self-sufficiency.

In support of this, the Philippine government gives priority to research and development, which have immediate relevance to the country's production system.

The Philippine's Lead Agency for Rice Research

PhilRice is a government corporation under the Department of Agriculture (DA). It is mandated to (1) lead, unify, and strengthen the manpower capabilities and improve the facilities of agencies involved in the national rice research and development program, and (2) serve as a vital force in attaining and sustaining the country's goal of self-sufficiency in rice and in promoting greater access of farmers to agricultural technology.

For 12 years since it started its operation in mid-1987, PhilRice has earned a good reputation in the national R&D environment. It has a strong and competent research group, composed mainly of

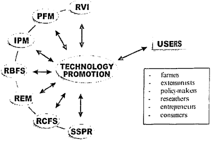

Legend:

RVI - Rice Varietal Improvement
PFM - Planting and Fertilizer Management
IPM - Integrated Pest Management
RBFS - Rice-Based Farming Systems
REM - Rice Engineering and Mechanization
RCFS - Rice Chemistry and Food Science
SSPR - Social Science and Policy Research

Fig.1. Old PhilRice R&D structure.

scientists trained and educated in premier universities here and abroad. Its capability in biotechnology research is strengthened through an aggressive manpower development and upgrading of research facilities.

Biotechnology research in PhilRice used to be concentrated in its Rice Varietal Improvement Program, which focused on the breeding of different varieties for irrigated, rainfed, upland, and adverse environments, including some special purpose rices. This setup followed the old R&D structure (Fig.1). However, because of the urgent needs to expedite the development of more and better rices, biotechnology is now integrated into four programs having varietal improvement components. The integration was made possible by the creation of an interdisciplinary R&D structure in 1998 (Fig. 2).

Biotechnology Strategy

The biotechnology research strategy of PhilRice is to benefit as much as possible from related research activities of laboratories around the world, and concentrate on areas of special interest to the Philippines. PhilRice collaborates very closely with scientists from the International Rice Research Institute (IRRI) in pursuing specific objectives in order to avoid duplication of research activities.

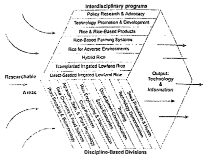
Interdisciplinary programs
Policy Research & Advocacy
Technology Promotion & Development
Rice & Rice-Based Products
Rice-Based Farming Systems
Rice for Adverse Environments
Hybrid Rice
Transplanted Irrigated Lowland Rice
Direct-Seeded Irrigated Lowland Rice
Researchable Areas
Plant Breeding & Biotechnology
Rice Chemistry & Food Science
Agronomy, Soils, & Plant Physiology
Crop Protection
Rice Engineering & Mechanization
Socio Economics
Development Communication
Training
Technology Demonstration
Seed Production & Health
Output: Technology & Information
Discipline-Based Divisions

Fig. 2. New PhilRice R&D structure.

Considering its cost and benefits, rice biotechnology research in the institute focuses on the specific problems of primary concern in its different programs. Currently, rice varietal improvement activities at PhilRice are largely supported by biotechnology research geared toward the development of high-yielding varieties adapted to the different agro-ecological conditions in the Philippines.

As one of the tools in varietal development, biotechnology is used especially in areas where conventional breeding has been shown to be not very efficient. These include research activities where conventional breeding takes a long period to generate advanced lines, where screening procedures are very tedious or difficult, and where desired traits are not known to be available in the rice gene pool.

The priority areas for the application of biotechnology at PhilRice are:

1. Utilization of the molecular marker technology in:

a) genetic mapping of important traits in rice such as yield components, seedling vigor, and resistance to the rice tungro disease (RTD), green leafhoppers, and blast;

b) analysis of genetic relationships of germplasm materials and breeding lines through DNA fingerprinting and genetic diversity studies;

c) development and application of marker-aided selection for RTD and bacterial leaf blight (BLB) resistance;

2. Utilization of *in vitro* techniques in the

Table 3. Rice biotechnology projects/activities in the different programs

Projects/Activities	Programs			
	Direct Seeded	Trans-planted	Hybrid	Adverse
1. Use of the DNA marker technology for rice improvement				
a. Pyramiding bacterial blight resistance gene		X	X	
b. Mapping/tagging				
-resistance genes (tungro, bacterial blight, blast)	X	X	X	X
-seedling vigor	X			
-CMS			X	
c. Varietal fingerprinting & biodiversity analysis		X	X	
2. Cloning of tungro resistance gene	X	X	X	
3. Genetic transformation – resistance to BPH, blast, and bacterial blight; salt tolerance, male sterility, seedling vigor, and beta carotene.				
a. Xa21, chitinase, pin2 and hva1 genes	X	X	X	X
b. beta glucanase gene	X			
4. Screening of GMO (bacterial blight, tungro, beta carotene)		X		
5. Anther culture (salt tolerance & cold tolerance)				X
6. Wide hybridization (tungro resistance)	X	X	X	

development of lines with tolerance to adverse conditions (*eg.* cold, salinity, and drought) and of improved grain quality;

3. Molecular cloning of important genes such as those for RTD resistance;

4. Genetic transformation of rice plants for male sterility and resistance to sheath blight and stemborers; and,

5. Transfer of resistance genes for tungro, sheath blight, and stemborers from wild *Oryza* species to cultivated varieties.

Significance of Integration

Biotechnology research at PhilRice is highly integrated in four component programs, namely: transplanted irrigated lowland rice, direct-seeded irrigated lowland rice, hybrid rice, and rice for adverse environments (Table 3). These programs develop varieties that are suited for specific locations and conditions. Biotechnology tools are used to speed up the development of these varieties and the incorporation of genes of interest.

Integrating biotechnology in the different programs is very important because it is one of the tools in improving rice productivity. As a tool, it has to be evaluated on whether it will provide the best option to remedy a particular constraint in the long term or in the short term. Like any other tool, it is most effective when combined with other tools.

Integrating biotechnology in the programs ensures that it addresses priority problems. Biotechnology is applied after other options have been considered, owing to the limited financial resources available to support rice R & D in the Philippines.

This set-up provides biotechnology researchers more opportunities to collaborate with other researchers in other disciplines and programs. This is because biotechnology application usually cuts across programs. A particular resistance gene (e.g. *Xa*-21) can be incorporated or transferred into rice lines for the lowland and upland ecosystems. Likewise, this allows funding of a particular biotechnology research which may be costly to be sourced out from different programs.

Integration also enhances interaction with other disciplines, which is important in the conduct of biotechnology research. Interaction with other experts such as entomologists, plant pathologists and plant breeders becomes part of the research agenda. This precludes the awkward setup of biotechnologists forming their own exclusive group.

Biotechnology Projects in the Different Programs

Transplanted Irrigated Lowland Rice.

Transplanting is widely practiced by Filipino farmers in Luzon and Mindanao. Compared with direct seeding; transplanting gives higher yield, increases efficiency of farm inputs, requires lower seeding rates, reduces weeding costs, facilitates use of rouging, and speeds up the application of fertilizer and other field operations. This method, however, is capital- and labor-intensive.

From 1987 to 1997, 25 varieties were released for the irrigated ecosystems. Average yield per season is targeted at 7.5 t/ha by 2002 and 10 t/ha by 2005. Research activities focus on the development of more diverse varieties for specific locations and conditions, widespread implementation of integrated pest management (IPM), and promotion of location-specific fertilizer recommendations.

Wild species have been crossed to transfer pest resistance genes: *Oryza rufipogon* for tungro resistance; *O. officinalis* for green leafhopper (GLH) and brown planthopper (BPH); and *O. brachyantha* and *minuta* for bacterial leaf blight (BLB), sheath blight, and yellow stemborers. The current focus is the transfer of rice tungro disease (RTD) resistance genes from *O. rufipogon* (acc. 105909) into modern rice varieties. Molecular markers are being used to analyze the backcross progenies with IR64 for cosegregation with tungro resistance.

Despite the difficulty of mapping resistance to tungro due to its complicated disease development, an rice tungro spherical virus (RTSV) resistance gene from ARC11554, together with a tightly linked GLH resistance gene, was localized in chromosome 4 using restriction fragment length polymorphism (RFLP). Tungro resistance genes in Utri Merah and Utri Rajapan are also being mapped. Physical mapping using yeast and bacterial artificial chromosomes generates high resolution genetic and physical maps around the region of the tungro resistance gene in ARC 11554. This enables the isolation of the gene through map-based cloning.

Molecular markers are also being used to assess the extent of biodiversity in farmers' fields (particularly in Regions 2 and 3), analyze genetic relationships in the existing modern rice germplasm, and verify the identity of varieties. DNA markers are also employed in the marker-aided pyramiding of BLB resistance genes (*xa*-5, *Xa*-21 and *O. minuta* gene) in modern cultivars, and in the genetic mapping of blast resistance in a Tequing ' Lemont recombinant inbred population.

Plant transformation at PhilRice is done mostly through the natural vector *Agrobacterium tumefaciens*. It aims to improve highly advanced elite new plant type lines and elite cultivars by incorporating one or two exogenous genes conferring resistance to sheath blight, blast, and tungro. Conditions for *tumefaciens*-mediated transformation have been optimized and transgenic lines containing the chitinase and glucanase genes are being generated. Evaluation of transgenic rice at PhilRice either produced or from institutional collaborations is now possible with the newly renovated containment level 2 screenhouse. Initial experiments include the evaluation of transgenic IR72-*Xa*21 for resistance to different races of BLB, and transgenic IR72 containing the RTSV coat protein.

Direct-Seeded Irrigated Lowland Rice

Direct seeding is widely practiced during the dry season in Pangasinan, upper Pampanga, Panay, and Bicol. Although this requires high seeding rates and thorough land preparation, it is still more practical for small farmers because it requires less water, and relatively cheaper labor cost.

This program targets an average yield of 7-8 t/ha in 2002 and 8-10 t/ha in 2005. Using biotechnology, promising parental cultivars for direct-seeded rice breeding have been analyzed for seedling vigor (SV) performance using controlled laboratory tests in conjunction with molecular marker assays. Molecular mapping of quantitative trait loci (QTLs) underlying traits for SV has also been conducted using RFLP, randomly amplified polymorphic DNA (RAPD), and amplified fragment length polymorphism (AFLP) markers. The development of a marker-aided selection technique for this character is being studied.

Hybrid Rice

The potential of hybrid rice production has been established in neighboring countries like China, which gained a tremendous increase in rice production. In the Philippines, the potential of this technology in attaining yields as high as 10 t/ha has been shown in selected technology demonstration sites. This program aims to strengthen hybrid rice R&D efforts in the country to maximize the technology's potential. Three hybrid rice varieties, PSB Rc26H (Magat), PSB Rc72H (Mestizo), and PSB Rc76H (Panay) were previously released. These are now cultivated in different parts of the country.

The hybrid rice program aims to develop and use hybrid rice technology to increase average yields per hectare by 15% or higher, thus promoting farmers' productivity and competitiveness and the attainment of rice self-sufficiency over the long term.

DNA fingerprinting is being done in cytoplasmic male sterility (CMS) lines using RAPDs, microsatellites, and AFLP to measure the genetic diversity of the existing germplasm. Assignment of breeding lines to different heterotic groups is one essential step in designing crosses for hybrid breeding. DNA fingerprints are also used in the analysis of genetic diversity of breeding materials for the prediction of F_1 performance.

Through genetic engineering, a new system in developing male sterility is being developed. A tapetum specific promoter of *Arabidopsis thaliana*, the *A9* gene was cloned into a GUS expression vector and is currently being tested in transgenic rice. Genes that will be effective in controlling the expression of the transgene in anthers to produce male sterile plants will be cloned in front of the promoter.

Rice for Adverse Environments

The many adverse areas in the country are mostly ecosystems-based, and they require unique R&D approaches and strategies. In the cool elevated areas of the Cordillera Administrative Region, for example, yields have averaged at a low 1.7 t/ha. In other low temperature areas like Cagayan Valley and Bukidnon, yields can decrease by about 20-80%. Efforts are being made to increase yields in these areas. Two salt-tolerant varieties, PSB Rc48 (Hagonoy) and PSB Rc50 (Bicol), have already been released. For upland areas, there are three PSB-recommended varieties: PSB Rc1 (Makiling), PSB Rc3 (Ginilingan Puti), and PSB Rc5 (Arayat).

The program aims to improve and sustain yields in saline-prone, acid upland, and cool elevated areas at an average of 3.5 t/ha; and in Zn-deficient, peat, and alkaline soils at 4 t/ha. Major R&D activities include the characterization of adverse areas, development of appropriate varieties, and development of cultural management practices.

Anther culture efforts in PhilRice-Central Experiment Station (CES) focus on the development of lines for saline and cool-elevated areas, while efforts in PhilRice-Los Baños focus on drought tolerance. Field conditions in adverse environments are unpredictable, making selection and generation advance complicated. Anther culture addresses this problem by the fact that doubled-haploid lines make it possible to conduct replicated trials much sooner. Aside from the anther culture-derived released variety PSB Rc50 of IRRI, PhilRice has produced three promising salt-tolerant lines, which are now in the National Cooperative Tests.

PhilRice's Capability for Biotechnology Research

The main laboratory facilities of PhilRice were provided by JICA in 1991. These facilities include a medium-term germplasm bank, several greenhouses, and research laboratories for plant physiology, soil analysis, chemistry, food technology, genetics, tissue culture, entomology, and plant pathology,. JICA, together with ARBN, RF and funds from the government also provided facilities in the genetics and tissue culture laboratories. At present, facilities are available for transgenic work, anther culture, and molecular marker analyses such as microsatellites, amplified fragment length polymorphism (AFLP), randomly amplified polymorphic DNA (RAPD), and restriction FLP (RFLP).

PhilRice pursues an aggressive manpower development program to implement the national R&D for rice. Eight out of 22 PhD's at PhilRice have been trained specifically for this purpose. Several more staff members are expected to finish their degrees in the immediate future and join the competent group of researchers specializing in biotechnology. The staff development of PhilRice in rice biotechnology is supported by the Rockefeller Foundation and the

Table 4. Projected specialization of senior biotechnology researchers at PhilRice.

Specialization	Present Core	Under Training	Future Training	Total by 2001-2003
Molecular Markers	4	1	0	5
Gene Cloning	1	2	1	4
Genetic Transformation	2	0	1	4
TOTAL	8	3	2	13

Japanese Government through its Monbusho Scholarship. The distribution of core staff according to specific areas of biotechnological research is shown in Table 4.

Concluding Remarks

Integrating biotechnology research into the mainstream of rice RD&E programs is a very important aspect of the newly re-focused National Rice RD&E Agenda. This strategy ensures that the biotechnology activities are in line with the priority concerns of the different programs. This also makes it easier to relate the outputs of biotechnology research with the other outputs from other research activities. With meager resources, integration and strong focus are a must.

References

Aldemita RR. 1997. Studies to improve transient GUS A expression in *A. tumefaciens*-mediated transformation of rice. In: Proc. of the First International Symp. on Biotech. of Tropical and Sub-Tropical Species, Brisbane Park Royal Hotel, Queensland, Australia, Sept. 29-Oct. 3, 1997, p 209.

Aldemita RR & Hodges TK. 1996. *A. tumefaciens*-mediated transformation of *japonica*and *indica* rice varieties. *Planta* 199:612-617.

Alfonso AA, Viray MC & Sebastian LS. 1997. Transfer of tungro virus resistance from the wild rice *Oryza rufipogon* Griff. to the cultivated rice *O. sativa* L. 19th Annual Scientific Meeting, National Academy of Science and Technology (Philippines), Jul. 9-10, 1997. Pasay City, Metro Manila.

Andaya CB, Sebastian LS, Leano CM & Andaya VC. 1997. Variability within doubled haploid lines from rice varieties RPKN2 and BW 203. Acta Horticulturae 461: 293-300.

Bato CB, Leano CM, Tabanao DA & Sebastian LS. 1996. Anther culturability of recombitant inbred lines derived from indica x japonica cross. Philip. J. Crop Sci. 21(1): 62.

Caldo RA & Sebastian LS. 1998. Molecular diversity of Philippine improved rice varieties and their progenitors using RAPD and SSR markers. In: Agricultural Biotechnology: Laboratory, Field and Market (P.J. Larkin, ed). Proc. 4th Asia-Pacific Conference on Agricultural Biotechnology, Darwin, Australia, 13-17 July 1998, p. 79-81.

Maramara MGV, Sebastian LS, Martin HC & Tiongco ER. 1997. Molecular mapping of resistance to tungro in Utri Rajapan (*Oryza sativa* L.). Pest Management Council of the Philippines (PMPC) Annual Meeting, Mar. 19-23, 1997, Iloilo City.

Obien, SR & Sebastian LS. 1998. Biotechnological research for rice improvement in the Philippines. Philipp. J. Crop Sci. 23(1)59-63.

Redoña ED & Mackill DJ. 1996. Molecular mapping of quantitative trait loci in japonica rice. *Genome* 39:395-403.

Redoña ED, Hipolito LR, Ocampo TD, & Sebastian LS. 1997. Molecular genetic diversity of CMS lines for hybrid rice breeding. Proc. 18th SABRAO Congress, Sept. 23-26, 1997, Seoul, South Korea. pp 125-126

Redoña ED, Hipolito LR, Ocampo TD, & Sebastian LS. 1997. DNA fingerprinting of hybrid rice germplasm. Federation of Asian and Oceania Biochemistry and Molecular Biology (FAOMB). Dec. 2-5, 1997, Quezon City, Philippines.

Redoña, E.D., L.R. Hipolito, T.D. Ocampo & L.S. Sebastian. 1998. Molecular polymorphisms of rice cytoplasmic-genetic male-sterile (CMS) lines based on AFLP, RAPD, and microsatellite markers. Philipp.

J. Crop Sci. 23(1):12-20.

Redoña ED, Hipolito LR, Ocampo TD & Sebastian LS. 1997. Molecular genetic diversity of CMS lines for hybrid rice breeding. International Symposium on the Genetics and Exploitation of Heterosis in Crops. Aug. 16-22, 1997. CIMMYT, Mexico City, Mexico.

Sebastian LS, Ikeda R, Imbe T, Huang N & McCouch SR. 1994. *Tagging genes for resistance to rice* tungro disease. In: Proc. 7th Meeting of the International Program on Rice Biotechnology. May 16-20, 1994 . p183.

Sebastian LS, Ikeda R, Huang N, Imbe T, Coffman WR & McCouch SR. 1996. Molecular mapping of resistance to rice tungro spherical virus (RTSV) and green leafhopper (GLH) in rice. Phytopathology 86(1):25-30.

Sebastian LS, Ikeda R, Huang N, Imbe T, Coffman WR, Yano M, Sasaki T & McCouch SR. 1996. *Genetic* mapping ot resistance to rice tungro spherical virus (RTSV) and green leafhopper (GLH) in ARC 11554. In: Rice Genetics III. (G.S. Kush, ed.). Proc. 3rd International Rice Genetics Symposium, Manila, Philippines. pp.560-564.

Sebastian LS, Maramara GV, Martin HC & Tiongco ER. 1997. Molecular mapping of resistance to rice *tungro spherical (RSTV) in Utri rajapan (O. sativa* L.). Meeting of the International Program on Rice Biotechnology – Rockefeller Foundation Rice, Sep. 15-19, 1997 in Malacca, Malaysia.

Sebastian LS. 1997. Safeguarding and Preservation of the Biodiversity of the Rice Genepool – On Farm Conservation – Country report presented during the Workshop on Safeguarding and Preservation of the Biodiversity of the Rice Genepool, Penang, Malaysia, Dec. 7-14, 1997.

Sebastian LS, Hipolito LR, & Garcia JS. 1998. Molecular contribution of landraces in the development of Philippine-bred modern rice varieties. SABRAO J. Plant Breeding and Genetics. 30(2):73-82.

Sebastian LS, Hipolito LR, Tabanao DA, Maramara GV & Caldo RA. 1998. Molecular diversity of Philippine-bred rice varieties. SABRAO J. Plant Breeding and Genetics. 30(2):83-90.

Sebastian LS, Hipolito LR, Garcia JS, Tabanao DA, Maramara GV and Caldo RA. 1998. Microsatellite marker analysis of the allelic composition of Philippine-bred modern rice varieties. Philipp. J. Crop Sci. 23(1)21-27.

Sebastian LS, Hipolito LR, Tabanao DA & Maramara GV. Applications of molecular markers in the identification and establishment of origin of selected Philippine rice cultivars. Philipp. J. Crop Sci. 23(1):28-34

Sebastian LS, Garcia JS, Quiloy SE, Hipolito LR, Sanchez PL, Calibo MC & Pham JL. 1998. Assessment of diversity and identity of farmers rice varieties using microsatellite markers. Plant and Animal Genome VI. Jan. 18-22, 1998. San Diego, CA, USA.

Tabanao DA, Andaya VC, Ocampo TD & Sebastian LS. 1997. *Pyramiding of bacterial leaf blight resistance* in popular Philippine rice cultivars. FCSSP Scientific Conference, May 26-30, 1997, Baguio City. PJCS. 22(1):56.

Philippine Journal of Science
128 (4): 281 - 287, December 1999
ISSN 0031 - 7683

REVIEW

Philippine Frogs of the Genus *Platymantis* (Amphibia:Ranidae)

Angel C. Alcala[1]* and Walter C. Brown[2]

[1]Silliman University-Angelo King Center for Research and Environmental Management,
Marine Laboratory, Dumaguete City, Philippines
[2]California Academy of Sciences, San Francisco, California 94118 U.S.A.

Philippine platymantine frogs, as currently understood, belong to the genus *Platymantis*. The Philippine species are subdivided into three groups: the *hazelae*, the *guentheri* and the *dorsalis* Groups. With the exception of *Platymantis dorsalis*, the other 25 species thus far recognized are endemic. The local distribution of the three groups varies, with the *hazelae* Group exhibiting the most restricted distribution and the *dorsalis* Group the widest. No *Platymantis* species has been recorded from the Palawan and Sulu island groups. The distribution and taxonomic data support the hypothesis that the Philippine platymantine frogs are Papuan in origin.

Key words: *Platymantis, hazelae* Group, *guentheri* Group, *dorsalis* Group, murid rodents

The platymantine frogs, as presently diagnosed (Duellman and Trueb 1994), include four genera: *Palmatorappia and Ceratobatrachus* in the Solomons; *Discodeles* in the Solomon, Bismarck, and Admiralty islands; and the genus *Platymantis* from the Fijis, Palaus, Solomons, Bismarcks, New Guinea, and the Philippines.

The earliest descriptions of any platymantine frogs are those of *Hylodes corrugatus* and *Cornufer dorsalis* (Duméril 1853). These were stated to be from Java but no further examples of these species or any other species of this genus have ever been collected in Java. The type specimens are conspecific with Philippine populations. This was confirmed by Inger (1954) for *H. corrugatus* and by Brown and Inger (1964) for *C. dorsalis*. The Melanesian genera of platymantine frogs (*Platymantis, Ceratobatrachus,* and *Discodeles*) were diagnosed by Boulenger (1884 and 1918). The fourth Melanesian genus (*Palmatorappia*) was diagnosed by Sternfield (1921).

As to the generic names, *Cornufer* and *Platymantis* have been used at different times for different groups of species [Guenther (1858), Boulenger (1882), Taylor (1920), and Inger (1954)]. The present restriction to the use of *Platymantis* for all species resulted from the determination that the Paris Museum syntype (MNHN 747) of *Cornufer unicolor* (Tschudi 1838) is an example of a species of *Eleutherodactylus* from the West Indies (Zweifel 1967).

The definition of the platymantine frogs has become more precise and restricted in the past seventy years and the concept of continental drift as opposed to fixed continents has received general

---

*Corresponding author: suakcrem@fil.net

[illegible] in the [illegible] years. These two concepts are summarized in the following diagnostic and biogeographic views expressed by various authors during this period.

Recognition of the subfamily Cornuferinae for these ranid frogs was first proposed by Noble (1931); however, his diagnosis was sufficiently broad as to include several Asiatic genera ([illegible], Micrixalus, Staurois, and Simomantis). Other recent publications have resulted in further confusion as to possible Asiatic relatives of the island platymantines. One was the description of three frogs occurring in western China and Tibet as species of [illegible] [illegible], [illegible], and [illegible] between 1877 and 1894. These three species along with several other Asian ranids were placed in a new genus [illegible] erected by Dubois (1986). They were all transferred to the genus [illegible] by Zhao and Adler (1993). Many subsequent authors, including some who restricted the platymantine frogs to the Melanesian and Philippine genera Ceratobatrachus, Discodeles, Platymantis, and possibly Palmatorappia, have continued to subscribe to the concept of dispersal from Asia (Darlington 1957, Savage 1973, Duellman and Trueb 1986, and Allison 1996).

The hypothesis of a non-Asiatic origin of the platymantine frogs has also had its proponents in the past two decades following the general acceptance of continental drift. In one of the earliest papers, Tyler (1979) proposed that Platymantis evolved in the Philippines from an Australian ranid stock during the Tertiary, with eastward dispersal and subsequent radiation in Melanesia following. Two recent papers (Brown 1997 and Inger 1999) refer to the platymantine frogs as Papuan in origin.

Philippine Platymantine Frogs

The platymantine species in the Philippines are currently all assigned to the genus Platymantis. Recently they have been divided into three species groups (Brown et al. 1997a and 1997b). These groups [illegible] are recognized on the basis of the following morphological characteristics of the fingers and the terminal phalanges. These characters are briefly summarized below.

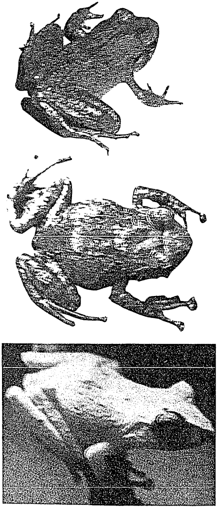

Figure 1. Representative species for the three groups of Platymantis. Top, Platymantis [illegible] (Brown, Alcala and Diesmos), middle, Platymantis [illegible] (Brown, Alcala, Diesmos and Alcala), and bottom, Platymantis [illegible] (Brown, Alcala, [illegible] and Diesmos).

The *hazelae* Group

Digits with broad disks, subtending part of digits wide, subarticular tubercles low and rounded, terminal phalanx a wide "T". This Group includes nine species: *hazelae, cornutus, isarog, lawtoni, montanus, panayensis, polilloensis, subterrestris,* and *sierramadrensis.*

The *guentheri* Group

Digits with broad disks, subtending part of digits narrow, subarticular tubercles strongly protruding and usually pointed, terminal phalanx a moderate to wide "T" This group includes six species: *guentheri, banahao, luzonensis, negrosensis, insulatus* and *rabori.*

The *dorsalis* Group

Digits blunt or with small to moderate disks, subtending part of digits narrow, subarticular tubercles strongly protruding and usually pointed, terminal phalanx not "T" shaped. This group includes 11 Philippine species: *corrugatus, dorsalis, levigatus, spelaeus, mimulus, naomii, pygmaeus, cagayanensis, taylori, pseudodorsalis,* and *indeprensus.* Five of these species (*sierramadrensis, cagayanensis, taylori, pseudodorsalis,* and *indeprensus*) have been described recently (Brown et al. 1999a and 1999b).

Ecology of Philippine *Platymantis*

The species of the *dorsalis* Group are ground dwelling forms, although they have been observed to climb low vegetation less than a foot above the ground. One species of this Group inhabits caves. Most of the species belonging to the two other Groups are arboreal, being found in microhabitats up to several meters above the ground, such as arboreal ferns, screw pines, moss growing on tree trunks, etc These microhabitats are part of original rain forests. Only occasionally are species such as *corrugatus* and *dorsalis* found in second growths or man-made forests that are adjacent to undisturbed areas. In favorable microhabitats, some of the species are fairly common.

Platymantis species do not require running streams. However, because these frogs undergo direct development, wet or moist condition of the habitats is necessary for reproduction. Six or seven species are known to deposit their large, unpigmented eggs beneath duff on the forest floor or arboreal situations afforded by leaf axils of screw pines and broad-leaved plants (Araceae), wet moss, and bird's nest ferns (Alcala 1962, Brown and Alcala 1983). The large unpigmented eggs of other species indicate a similar development process.

These frogs are found in suitable habitats from lowland or dipterocarp forest and montane (mossy) forest at altitudes ranging from near sea level to 2,250 m above sea level. However, species of the *hazelae* and *guentheri* Groups occur primarily in the submontane and montane zones. Temperatures in their habitats range from 15° to 25° C. Of the 26 recognized species, 15 are found in arboreal microhabitats and 11 are in forest floor microhabitats.

Advertisement calls of most species have been heard during the rainy months, which include the breeding period. Thus far, no calls have been heard during the non-rainy months for most of the species.

Endemism

Of the 26 species currently recorded from the Philippines, 25 (all but *dorsalis*) are endemic. Populations in Palau, New Guinea, Bismarck, and Solomon Islands are also referred to *P. dorsalis.*

Distribution Patterns in the Philippines

The *dorsalis* Group, as presently diagnosed, has a wide range in the Philippines. The ranges of the other two groups, as presently defined, are limited to the Philippines (Table 1).

The *hazelae* Group exhibits the most restricted distribution, known only from the oceanic islands (Greater Negros-Panay and Tablas-Romblon-Sibuyan as well Greater Luzon island areas). The *guentheri* Group is known from Greater Mindanano islands as well as Greater Negros-Panay and Greater Luzon island areas (Fig.2). The range of the *dorsalis* Group includes Mindoro Island in addition to the three island groups already mentioned. No species of *Platymantis* has been recorded from Palawan or the Sulu Islands (but geologically and biogeographically Greater Palawan and probably the Sulus are part of Sundaland, not the Philippine Archipelago). Based on present data, there are seven species of *Platymantis* in Greater Negros-Panay-Masbate, four in Greater

Table 1. Distribution patterns for the recognized Groups of *Platymantis* Species in the Philippines.

Location	*Platymantis* Group		
	hazelae	*guentheri*	*dorsalis*
Greater Sulus	0	0	0
Greater Mindanao	0	2	2
Greater Bohol	0	2	2
Greater Luzon	6	2	9
Camiguin	0	0	1
Greater Negros-Panay	2	2	3
Greater Mindoro	0	0	2
Tablas, Romblon, Sibuyan	1	0	2
Greater Palawan	0	0	0

Mindanao and Bohol, 17 in Greater Luzon, two in Greater Mindoro, three in Tablas-Romblon-Sibuyan, one in Camiguin, and none in Palawan or the Sulus (Fig. 2 & Table 1).

Isolating Mechanisms and Speciation

Three isolating mechanisms have operated to produce the speciation occurring in Philippine *Platymantis* (Brown, Brown and Alcala 1997b). One is the presence of marine barriers that have isolated the islands of Negros, Panay, Sibuyan, Romblon, Tablas, and Mindoro from each other as well as from Luzon. Negros, Panay and Cebu were probably connected by land to each other as recently as 18,000-20,000 years ago. There are no records of arboreal platymantine species on Cebu, probably because of the total disappearance of original forests on this island early in this century. It is possible that land connections between Sibuyan and Tablas on the one hand and Luzon on the other existed much earlier during Pleistocene times about 100,000 to 500,000 years ago (Morley and Flenley 1987).

The second isolating mechanism operating for the Luzon populations is the habitat preference of these frogs for humid or wet montane forest habitats on isolated mountains. Such mountains are separated by swaths of lowland forest or man-made habitats.

The third isolating mechanism is past fragmentation of some of the larger islands, such as Mindanao and Luzon.

Discussion

As currently diagnosed, there are 26 species of platymantine frogs in the Philippine Islands, and all but one (*dorsalis*) are endemic. The rest of the Philippine frogs with the exception of two species of *Oreophryne* are related to the frogs of Borneo.

In contrast to the platymantine frogs, only 28 of 55 Sundaland-related frogs are endemic. If one contrasts only the Bornean-related ranids, eight of 17 species are endemic.

When distribution patterns are contrasted, the Bornean-related ranids are rather evenly distributed including Palawan and the Sulus. When the contrast includes all families of frogs, they again are found in all Philippine faunal regions, but with the largest number in the Greater Mindanao region (Table 2)

To provide a contrast with a non-amphibian Sundaland-related fauna, we chose the murid rodents. They have entered by the same pathways (Palawan and Sulus) as the Sundaland frogs and include both surface-dwelling and arboreal forms. Our knowledge of their distribution patterns is current (Heaney et al. 1998). Again, as with the Sundaland-related frogs, the murid rodents are recorded from all nine faunal regions (Table 2). Fifty-three of the 61 species are endemic in contrast to only 28 of the 55 Sundaland-related frogs.

Conclusion

We conclude that the hypothesis of a Papuan origin for the Philippine platymantine frogs is strongly supported by the data presented in this review. Research, using currently available methods of comparing populations and diagnosing species, is urgently needed, especially in such geologically complex regions as Greater Mindanao and Greater Mindoro. The urgency is due to the current rapid depletion of suitable forest habitats on most of the larger islands.

We predict that the number of species of platymantine frogs will be greatly increased by prompt undertaking of the proposed research. We further predict that endemism for Sundaland-related frogs is probably greater than currently recognized.

One major problem is that of determining the relationship of the platymantines to other ranids. A phylogenetic study is currently being pursued by Rafe M. Brown at the University of Texas in Austin. Results of this investigation should provide a better understanding of the evolution of the platymantine frogs, their dispersal routes, and present ranges.

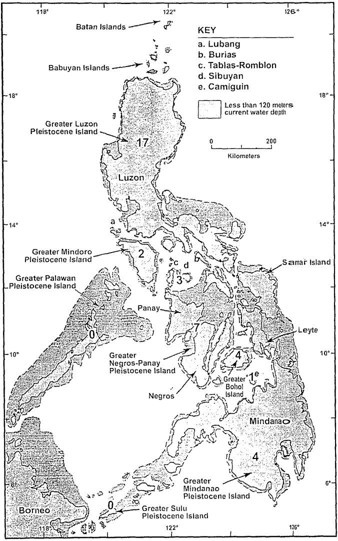
118°
122°
126°
Batan Islands
KEY
a. Lubang
b. Burias
c. Tablas-Romblon
d. Sibuyan
e. Camiguin
Babuyan Islands
18°
Less than 120 meters current water depth
Greater Luzon Pleistocene Island
17
0
200
Kilometers
Luzon
14°
a
Greater Mindoro Pleistocene Island
2
c
d
b
3
Samar Island
Greater Palawan Pleistocene Island
Panay
7
0
Leyte
10°
Greater Negros-Panay Pleistocene Island
4
Greater Bohol Island
1
e
Negros
Mindanao
4
Greater Mindanao Pleistocene Island
6°
Borneo
0
Greater Sulu Pleistocene Island
118°
122°
126°

Figure 2. Distribution of *Platymantis* in the Ice-Age islands of the Philippines. Figures represent number of species.

Table 2. Distribution patterns of platymantine frogs, Bornean-related ranids, all Bornean-related frogs and Bornean-related murid rodents in the Philippines. **A**, Platymantis; **B**, Bornean-related ranid frogs; **C**, All Bornean-related frogs; **D**, Bornean-related murid rodents (Mammalia).

Faunal Region	A	B	C	D
Greater Sulus		3	8	1
Greater Mindanao	4	8	26	17
Greater Bohol	4	5	14	4
Greater Luzon	17	5	15	26
Camiguin	1	5	8	3
Greater Negros-Panay	7	6	9	7
Greater Mindoro	2	3	9	10
Tablas, Romblon, Sibuyan	3	2	2	4
Greater Palawan		5	12	8
Total species in the Philippines	26	17	55	61

Acknowledgments

We wish to thank Robert F. Inger for his constructive comments on an earlier draft; Lawrence Heaney, Danilo Balete, Arvin Diesmos, Rafe Brown, Ely Alcala, Jose Lago, and Roy Quiber for assistance in the field; and Dolores Felicitas and Jeanette Brown for typing the manuscript.

References

Alcala AC. 1962. Breeding behavior and early development of frogs of Negros, Philippine Islands. Copeia 1962: 679-726.

Allison A. 1996. Zoogeography of amphibians and reptiles of New Guinea and the Pacific Region: Pp. 407-436. In: The Origin and Evolution of Pacific Island Biotas, New Guinea to Eastern Polynesia: Patterns and Processes, A. Kaost and S.E. Miller, eds. Academic Publishing, Amsterdam.

Boulenger GA. 1882. Catalogue of Batrachia Salientia Ecaudata in the Collection of the British Museum, London. 1:503 pp.

Boulenger GA. 1884. Diagnosis of new reptiles and batrachians from the Solomon Islands, collected and presented to the British Museum by H.B. Guppy, Esq. Proc. Zool. Soc. London, 1884:210-213.

Boulenger GA.1918. Remarks on the Batrachian genera *Cornufer* Tschudi, *Platymantis* Guenther, *Simomantis*, g.n., and *Staurois* Cope. Ann. Mag. Nat. Hist. (9): 372-375.

Brown WC. 1997. Biogeography of amphibians in the islands of the southwest Pacific. Proc. Calif. Acad. Sci. 50 (2): 21-38.

Brown WC & Alcala AC. 1983. Modes of reproduction of Philippine anurans. Pp. 415-428 *in* Advances in Herpetology and Evolutionary Biology. A.G.J. Rhodin and K. Miyata. Eds. Harvard Univ. Press, Cambridge.

Brown WC, Alcala AC & Diesmos AC. 1997a. A new species of the genus *Platymantis* (Amphibia:Ranidae) from Luzon Island, Philippines. Proc. Biol. Soc. Washington 110 (1):18-23.

Brown WC & Inger RF. 1964. The taxonomic status of the frog *Cornufer dorsalis* A. Dumeril. Copeia 1964:450-451.

Brown WC, Brown RM & Alcala AC. 1997b. Species of the *hazelae* Group of *Platymantis* (Amphibia:Ranidae) from the Philippines, with descriptions of two new species. Proc. Calif. Acad. Sci. 49 (11):405-421.

Brown WC, Alcala AC, Diesmos AC & Alcala E. 1997c. Species of the *guentheri* Group of *Platymantis* (Amphibia: Ranidae) from the Philippines, with descriptions of four new species. Proc. Calif. Acad.Sci. 50 (1):1-20.

Brown WC, Alcala AC, Ong PS & Diesmos AC. 1999a. A new species of *Platymantis* (Amphibia:Ranidae) from the Sierra Madre mountains, Luzon Island, Philippines. Proc. Biol. Soc. Washington 112 (3):510-514.

Brown WC, Alcala AC & Diesmos AC. 1999b. Four new species of the genus *Platymantis* (Amphibia:Ranidae) from Luzon Island, Philippines. Calif. Acad. Sci. 51 (12):449-460.

Darlington PJ. 1957. Zoogeography: The Geographical Distribution of Animals. Wiley and Sons, New York. 675 pp.

Dubois A. 1986. Miscellanea taxinomica [sic] batrachologica (1). Alytes 5:7-95.

Duellman WE and Trueb L. 1994. Biology of Amphibians. Johns Hopkins Univ. Press, Baltimore, MD. 670 pp.

Duméril A. 1853. Memoire sur les Batraciens Anoures, de la famille des Hyla-formes ou Rainetes , conprenant la description d'un genre nouveau et de onze especes nouvelles. Annales des Sciences Naturelles (3) 19:135-179.

Guenther A. 1858. Catalogue of the Batrachia Salientia in the British Museum. (London), 160 pp.

Heaney LR, Balete DS, Dolar ML, Alcala AC, Dans AT, Gonzales PC, Ingle NR, Lepiten MV, Oliver WL, Ong PS, Rickart EA, Tabaranza BR & Utzurrum RC. 1998. A synopsis of the mammalian fauna of the Philippine Islands. Fieldiana:Zoology, 88:1-61.

Inger RF. 1954. Systematics and zoogeography of Philipine amphibia. Fieldiana:Zool. 33:181-531.

Inger RF. 1999. Distribution of amphibians in southern Asia and adjacent islands. Pp. 445-482 in W. E. Duellman, ed. Patterns of Distribution of Amphibians: A Global Perspective, Johns Hopkins Univ. Press, Baltimore, MD. 670 pp.

Morley RJ & Flenley JR. 1987. Late Cenozoic vegetational and environmental changes in the Malay Archipelago. Pp. 50-59 *in* Biogeographical Evolution of the Malay Archipelago, Oxford Monogr. Biogeog. 4, T.C. Whitmore, ed. Clarendon Press. Oxford.

Noble GK. 1931. Biology of the Amphibia. McGraw-Hill, New York. 577 pp.

Peters W. 1873. Uber eine neue Schildkrotenart, *Cinosternon effeldtii* und einige andere neue oder weniger bekannte Amphibien. Monstsber. Adad. Wiss. Berlin 1873:603-618.

Savage JM. 1973. The geographic distribution of frogs: patterns and predictions. Pp. 351-445 *in* Evolutionary Biology of Anurans, J.L. Vial, ed. Univ. Missouri Press. Columbia.

Sternfield R. 1921. Zur Tiergeographie Papuasiens und der pazifischen Inselwelt. Aband. Senckenberg. Naturf. Ges., 36 (for 1920), pp. 375-436.

Taylor EH. 1920. Philippine Amphibia. Phil. J. Sci. 16:213-359.

Tschudi JJ. 1838. Classification der Batrachier. mit Berucksichtigung der fossilen Theire dieser Abtilung der Reptilien. Neuchatel, Switzerland. (A preprint, also in Mem. Soc. Sci. Nat. Neuchatel, 2,1839 [1840].)

Tyler MJ. 1979. Herpetological relationships of South America and Australia. Monogr. Mus. Nat. Hist. Univ. Kansas 7:73-106.

Zhao Er-Mi & Adler K. 1993. Herpetology of China. Society for the Study of Amphibians and Reptiles, in cooperation with the Chinese Society for the Study of Amphibians and Reptiles, 152 pp.

Zweifel RG. 1967. Identity of the frog *Cornufer unicolor* and application of the generic name *Cornufer*. Copeia 1967:117-121.

Philippine Journal of Science
128 (4): 289 - 294, December 1999
ISSN 0031 - 7683

REVIEW

Production Systems Modeling for Sawmills: An Overview

Roger J. Meimban and Guillermo A. Mendoza*

Department of Natural Resources and Environmental Sciences
University of Illinois at Urbana-Champaign
1102 S. Goodwin Avenue, Urbana, IL 61801, U.S.A.

In this paper, we present an overview of hardwood sawmilling operation and the results of some of our modeling experiments. The methodology involves the development of modeling techniques to differentiate and quantify the various sawmilling by-products, including lumber quality. Empirical and simulation studies have shown that more than 70 % of sawmilling costs is due to the cost of materials or logs. It is for this reason that focus is given to develop models that could predict the recovery of sawmill components. Such models could provide insight regarding the efficiency of individual sawmill operations and sawing practices. For example, our simulation resulted in 12.8% recovery of the high grade First and Second (FAS) lumber if gradesawing is used while only 5.5% is recovered through livesawing. Empirical studies on the same set of logs showed an actual FAS grade recovery of 15.3%. Overall, simulated gradesawing resulted in 52.6% recovery of Selects and better grade compared to 19.5% from livesawing. Empirical gradesawing study recovered 49.8% of Select and better grade materials. However, the processing time for gradesawing more than doubles that of livesawing. The paper further presents some sawmill modeling issues that confront mill analysts.

Key words: wood processing, simulation, discrete-event simulation, sawmilling

Several interrelated steps are involved in converting logs into lumber. These steps include log breakdown or headsawing, edging, and trimming. In each of these manufacturing stages, several sawmilling by-products are produced such as lumber, bark, slabs, edgings, trims, and dog boards. Knowledge of the volume of each of these sawmilling components is essential in achieving efficient lumber manufacturing operation. The volume of each of the by-products, other than lumber, represents the amount of wood lost due to sawing practices and equipment. Steele et al. (1992) estimated that raw material might comprise 75 % or more of the total sawmill manufacturing cost. Thus, it is important to improve conversion efficiency and recover as much lumber as possible with the least amount of processing waste. With information on the amount of wood lost at each stage of lumber manufacturing, one can identify the areas in sawmilling where potential profits can possibly be increased.

---

*Corresponding author: gamendoz@uiuc.edu

Abbreviations used: cumulative distribution function (CDF), first and second (FAS), probability distribution function (PDF)

This paper aims to describe some simulation modeling techniques to quantify and analyze the conversion of hardwood logs into lumber. Some of these techniques can be implemented in standard programming languages such as Fortran or C or by using dedicated simulation packages such as SLAM and ARENA. The methodology allows the detailed analysis of various interacting variables without physically sawing a log. We further present a methodology of incorporating the temporal attributes of the sawmill and the results of some of our modeling experiments. For illustrative purposes, the modeling framework of the SIMAN/CINEMA (currently known as ARENA) simulation package is utilized in some of the discussions.

Modeling Sawing Patterns and Decisions

Modeling of sawmill activities primarily focus on two areas: the algorithmic representation of log conversion activities to maximize yield or value and the representation of sawmill material and information flow over time. In the following discussions, we first develop the basic algorithm for log breakdown and then implement the idea into a discrete-event simulation model.

Log Breakdown

Figure 1 presents the schematics and pseudo-codes for two popular sawing patterns: live sawing and grade sawing. In live sawing, all cuts are parallel to each other. Once the initial sawing face is determined, there are no further decisions except for thickness setting and when to turn the log. In grade sawing, the log is visually divided into quadrants and turned to a face in search of better grade boards. Because of the greater number of cuts or sawlines generated in grade sawing, one would expect a lower volume recovery of lumber compared to live sawing.

To quantify the volume of materials, we assume a truncated cone geometry which is typically used in representing hardwood logs (see for example: Richards, 1973; Savsar and Kersavage, 1982, Meimban et al., 1992) Further assume a non-tapered sawing method and that all saw cuts are parallel to the central or longitudinal axis of the log. The resulting facial configuration of the material can be approximated by a trapezoid whose volume (V) can be expressed as:

$$V = L\int_{z^2}^{z^1}(\sqrt{R^2 - z^2} + \sqrt{r^2 - z^2})dz \qquad (1)$$

where L is the length of the log, R is the radius of debarked log at big end, r is the radius of debarked log at small end and z_1 and z_2 are face distances of cuts from the origin on the Z-axis (Figure 1.). The above expression can be used to calculate the volume of boards, and can be modified to quantify other by-products such as edgings, trims, and sawdust (Kersavage et al. 1990).

It is often of interest to determine the amount of 'chippable' materials a sawmill produces. Materials such as edgings and trims and even sawdust have some economic value as these can be marketed to fiberboard and particleboard plants. The calculation of the weight of material is straightforward:

$$W = (\frac{MC}{100} + 1)G_o \sum V_i \qquad (2)$$

where W is the weight of the by-product, MC is moisture content in percent, G_o is the oven dry density of the species which can be found in wood handbooks, and V_i is the volume of the individual trapezoids as calculated in Equation 1 or as components of such trapezoids.

Assigning Lumber Quality

Among the issues confronting sawmill model-builders is the representation of lumber quality or grades. In practice, grades largely influence a sawyer's selection of cutting patterns. The heterogeneous characteristic of wood makes it difficult to model the human decisions in terms of the number of cuts to make from each side or quadrants of a log or when to rotate the log from the current cutting face. Current efforts are being undertaken by some researchers in log scanning technology to enable the detection of defects inside a log (Schmoldt et al. 1999; Chen and Occena, 1996).

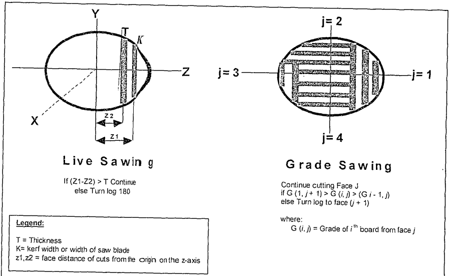
Y
T
K
Z
X
Z2
Z1
Live Sawing
If (Z1-Z2) > T Continue
else Turn log 180
Legend:
T = Thickness
K= kerf width or width of saw blade
z1,z2 = face distance of cuts from the origin on the z-axis
j= 2
j= 3
j= 1
j= 4
Grade Sawing
Continue cutting Face J
if G (1, j+ 1) > G (i, j) > (G i - 1, j)
else Turn log to face (j + 1)
where:
G (i, j) = Grade of i th board from face j

Figure 1. Common sawing patterns and cutting decisions.

A typical approach in incorporating lumber quality into a simulation model is the use of table-lookup procedures. Available information on the grade yield proportions of lumber from logs can be used to generate the quality of a board from a simulation process. This would involve the following steps:

1. Calculate the Probability Density Function (PDF) for each log diameter and species.
2. From the PDF, construct the Cumulative Density Function (CDF) for each log class.
3. By inverse transformation, generate the grade of the board from the CDF.

Hence, if F(x) is the probability that the proportion of lumber grade G will be at most x, the CDF is defined for every x by:

$$F(x) = P(G \leq x) = \sum p(y) \qquad (2)$$

where $y \leq x$. Once the CDF is constructed, the realization of x in Equation 3 can be obtained by inverse transformation. This involves solving the function $x = F^{-1}(r)$ where $F^{-1}(r)$ is the inverse CDF of x and r is a random variable uniformly distributed in the interval [0,1].

We utilized the above procedure in developing the grade sawing decisions in Figure 1. To implement, the lumber grades found in the grading rules handbook can be indexed with one as the highest quality corresponding to the First and Second (FAS) grade. For brevity of presentation, let G(i, j) be the grade of the ith board from the jth face and j=1...4. Note that j represents the order of sawing the faces as determined by evaluating the face grade and j=1 indicates the highest grade face. The grade boundaries of the ith board sawn from the jth face, which is used to determine log turning decisions, can be expressed as:

$$G(1, j+1) \geq G(i, j) \geq G(i-1,,j), \qquad j>2 \quad (4)$$

Unless the current cutting face is the fourth face (j=4), log turning to face j+1 is made if there is no

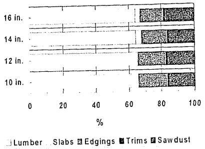

Figure 2. Simulated recovery of live sawing by-products.

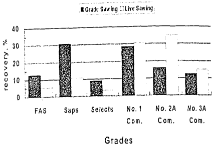

Figure 3. Comparison of grade recoveries in live sawing and grade sawing.

more G(i, j) grade that will satisfy the above relationship. Note that the condition j > 2 is justified operationally as sawyers often make 2 cuts to expose the inside grade of a face.

Simulated Results of Product Recovery

Figure 2 presents the results of some simulation experiments in the livesawing of various log sizes. We assumed a kerf width of 5/16" and 4/4" boards were sawn 1/8" oversize. Simulated lumber recoveries came within 3 % of actually sawing the same set of logs used by Clark (1976). Total chippable residues were within 5% of actual values. Note that as log diameter increases, lumber recovery increases with decrease in the proportion of wastes in form of slabs and edgings.

Figure 3 compares the grade recoveries between live sawing and grade sawing. The simulation runs made on 50 poplar logs assumed minimal saw kerf in order to isolate the effect of within board sawing variation in volume recovery. Our simulation resulted in 12.8% recovery of the high grade First and Second (FAS) lumber if gradesawing is used while only 5.5% is recovered through live sawing. Empirical studies on the same set of logs showed an actual FAS grade recovery of 15.3%. Overall, simulated gradesawing resulted in 52.6% recovery of Selects and better grade compared to 19.5% from livesawing. Empirical gradesawing study recovered 49.8% of Select and better grade materials. The pattern of grade recovery conforms with the actual observation that live sawing method results in lower proportion of high-grade lumber.

Modeling the Dynamics of Sawmilling

The static models presented in the previous sections cannot fully reflect the overall performance of actual sawmill production. For example, it is very likely that the economic gains due to increases in volume recovery arising from a sawing method can be negatively offset by longer production time. In the following sections, we discuss some methodologies of integrating the temporal components of lumber production.

Discrete-Event Simulation

Discrete-event simulation involves modeling a system as it evolves over time and where changes in the state of the system occur only at discrete points in time (Law and Kelton, 1991). In log breakdown operation for example, the events would include the log arrival at the headsaw area, log turning, sawing, release of boards, and so forth. Simulation is executed by advancing the simulation time and updating the state of the system when necessary. The sum between the times of successive occurrence of events would lead to the determination of the total time spent by a log in the headsaw station. A sample pseudo-code to include time delays in log breakdown would be as follows:

```
Release log from QUEUE
DELAY by log loading time (sample from distribution)
```

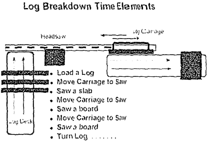

Figure 4. Schematic diagram and algorithm for a log breakdown process.

```
DO until (z1 -z2) < (thickness of board or kerf)
    SEIZE headsaw machine
    DELAY by headsawing time (sample from
    service time distribution)
    RELEASE headsaw machine
    Update z1 and z2
```

In the SEIZE block, the log is allocated the machine resource and delayed by a specified amount, e.g., sample from a *log-normal distribution of service* time.

Model Integration

We now demonstrate a methodology to simulate the log sawing patterns and decisions with time delays. This approach provides a sound basis for evaluating the economic impact of changes in production time as a result of changes in sawing policy. For illustrative purposes, consider the log breakdown schematic shown in Figure 4.

The model treats materials such as logs, boards, and lumber as entities and machines as resources. As an entity is processed, *event* subroutines are called at each occurrence of an event. These subroutines execute the logic associated for breaking down a log into flitches and flitches in boards. A log entity processed through the headsaw machine is replicated into boards whose quantity is calculated by the log breakdown model. The species attribute of the mother entity (log) is passed on to offspring entity (board) and enhanced to further include board thickness, width, volume, grade, and the next routing station (i.e., edger or trimmer machine).

Note from Figure 4 that boards are produced one *at a time as the log engages* the headsaw. In an event a headsaw machine is engaged, the associated time delays are collected and treated as components of log sawing time.

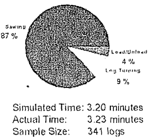

Figure 5. Simulated time elements in the grade sawing of hardwood logs.

Results of Simulated Processing Time

The approach presented previously was validated by using the same set of logs processed by Adams (1988) in calibrating the DESIM simulation system. The results, as summarized in Figure 5, are from 30 simulation runs for a 10-hour shift of an actual sawmill operation. The values were collected under steady-state condition.

The bulk of the time in grade sawing is spent in turning or orienting the logs in search of better quality boards. A similar simulation run on the same set of red oak logs using the live sawing method resulted in lower average headsawing time of 1.42 minutes per log (Mendoza, et al. 1991; Meimban et al. 1992).

Conclusion

What we have presented in this paper are techniques that can be used to develop sawmill simulation models in a larger scale. Individually or collectively, these can be implemented to analyze sawmill-fiber balances, evaluation of log breakdown procedures and sawing parameters (e.g., effect of kerf width) or as a tool for creating time schedule for production.

There are however other sawmill modeling issues that are not presented. Among the most important issues, especially in the selection of equipment, is the inclusion of sawing variations in the models. In practice, the saw blade or kerf "wanders" as it engages the log resulting in within board variation and wood loss.

Another interesting component that remains to be modeled is the inclusion of the optimal mixture of lumber thicknesses to account for possible product-mix specifications of customers.

References

Adams EL. 1988. Testing DESIM for designing and simulating the operation of hardwood sawmills. For. Prod. J. 38(7/8):41-45.

Chen W & Occena L. 1996. A 3-D shape model for generating log and knot defects. Proc., 5th Industrial Engineering Research Conference. Minneapolis, MN, pp 393-398.

Clark A. 1976. Sawmill residue yields from yellow poplar logs. Forest Prod. J. 26(1):23-27

Law AM & Kelton WD. 1991. Simulation modeling and analysis. 2nd ed. McGraw-Hill Inc.

Kersavage P, Savasar M & Meimban R. 1990. A mathematical analysis to determine the volume of residues and lumber produced in the sawmill edging process. Wood Fiber Sci. 22(3):371-382.

Meimban R, Mendoza G, Araman P & Luppold W. 1992. A simulation model for a hardwood sawmill decision support system. J. Forest Eng. 4(1): 39-47.

Mendoza GA, Sprouse W, Luppold W, Araman P & Meimban R. 1991. An integrated management support and production control system for hardwood forest products. Computers in Industry 16(4):343-351.

Richards J. 1973. Hardwood lumber yields by various simulated sawing methods. Forest Prod. J. 23(10):50-58.

Savsar M & Kersavage P. 1982. Mathematical model for determining the quantity of materials produced in sawmilling. Forest Prod. J. 32(11/12): 35-38.

Schmoldt D, Occena L, Abbot AL & Gupta NK. 1999. Nondestructive evaluation of hardwood logs: CTscanning, machine vision and data utilization. Nondestructive Testing and Evaluation. 15(5): 1058-1059.

Steele P, Wade M, Bullards S, & Araman P. 1992. Relative kerf and sawing variation values for some hardwood sawing machines. Forest Prod. J. 42(2):33-38.

Philippine Journal of Science
128 (4): 295 – 318, December 1999
ISSN 0031 - 7683

The Subfamily Turrinae in the Philippines: The Genus *Turris* (Röding, 1798)

Baldomero M. Olivera*

Department of Biology, University of Utah, 257 South 1400 East #201,
Salt Lake City, Utah, 84112-0840, USA

Marine gastropods of the family Turridae, commonly known as turrids, comprise the largest living group of venomous snails. The taxonomy of this group, however, has been generally neglected. In this work, the genus *Turris* (Röding 1798) is discussed. Out of more than 200 different turrid genera, this genus comprises some of the largest and most distinctive living turrid species. The last comprehensive treatment of this particular genus (Powell 1964) identified seven species from the Philippines. In this paper, twelve distinct species of *Turris* found in the Philippine waters are recognized. Four new species are described: *Turris dollyae*, *T. normandavidsoni*, *T. pagasa* and *T. totiphyllis*. Insufficient material makes it premature to conclude whether three additional distinctive *Turris* forms are separate species, or unusual varieties of other species. The taxonomic status of the genus *Turris* and its relationship to other Turrinae is further discussed. Alternative hypotheses regarding the evolutionary origins of this group are also considered. In addition, two species of *Gemmula*, with particular affinities for species clades in *Turris* are noted: one is a new species and one is a renamed homony.

Key words: Conacea, Turridae, toxoglossate, mollusc, clades, evolution

Toxoglossate molluscs (Conacea = Toxoglossa) comprise what is arguably the largest superfamily of venomous animals in terms of number of species (>3,000) (Powell 1966). Traditionally, toxoglossate molluscs are divided into three familiar groups: Conidae (cones), Terebridae (augers) and Turridae (turrids). Generally speaking, the cones and terebrids are easily recognized from their shells, and recent comprehensive taxonomic accounts of these groups have been published (Bratcher & Cernohorsky 1987, Röckel et al. 1995). The taxonomy of *Conus* has been analyzed not only by traditional malacological criteria. Recently, biochemical and molecular data that could be useful for deciding between different phylogenetic alternatives have been collected (for overviews, see Olivera et al. 1990 and Olivera et al. 1999). One of the first attempts to carry out molecular analysis of any toxoglossate molluscan group for purely taxonomic purposes (Dia-Monje 1994) was recently published in this journal (Monje et al. 1999).

The turrids are geologically the oldest of the three classical toxoglossate types, being well-represented in the Mesozoic. They are probably the most species-rich of all living gastropod lineages. Compared to cones and terebrids, turrids are remarkably diverse and much more heterogeneous.

---

*Send correspondence to: olivera@biology.utah.edu

The only characteristic that all turrids share is the presence of a slit (or posterior sinus). Virtually nothing is known about most of the several thousand different turrids. More than 200 different turrid genera have been proposed and there is no consensus on how many different families comprise the turrids. It has recently been suggested, based on a cladistic analysis, that some of the traditionally turrid genera might, in fact, be more closely related to cone snails than to other turrids and that these are more properly placed within the family Conidae (Taylor et al. 1993).

The most familiar and best-known of all the turrids in the Philippines are those belonging to the genus *Turris* (Röding 1798) as narrowly defined by Powell (Powell 1964, Powell 1966). This genus includes some of the largest and most striking turrid species. The Indo-Pacific arc (from the Philippines to New Guinea) appears to be the center of distribution for this group. However, most species are found in moderately deep water. As a consequence, most *Turris* species have not been widely available for study. As Powell stated in his 1966 monograph, classification of the Turridae is greatly hampered because "a range of specimens is not often available, even by dredging."

Because of the impressive creativity of the Philippine shell gathering industry, new technologies for collecting deep-water molluscs of interest to collectors have been developed. In the last few decades, through the use of gill nets and hookah collecting in the central and southern Philippine Islands, Philippine shell-gathering fishermen have found turrid species that were previously rare or uncommon. Because of their availability, the author has initiated biochemical and molecular work on turrid venoms. In order to do proper work of any type with the turrids, a reasonable understanding of their basic taxonomy is essential. However, in many cases, even the most rudimentary separation into species is proving to be problematic. Given the more than 2,000 turrid species, the only practical way to address this problem is to examine one genus (or group of related genera) at a time. We shall initially concentrate our efforts on the subfamily Turrinae. A logical starting point is therefore the nominate genus of this group: *Turris*.

Scope of this paper

In this paper, all known living forms conventionally assigned to the genus *Turris* (narrowly defined), which have been collected in the Philippines, are presented. The availability of a larger suite of specimens has made it possible to define four new species in this genus. A proposal for the evolutionary relationships between species clades in the genus and the possible origins of these clades is presented.

Like most taxonomic work, the proposals in this paper must be regarded as tentative. More material may reveal that forms proposed to be different species may in fact intergrade once a larger series is available and forms assigned to the same species may prove distinct upon closer examination of a larger sample set. However, this study comprises the minimal taxonomic characterization required before an effective molecular and biochemical characterization can be initiated on the venoms of *Turris* species. Taxonomic characterization is a necessary starting-point for other studies, however, results of the molecular studies and venom characterization should provide feedback that will be useful for rigorously evaluating the taxonomic framework proposed.

Previous monographs on *Turris* from the Philippines

The standard references on Indo-Pacific Turrinae are Powell's three monographs (Powell 1964, 1966, 1967). Powell recognized seven distinct species of *Turris* from the Philippines out of the eight total in his monograph. The only other subsequent treatment of *Turris* from the Philippines is the *Shells of the Philippines* by Springsteen and Leobrera (1986) which discussed and illustrated seven species. In that work, the authors did not include *Turris annulata* (presumably because no specimens could be found in any Philippine collections) but illustrated *Turris nadaensis*, a species described after the monographs of Powell.

Materials and Methods

Specimen collection

Turris specimens examined were mostly from the author's collection. These were collected from

Table 1. Summary of distinct forms in the genus *Turris* found in the Philippines (as defined by Powell 1964 and Powell 1966)

Turris	Specimen # in Plate I	Also Shown in Plate
annulata**	9	X
babylonia	5	IV, VI
crispa	1a, b	II, VI
cryptorrhaphe*	13	VIII, XI
dollyae, n. sp.	2	II, VI
garnonsii	8	VI
nadaensis*	10a, b, c	VIII
normandavidsoni, n. sp	3	III, VI
pagasa, n. sp	4	V, VI
spectabilis	14	VII
totiphyllis, n. sp	15	VII
undosa*	12	VIII, XI
Uncertain taxonomic status		
"niniveh" form (T. bablylonia?)	6	IV, VI
"Sulu Sea" form (T. babylonia?)	7	IV
"angular" form (T. nadaensis?)*	11	

Clade 1, no asterisk; Clade 2 *; Clade 3 **

various Philippine localities over the last 45 years. Specimens more recently obtained were collected primarily by using tangle nets in deep water (50-200 m) by trawling or by hookah in the localities indicated under each species.

Species characterization

The primary diagnostic keys used were the monograph of Powell (1964) and the book of Springsteen and Leobrera (1986). Morphological observations were restricted to the shells of each species.

Result and Discussion

Overview of *Turris* Species in the Philippines

For the purpose of this monograph, the fifteen distinctive Philippines forms assigned to *Turris* (see Table 1 and Plate I) were divided into three groups. These appear to be coherent clades, which probably reflect general evolutionary relationships between the various species traditionally assigned to this genus.

Clade I: The *babylonia* clade. This includes the largest group of species. The monograph of Powell (1964) discussed four species from the Philippines in this group: *Turris crispa crispa*, *Turris babylonia*, *Turris spectabilis* and *Turris garnonsii*. These four species are also figured and discussed by Springsteen and Leobrera (1986). In the treatment of the Clade I below, we include eight species, and two forms whose assignment is uncertain.

Clade II: The purple clade. These include three species that were recognized by Springsteen and Leobrera (1986): *Turris cryptorrhaphe*, *Turris undosa* and *Turris nadaensis* (the first two are also discussed by Powell), and a distinct form tentatively assigned to *T. nadaensis*. This group is characterized by the distinctive purple color of the aperture region, often extending into the canal.

Clade III: The *Annulaturris* clade. This includes only one Philippine species, assigned to *Turris annulata*, which appears to have little affinity with Clade I and Clade II species. Powell (1966) proposed the subgenus *Annulaturris* for *T. annulata*. We raise the possibility in this monograph that *Turris* (*Annulaturris*) *annulata* does not properly belong within the genus *Turris*. In this paper, we describe a new species of *Gemmula*, which at least superficially seems to be similar in general shape to *T. annulata*. However, we believe that the new species is properly assigned to *Gemmula*, and not *Turris*. This therefore raises the question of whether *T. annulata* and the subgenus *Annulaturris* is properly in *Turris*, in *Gemmula*, or is part of a distinctive transitional group intermediate between *Gemmula* and *Turris*.

Clade I: The *babylonia* clade

The type of the genus is *Turris babylonia*. In the Philippines, several forms appear to be part of a taxonomically confusing species complex closely related to both *T. crispa* and *T. babylonia*. Four new species that are part of this clade are described: *Turris dollyae*, *Turris normandavidsoni*, *Turris pagasa* and *Turris totiphyllis*. Some of the new species described here have been illustrated previously and identified as either *T. babylonia* or *T. crispa* by several authors. References in which these newly recognized forms have previously been illustrated will be cited where appropriate.

Turris crispa crispa (Lamarck, 1816)

(Plate I, Specimens 1a and 1b; Plates II and VI)

This is the largest of all living species in both the genus and the subfamily. This species can exceed 185 mm in length. *T. crispa* is primarily a deep-water species. Plate I shows the two variants of *T. crispa crispa* found in the Philippines. The large size and characteristic maculations on the typical form of this species are unmistakable (Plate I, Specimen 1A; Plates II and VI). *T. crispa* is trawled or collected by gill nets from a wide variety of different Philippine localities at depths of 80 to 150 meters. There is a white variety with almost no maculations (Plate I, Specimen 1b) which I assign to *T. crispa*; this is generally narrower than typical *T. crispa*. This form is much rarer in collected material from the Philippines.

In most previous treatments of *T. crispa*, a third form has been included within the species. From the much greater amount of material available, it seems clear that this form is distinct from *T. crispa*. Both typical *T. crispa* and this form apparently occur in several Philippine localities such as at Bogo, Cebu and around Panglao, Bohol. Since no intermediates between the two forms have been discovered, and this *T. crispa*-like form has not previously been described, a new name is proposed here, *T. dollyae*.

***Turris dollyae*, new species**

(Plate I, Specimen 2; Plates II and VI)

Description. The shell is large (80-123 mm), narrowly fusiform with a long siphonal canal. Adult specimens have 15-17 whorls; spire angle is 20-22°, ratio of aperture plus siphonal canal to total length is 0.48. Next to the upper suture are two fused spiral cords, the one adjacent to the suture generally smaller. Between the subsutural cords and the sinus cord is a deeply excavated area, with flat white threads. There are typically 5 or 6 spiral cords which are broad but come to a sharp apex, with secondary fine cords or threads in between. The canal is completely covered with additional spiral cords. The entire shell is marked with axial black maculations, much longer axially than along the spiral cord, with continuity between maculations across many cords in most but not all specimens. The large size, thin black axial markings and broadly excavated spiral area between the subsutural cords and the sinus cord are distinctive characteristics of the species.

Discussion. Most specimens labeled *T. crispa* collected from the Philippines are in fact *T. dollyae*, many collected from one locality (Tabaco Bay, Albay, Luzon Island) in fair numbers between 1960-1975. The holotype of *T. dollyae* from this locality is illustrated along with three paratypes in Plate II, and compared with a Philippine specimen of *T. crispa*.

The figure identified as *T. crispa crispa* from Luzon in the 1964 Powell monograph is in fact *T. dollyae* (Plate 181, Specimen 11). A specimen of *T. dollyae* is also figured in Springsteen and Leobrera (1986) and identified as *T. crispa* (Specimen 76, number 2, specimen on the right). Wilson (1994) illustrates a specimen of *T. dollyae* from Townsville, Queensland, Australia (Plate 38, Specimen 10B) (the other specimen labeled *T. crispa* from Queensland is the white form of *T. crispa crispa* without maculations). These literature records suggest that this species can be found throughout the Indo-Pacific arc, from Luzon to Queensland, Australia.

Comparison. *T. dollyae* is generally similar to *T. crispa* and *T. babylonia*, with mature *T. dollyae* larger than *T. babylonia*, and broader in outline, with a thicker canal than *T. crispa*. In many specimens of *T. crispa*, the maculations on the body whorl are restricted to the spiral ridges and are characteristically purplish-brown. The markings on *T. dollyae* are black and often run continuously in an irregular axial manner over several cords, particularly in the canal. When axial flammules do occur in *T. crispa*, the markings on the cord interstices are lighter in color than on the spiral cords. In *T. dollyae*, the markings are uniform black whether on the spiral cords or in between. The maculations of *Turris crispa* are aligned, with the longest dimension along the spiral cord, while these markings in *T. dollyae* are longer axially. In Philippine specimens, the spiral cords on *T. crispa* are generally narrower, making the intercord areas seem larger on the body whorl; in *T. dollyae* the cords are essentially contiguous to each other throughout the body whorl and siphonal canal. Another difference between the two species is that the gap between the subsutural area and the sinus cord is usually gently sloping in *T. crispa*, and sharply terraced in *T. dollyae*. In most specimens of *T. dollyae*, the peripheral cord is the most prominent spiral cord, while in Philippine specimens of *T. crispa*

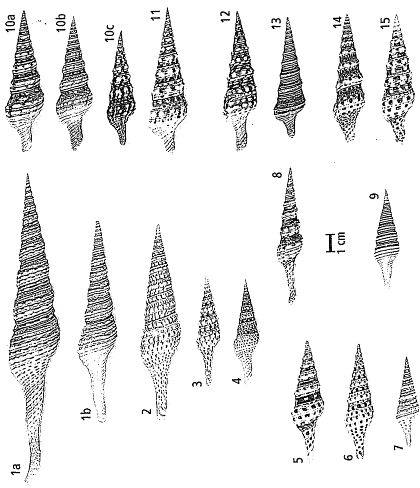

Plate I. Fifteen distinctive forms found in the Philippines of the genus *Turris*. 1. *Turris crispa crispa* (1A, regular form; 1B, unspotted form). 2. *Turris dollyae*. 3. *Turris normandavidsoni*. 4. *Turris yeddoensis*. 5. *Turris babylonia* (typical, "babylon" form). 6. "Niniveh" form (*Turris babylonia*?). 7. "Sulu Sea" form (*Turris babylonia*?). 8. *Turris garnonsii*. 9. *Turris annulata*. 10. *Turris nadaensis* (10A, typical form; 10B, lighter broad variety; 10C, exceptionally dark form). 11. "Angular" form (*Turris nadaensis* variety?). 12. *Turris undosa*. 13. *Turris cryptorrhaphe*. 14. *Turris spectabilis*. 15. *Turris totiphyllis*. The size bar is 1 cm.

all primary cords on the body whorl have similar size.

Nomenclature. This new species is named for Dolores (Dolly) Hernandez, to honor her outstanding contributions to Philippine science education. Before she obtained her graduate training, Dolly Hernandez was the author's teacher in his first chemistry and biology courses. I want to express my deep personal gratitude to Dolly Hernandez for steering me towards a scientific career combining chemistry and biology.

Types. The holotype will be deposited in the Philippine National Museum; paratypes will be deposited in the British Museum of Natural History, in the American Museum of Natural History and the U.S. National Museum. Other paratypes are in the Olivera collection (see Appendix for measurements of individual types).

Turris normandavidsoni, new species

(Plate I, Specimen 3; Plate III)

Description. The shell is 58-85 mm in length, narrowly fusiform with a long siphonal canal, and covered with spiral cords decorated with regularly spaced blackish-brown maculations. There are two distinctly brownish zones in the body whorl, just anterior to the subsutural cord and between the body whorl and the siphonal canal. Spire angle of *T. normandavidsoni* is 20-22°, and the ratio of aperture plus siphonal canal to total length is 0.44. Next to the upper suture is a broad, complex subsutural cord with large black or dark brown maculations, followed by an excavated light brown area between the subsutural cord and the terraced sinus cord. On the larger spire whorls, two additional spiral cords are visible. There are 6-7 broad spiral cords on the body whorl and base, and an additional 6-7 spiral cords on the canal, with intermediate spiral cords in some specimens. The spiral cord next to the large peripheral cord is characteristically the smallest of the four primary cords on the body whorl.

Discussion. *T. normandavidsoni* is a species superficially intermediate between *T. babylonia* and *T. crispa*. Very few specimens were known in Philippine collections until quite recently, and these were invariably confused with one of those two species. Powell figured what is probably a specimen of *T. normandavidsoni* in his 1964 monograph (Plate 181, Number 5) and assigned it to *T. babylonia* (although he recognized that it might be distinct). In Hinton's Seashells from New Guinea and the Central Indo-Pacific (Hinton 1972), a specimen of *T. normandavidsoni* is figured as *T. crispa* (Plate 30, Specimen 1). The availability of many more Philippine specimens, particularly from the Sogod, Cebu area has made it easier to define this variable species, which has either been regarded by collectors as a small *T. crispa* form or an exceptionally thin *T. babylonia*. Shell pattern can be variable, from thin axial markings in the body whorl (see paratype 1) to rectangular spiral maculations (see paratype 5, Plate III).

Comparison. *T. normandavidsoni* is very similar to, and has been confused with *T. crispa*, *T. garnonsii*, *T. dollyae* and the narrow "niniveh" form of *T. babylonia* (see below). *T. normandavidsoni* is generally smaller than either *T. crispa* or *T. dollyae*. The species is distinguished by the combination of the broad, strongly maculated subsutural cord complex and the sharply terraced sinus cord, making the zone between the subsutural cord and the sinus seem deeply excavated. In most Philippine specimens this region is colored uniformly olive brown or very light brown, often darker where the black maculations on the subsutural cord occur. In addition, most Philippine specimens have an olive brown color between cords at the base of the body whorl. However, some specimens from Olango Island, Cebu are lighter in color and smaller, while the few specimens from Luzon appear to be larger and darker, with the light brown zone greatly expanded in some specimens (Plate III, paratype 4).

The species is very variable in shell pattern (see Plate III). It is probably most closely related to *T. dollyae*, and like that species, in many Philippine specimens the maculations tend to have an axial rather than a spiral orientation. However, *T. normandavidsoni* is smaller in size with proportionally larger subsutural maculations.

The species range will extend at least to New Guinea and Fiji. Museum collections with specimens labeled *Turris crispa* from Fiji appear to be likely assignable to *T. normandavidsoni*.

Nomenclature. This species is named for Professor Norman Davidson, Caltech, Pasadena,

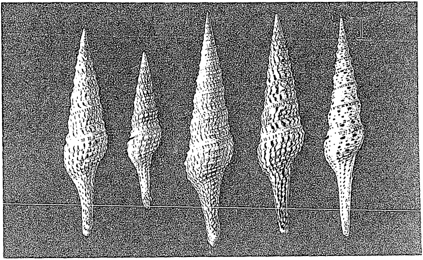

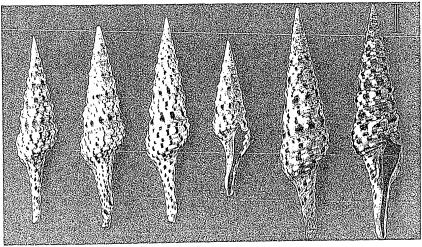

California, a wonderfully creative scientist and great mentor. It was the lucky break of my life to have become a graduate student in his laboratory.

Types. The holotype of *T. normandavidsoni* as well as most paratypes were collected from Sogod, Cebu by fishermen trawling in waters from 50 to 100 meters. Two paratypes were collected by hookah off Olango Island, Cebu, Philippines. The holotype and several paratypes are illustrated in Plate III. The holotype will be deposited in the Philippine National Museum, and paratypes will be deposited at the British Museum and the U.S. National Museum.

Turris babylonia (Linnaeus, 1758)

(Plate 1, Specimen 5; Plate IV)

The type species of the genus, *T. babylonia*, was originally described by Linnaeus. This remains one of the more problematic species in terms of taxonomy. In the Philippines, at least three distinct forms have been assigned by most workers to *T. babylonia*. There is a thick, sturdy form with a heavy shell, rather broad in outline. We will refer to this as the "babylon" form. Even within the typical form however, there is considerable variation, shown in Plate IV. The subsutural region and the base of the last whorl may be white, brownish-purplish or brownish-black. Plate IV illustrates an unusually melanistic Philippine specimen.

"Niniveh" form (*Turris babylonia*?) (Plate I, Specimen 6; Plate IV). A second form generally assigned to *T. babylonia*, which we refer to as the "niniveh" form, is proportionally narrower in outline and usually smaller than the typical *T. babylonia*. In addition, the shell is thinner and lighter. In the Philippines, specimens of the "niniveh" form have shells with a shiny surface, in contrast to the generally matte texture of the "babylon" form. The author has examined a large series of Philippine specimens and found that these two forms are always clearly separable.

Thus, based on Philippine specimens alone, the two forms would appear to be separable species. However, I have taken a conservative approach and have not designated the "niniveh" form as a separate species in this paper for two reasons. First, a casual examination of non-Philippine specimens reveals that the "niniveh" form tends to have a thicker and heavier shell in other localities, particularly the Moluccas. Thus, the possibility that intermediate forms will be found outside the Philippines between the "babylon" and "niniveh" forms needs to be thoroughly examined. I suspect that a wider geographic survey of the two forms will still prove them to be distinct, but this tentative judgement needs to be documented by a larger number of specimens from localities outside the Philippines. In addition, a number of names have been applied to the *babylonia* complex, and a careful examination of types is essential to determine which form each name refers to.

The comments of Powell in his monograph indicated that one potential name for the "niniveh" form might be *Turris raffrayi* (Tapparone-Canefri 1878). However, the summary statement in the original description of *Pleurotoma raffrayi* by Tapparone-Canefri is: "It has a strong resemblance to other Pleurotomas of the same group, specifically with *Pleurotoma spectabile* (= *Turris spectabilis*), but the canal is proportionally shorter, the shell larger and the spots have a different quality." The figure of the species which accompanied the original description shows a pattern of flammules on the body whorl (most similar to *T. nadaensis*, see below) rather than dots on the spiral cords. Together, the comparison to *T. spectabilis*, the comment that *P. raffrayi* has a shorter canal than *T. spectabilis* and the axial flammules shown in the original figure all make it unlikely that *P. raffrayi* is an appropriate name for this "niniveh" form.

In the Philippines the "babylon" and "niniveh" forms show characteristically different types of variants. In typical *T. babylonia*, there is a tendency for darker pigmentation in the subsutural and base regions. In some exceptional specimens, the entire shell is colored light brown or even black (see Plate IV). In the "niniveh" form, variants that have reduced maculations on the first few primary spirals of the body whorl, as well as color variants with lighter brown, instead of black maculations are found (Plate IV).

"Sulu Sea" form (*Turris babylonia*?) (Plate I, Specimen 7; Plate IV). There are a series of specimens from the Sulu Sea that are generally smaller with much thinner and more delicate shells

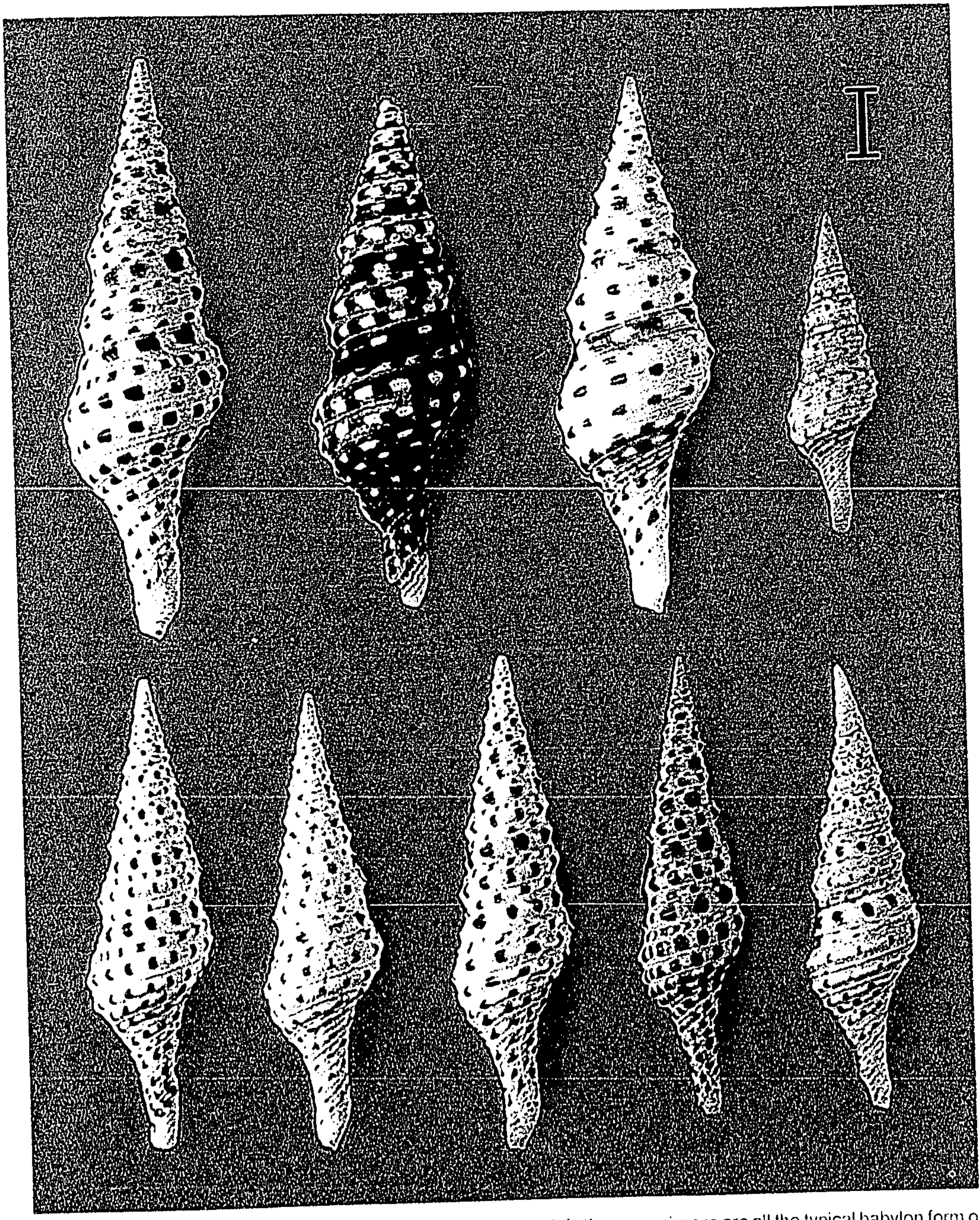

Plate IV. Three forms traditionally assigned to *Turris babylonia*. Top row, left three specimens are all the typical babylon form of *Turris babylonia*. The second specimen was collected by trawlers from off Cagayan de Oro, Northern Mindinao. The two other specimens are from unknown localities in the Philippines. Top row, rightmost, shows the "Sulu Sea form" (*T. babylonia* variety?). This form is noticeably thinner than typical *Turris babylonia*, or the niniveh form. Bottom row, various specimens of the narrow "niniveh form." Localities of specimens from top to bottom: Mindoro Island, Philippines, Dipolog, North Mindinao, Philippines; Olango, Cebu Island, Philippines; Cebu Island, Philippines. Sulu Sea, Philippines. Rightmost two specimens show extremes in coloration. The size bar is 1 cm.

(see Plate I, Specimen 7 and Plate IV). This is a variable form, most specimens lightly colored with less distinct maculations (in some specimens, coloration of maculations is the purplish-brown found in *Turris crispa*, instead of the black coloration of both forms assigned to *T. babylonia* above). Powell illustrated this form from Papua New Guinea, but some Philippine specimens are even lighter. The monograph on Australian gastropods by Wilson (Wilson et al. 1994) illustrates similar specimens from deep waters off West Australia, identified as *T. crispa* (see Plate 39, figs. 5A and B). If this is a distinct species, it is apparently present in West Australia while both "babylon" and "niniveh" forms have not been reported from there.

The "niniveh" form is easily confused with *T. normandavidsoni*. However, the region from the subsutural cord to the sinus cord is sharply terraced in *T. normandavidsoni*. In general, *T. normandavisoni* is narrower in outline than all three *babylonia* (?) forms described above.

Turris pagasa, new species

(Plate I, Specimen 4; Plate V)

Description. The shell is moderately large (61 to 98 mm), narrowly fusiform, with a turret-like spire and a moderately long siphonal canal. The protoconch is small with two smooth whorls. Adult shells have 13-16 teloconch whorls. The spire angle is 25° and ratio of aperture to total length is 0.42-0.46. Spire whorls have a broad subsutural cord that comes to a sharp apex, maculated with dark brown blotches. The sinus cord is narrow, raised and square in outline with smaller dark brown maculations. A striking characteristic is the presence of numerous thin, raised, scaly axial lamellae between the subsutural and sinus cords extending to more anterior areas in some specimens. There is an unmaculated white gap between the sinus cord and larger peripheral cord. In the larger spire whorls, two smaller spiral cords are present below the larger peripheral cord, all with small squarish dark brown maculations. On the body whorl, 3 or 4 spiral cords are found at the periphery, followed by a gap where the future suture will form, with an additional 3 to 4 cords to the base and 3-4 primary cords on the canal with weaker secondary cords between them. All have fine squarish dark brown maculations, more-or-less equal in size (in contrast, in the spire whorls, the peripheral cord is noticeably stronger with larger maculations). The major cords on the body whorl have between 24-36 square maculations per spiral cord. The siphonal canal is noticeably curved, with a false umbilicus in larger specimens.

Discussion. This new form was unknown in Philippine material until recently. The shell is superficially similar to *T. crispa* and *T. babylonia* but it is probably most closely related to *T. crispa yeddoensis* from Japanese waters and *T. crispa intricata* from Hawaii. However, since it occurs in the same localities as *T. crispa crispa*, it cannot be considered a geographic subspecies of *T. crispa*, and is treated here as a distinct species.

T. pagasa has not previously been figured or recorded from the Philippines, and the few specimens known have been trawled or collected by gill nets in the central and southern Philippines.

Comparison. The shell of *T. pagasa* is much heavier than most Philippine *Turris*, reminiscent of dense white porcelain. The shell markings are finer and more square-shaped than in most *Turris* species. Since the sinus cord is about midway between the subsutural and peripheral cord, the noticeable white gap between the sinus and peripheral cords is characteristic of the species. In *Turris pagasa*, the black maculations on the sinus cord are set deeper than in most *Turris*, giving the sinus cord an irregular weakly gemmulate character.

T. pagasa differs from *T. crispa yeddoensis* in that the shell is thicker and has a more turreted outline, the maculations are generally less dense, particularly in the canal region where *T. pagasa* specimens tend to be pure white, and the canal is distinctly curved instead of straight as in *T. crispa yeddoensis*. The subsutural cords differ in structure and maculations. Many specimens of *T. crispa yeddoensis* tend to a grayish background cast; *T. pagasa* generally has a pure white background. Specimens of *T. pagasa* and two Japanese varieties, both assigned to *T. crispa yeddoensis* are compared in Plate V.

Nomenclature. The Filipino word "pagasa" means hope. This name seems appropriate for a species discovered in the closing days of the

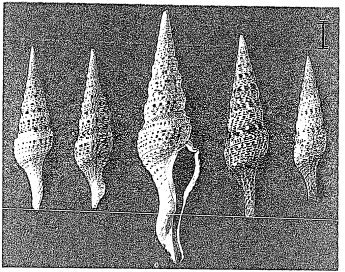

Plate V. *Turris pagasa*, new species, compared to Japanese specimens of *Turris crispa yeddoensis*. The three specimens on the left are *T pagasa*. From left to right: holotype, from Pamilacan Is., Bohol (gill nets 100 to 150 m); paratype #1, off Dipolog, Northern Mindinao, Philippines (collected by gill nets, 80 to 150 m); paratype #2 from Bogo, Cebu Island, Philippines (trawled, 50 to 100 m). The two specimens on the right are *Turris crispa yeddoensis*. The darker specimen is labeled "Tosa, Japan, 30 to 50 fathoms, March 1960, ex. M. Azuma collection." The rightmost specimen is labeled "Mada-cho, Wakayama Prefecture, Japan." The size bar is 1 cm.

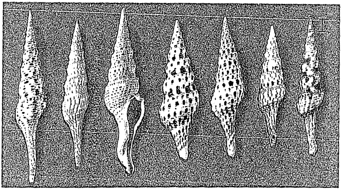

Plate VI. The *Turris babylonia/Turris crispa* complex. Specimens have been chosen that are approximately the same size, to emphasize differences in shell morphology between the seven species of Clade I with longer canals. (The comparative size of mature specimens was illustrated in Plate I.) From left to right: 1) *Turris crispa*; 2) *Turris dollyae*, 3) *Turris pagasa*; 4) *Turris babylonia*; 5) niniveh form (*T babylonia*?); 6) *Turris normandavidsoni*; 7) *Turris garnonsii*. Thus, most specimens of *Turris crispa* are much larger than specimens of *Turris garnonsii*, but a smaller-than-average specimen of the former and the largest specimen of the latter available are shown in this figure. The size bar is 1 cm

millennium, representing the hope that in the new millennium, a new generation of Philippine scientists will devote themselves to the study and conservation of our unique and threatened fauna, both terrestrial and marine.

Types. The holotype will be deposited in the Philippine National Museum.

Turris garnonsii (Reeve, 1843)

(Plate I, Specimen 8 and Plate VI, rightmost specimen)

The "narrow form" of this species (Powell 1964) was previously known from just a few specimens in Philippine collections, but has now been available in fair quantities from both gill-net and hookah collecting. It is very distinctive and readily identified by its extremely narrow outline combined with a sharply constricted sutural region. In addition, the broad maculations of the subsutural region extend all the way from the suture to the sinus cord. Philippine specimens of *T. garnonsii* are not readily confused with any other *Turris* species. Both Powell (1964) and Springsteen and Leobrera (1986) illustrated typical Philippine specimens of this species. Specimens of *T. garnonsii* have been collected in Balicasag Island, Bohol by gill nets in 100-150 m and in the area around Olango Island between Cebu and Bohol by hookah at depths of about 50 m.

A few specimens of *T. garnonsii* with very short canals are present in old Philippine collections, but the collection locality has not been established. These are very similar to, but distinctly narrower than *T. totiphyllis* (see below).

Species comparison

The six species described above, and one of the distinct forms are illustrated in Plate VI. Typical specimens of each, selected to be comparable in size, are illustrated to make differences in shell proportion and pattern easier to compare. These are the species in Clade I with longer canals. The two remaining species have much shorter canals, more similar in proportion to *Xenoturris* (as noted, *T. garnonsii* also has a short-canal form). However, in all other aspects of their shell morphology, these clearly belong in the Clade I *Turris* group.

Turris spectabilis (Reeve, 1843)

(Plate I, Specimen 14; Plate VII)

T. spectabilis is a striking species, and is one of the two species in Clade I with a relatively short canal and long spire. The massive peripheral cord with its broad black and white maculations, and the brown coloration of each whorl posterior to the peripheral cord and in the base region are distinctive characteristics. Although there is considerable variation within the species in the coloration and distribution of brown and white areas, upon close scrutiny, the species can only be confused with *T. totiphyllis* (see below). The diagnostic differences are outlined in the discussion of that species. The original type in the Cuming collection was reported from Ticao Island but this could not be located in the British Museum (Powell 1964); other specimens in the Cuming collection figured by Reeve are labeled "Island of Cebu," which is still a locality where many Philippine specimens have been collected in recent years.

Turris totiphyllis, new species

(Plate I, Specimen 15; Plate VII)

Description. The shell is moderately large, 67 to 91 mm, with a high spire and relatively short siphonal canal. The spire angle is 24-26°, and ratio of aperture plus siphonal canal to total length is 0.38. Adult shell has 11-13 whorls. Each whorl has a subsutural cord region with unusually large black or blackish-brown maculations, followed by a continuous lighter brown zone, and a flat siphonal cord, with alternating blackish-brown or brown maculations, much reduced and almost white in some specimens. On the larger spiral whorls, in addition to the large, broad peripheral cord, two additional spiral cords, also maculated in black or brownish-black are visible. The body whorl has 4-5 spiral cords on a white background, and at the boundary with the siphonal canal is a uniformly colored black or brownish-black zone with 2-4 spiral cords. The siphonal canal is white or much lighter brown with three to four primary cords, and weaker cords interspersed.

Discussion. Shells of *T. totiphyllis* have been confused with *T. spectabilis*; both have a generally

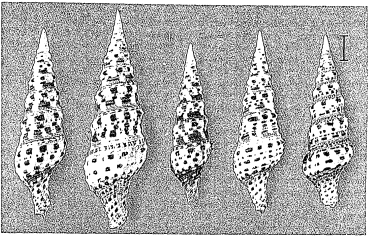

Plate VII. *Turris totiphyllis*, new species, compared to *Turris spectabilis*. All of the specimens shown are *Turris totiphyllis*, except the specimen on the extreme right. From left to right, holotype (collected between Olongo Island, Cebu and northern Bohol, by hookah 20 to 60 m); paratype #1 (same locality); paratype #2 (Balicasag, Bohol Island, collected by gill nets 50 to 150 m). The two rightmost specimens are *Turris totiphyllis* and *Turris spectabilis*, both collected between Olango Island, Cebu and northern Bohol. This pair illustrates the differences in the slit region of these two species; note the two threads that border the slit in *Turris spectabilis*, and the single sinus rib in *Turris totiphyllis* (see text). The size bar is 1 cm.

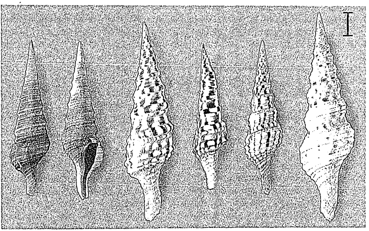

Plate VIII. Clade II *Turris* species. Left to right: *Turris cryptorrhaphe* (Marinduque Island, Philippines); *Turris cryptorrhaphe* (Olango Island, Cebu, collected by hookah 20 to 60 m); *Turris undosa* (Balicasag, Bohol Island, Philippines, gill nets 50 to 150 m); *Turris undosa* (Olango Island, Cebu, hookah between 20 to 60 m); *Turris nadaensis* (Olongo Island, Cebu, hookah 20 to 60 m); *Turris nadaensis* (Sogod, Cebu Island, trawled 50 to 100 m). The size bar is 1 cm.

elongated spire, short canal and share similar shell patterns. However, although easily separable from most Philippine specimens of *T. garnonsii* (the latter much more slender with a proportionately longer canal), *T. totiphyllis* is most similar to the *T. garnonsii* variety with a short canal.

Comparison. The shell pattern of *T. totiphyllis* generally resembles *T. babylonia* and *T. spectabilis* in that the primary cords have black maculations on a generally white (sometimes grayish) background. The body whorl has two brown-colored zones, one between the suture and the sinus cord, and the second at the base (i.e., the border between the body whorl and the canal. The color pattern of *T. spectabilis* is similarly organized (a pattern also found in certain morphological variants of *T. babylonia*). Most specimens of *T. babylonia* do not have these prominent dark brown areas characteristic of *T. spectabilis* and *T. totiphyllis* and have a proportionally longer and very straight canal, and a single smooth subsutural cord. *T. spectabilis* and *T. totiphyllis* are easily confused, but several differences are quite diagnostic. The sinus cord of *T. spectabilis* is typically not congruent with the posterior sinus, which is unusually wide for *Turris* species. In the body whorl of the mature *T. spectabilis*, a thin, raised black and white thread is aligned with the posterior edge of the sinus, with a second parallel thread slightly anterior, and not overlapping with the sinus. These threads define where the sinus is located, and are both posterior to the major peripheral cord. The presence of the two threads between the subsutural cord and the primary peripheral cord is highly characteristic of the mature body whorl of Philippine specimens of *Turris spectabilis*. In *T. totiphyllis*, the sinus cord is typically steeply terraced from the subsutural area. A second diagnostic difference is that in *T. spectabilis*, the subsutural cord may be reduced or minor, or moderately expanded (two cords can be fused); this is a variable characteristic. In *T. totiphyllis*, the subsutural cord area is massive and broadly maculated even in early spire whorls. The proportion of brown banding and white color on the whorls is also different; the brown zones are much more dominant in *T. spectabilis* than in *T. totiphyllis*, where in the subsutural area in particular, the brown zone is sometimes discontinuous (as in *T. garnonsii*). The new species can be distinguished from the short-canal variety of *T. garnonsii* in its much broader outline, and the presence of a continuous brown zone between the maculations in the subsutural area and the sinus cord.

Nomenclature. This new species is named for Toti and Phyllis Zaballero, for all the good times together.

Types. The holotype will be deposited in the Philippine National Museum, and paratypes have been deposited at the British Museum of Natural History and the U.S. National Museum. Other paratypes are in the Olivera collection. The holotype and most paratypes were collected in the central Philippines in the Cebu-Bohol area. One paratype is a specimen from an old collection, collected before 1970 from an unspecified Philippine locality. Recently collected specimens were found by hookah divers at night between 30-80 meters, and by gill nets in even deeper water.

Clade II: The Purple-mouthed *Turris*

The Clade II species have certain common features, most characteristic is the purplish coloration of the aperture, often extending to the canal. In addition, the canal is relatively short. Finally, when present, the axial markings are qualitatively different from the spiral cord maculations of Clade I species, in that they are not primarily located on spiral cords but are continuous broad streaks. At least three Philippine species are included in this group, *T. cryptorrhaphe*, *T. undosa* and *T. nadaensis*. More deep water material may reveal that at least one form tentatively assigned here to *T. nadaensis* may be a distinct species. This clade may be widespread in Indian Ocean localities as well, since the rare *T. tanyspira* (Kilburn, 1975) from Mozambique is almost certainly a member of this species clade.

Turris cryptorrhaphe (Sowerby, 1825)

(Plate I, Specimen 13; Plate VII)

T. cryptorrhaphe is a very distinctive species; the uniform blackish-brown color, lack of maculations and purplish aperture distinguish this form from any other *Turris* species. One characteristic of many *T. cryptorrhaphe* specimens is the presence of a darker thread at the apex of several primary cords. *T. cryptorrhaphe* was previously rare, but it is now collected in fair numbers in the Cebu-Bohol area, in ~30-60 m by hookah. Most specimens from this locality have multiple growth scars.

Superficially, *T. cryptorrhaphe* seems very distinctive from *T. undosa* and *T. nadaensis*, since the two latter species both have dark brown maculations. However, the three species may be more closely related than the shell patterns would suggest. The characteristic presence of a dark brown thread at the apex of spiral cords in specimens of *T. cryptorrhaphe* is also found in the spiral cords of the body whorl of many specimens of *T. nadaensis* and more rarely in *T. undosa*. This feature has not been observed in other *Turris* species.

Turris undosa **(Lamarck, 1816)**

(Plate I, Specimen 12; Plate VIII)

T. undosa is a distinctive species closely similar to *T. nadaensis*. The two species have been confused by many authors. However, *T. undosa* can be distinguished by its prominent, massive subsutural cord. As a result, this species does not appear at all constricted in the sutural region giving the spire a straight outline in contrast to the more rounded whorls of *T. nadaensis*. Powell (1964) figured *T. undosa* in Plate 181, Specimen 20 of his 1964 monograph, but in Plate 25, figs. 9 and 10, the species illustrated as *T. undosa* are in fact *T. nadaensis*. Springsteen and Leobrera (1986) illustrate the two species correctly. *T. undosa* is relatively constant in its shell morphology and pattern, in contrast to *T. nadaensis*, which is much more variable.

Turris nadaensis **(Azuma, 1973)**

(Plate I, Specimen 10; Plate VIII)

T. nadaensis, though relatively recently recognized, appears to be relatively widespread in the central and southern Philippines. However, it is variable. The majority of specimens collected to date are from the Cebu-Bohol area and there is considerable variation in how light or dark the maculations are (see Plate I, specimens 10a,b,c and Plate VIII).

T. nadaensis can be confused with *T. undosa* because both have a purple aperture and brownish-black maculations. In general, the dark markings on *T. nadaensis* are narrower and less prominent than those on *T. undosa*, extending from the peripheral cord to the suture. As is discussed under *T. undosa* above, one diagnostic difference is that the massive, raised subsutural cord region of *T. undosa* is absent in *T. nadaensis*, giving the latter much more rounded whorls. Specimens of *T. undosa* are uniformly maculated in all whorls, but in *T. nadaensis*, there is a tendency for the last whorl in mature specimens to be much lighter with more sparse maculations (see Plate I, Specimen 10B and Plate VIII, rightmost specimen). There is also considerable variation from locality to locality in how dark specimens are. The range of variations is shown in Plate I, specimens 10a, b, c and in Plate VI. The violet color of the canal and the aperture also varies considerably from one specimen to another. In immature specimens, a sharply delineated region is either light purplish or dark violet from the base all through the siphonal canal. In mature specimens, this purplish region can be much reduced and in some specimens is only obvious when seen from the aperture. In contrast, in *T. undosa*, the canal region is always purple, even in mature specimens. Mature specimens of *T. nadaensis* often have a false umbilicus. As noted above, many specimens have a dark thread at the apex of some of the spiral cords, particularly towards the base (Plate VIII, specimen at right) but this is not a consistent characteristic.

One exceptional specimen, collected in Balut Island, is quite distinct from typical Philippine *T. nadaensis* specimens in its broader outline and thicker canal (Plate I, Specimen 10b). The maculations on the last whorl are absent, though earlier whorls seem to have a similar pattern to typical *T. nadaensis*. The spiral cords are obsolete in the specimens illustrated, but dark brown threads are present. The Balut Island specimen is the closest Philippine example to an unusual specimen of *T. nadaensis* illustrated by Wilson (1994) from Queensland, Australia (Plate 39, Specimen 15) which was identified as *T. undosa*. The illustration of Tapparone-Canefri (Tapparone-Canefri 1878) of *T. raffrayi*, which was collected in New Guinea, seems closer to the Australian specimen of *T. nadaensis* than to any other *Turris* species known to the author. If this assignment were indeed the correct one, and could be definitively confirmed, then the name *T. raffrayi* would have priority over *T. nadaensis*.

"Angular" form (*Turris nadaensis* variety?) (Plate I, Specimen 11). There is another distinctive variety collected in the Philippines known from a single specimen which is tentatively assigned to *T. nadaensis*. More specimens may show that this is a different species (see Plate I, Specimen 11). This form has a greater similarity to *T. undosa* in shell pattern than other forms of *T. nadaensis*, but does not have the massive subsutural cord. The whorls are much more angular than *T. nadaensis* and the peripheral cord is proportionally larger and sharper in outline than in specimens of *T. undosa* and *T. nadaensis*. A similar specimen was figured by Hinton (1972) from Papua New Guinea as *T. undosa* (Plate 30, Specimen 6), suggesting that this form may have a widespread distribution in the Indo-Pacific, and is not a localized variant of *T. nadaensis*. However, more specimens are needed for the taxonomic status of this form to be clarified.

Clade III: the *Annulaturris* clade

Turris annulata (Reeve, 1843)

(Plate I, Specimen 9; Plate X)

So far this species is rare with very few Philippine specimens known. No specimens were illustrated by Springsteen and Leobrera (1986) in their comprehensive illustration of Philippine turrids. Philippine specimens are similar to the specimen figured as *T. annulata* by Powell (1964) from Tosa, Japan. The only other recent figure of any specimen assigned to this species is found in the catalog of the Ninomiya collection (Horikoshi, 1989) where a specimen from Phuket Island, Thailand is illustrated as *T. annulata* (Plate 32, Figure 1). The latter conforms to what Powell (1964) refers to as the "typical form," and it clearly differs in a number of respects from Philippine and Japanese specimens. Powell (1964) suggested that the two forms might be separable at the subspecific level.

T. annulata appears from shell morphology to be highly divergent from the two clades described above. One notable feature of the two specimens examined is that although one has relatively smooth cords throughout, in the specimen figured the sinus cord is weakly gemmulate. Furthermore, Powell indicated that the sinus cord was not the peripheral cord, but this is much more ambiguous in Philippine specimens. Indeed, in the specimen figured, the sinus cord appears to be peripheral, a feature which makes assignment to the genus *Turris* even more uncertain. The apparent gemmulate nature of the sinus cord was figured by Tyron (1884), but not present in the specimens examined by Powell (1964); this may be a variable feature of the species.

The Genus *Turris*: Monophyletic or Polyphyletic?

In the genus *Turris*, as defined by Powell (1964, 1967), the fifteen distinct forms found in Philippine waters appear to fall naturally into three clades. In this section, we address whether the three clades form a natural taxonomic group at the generic level. A consideration of the shell morphology is suggestive that this might not be the case. The only known Philippine species in Clade III, the broader form of *Turris annulata*, seems greatly diverged from the species in the other two clades. In proposing the subgenus *Annulaturris*, Powell noted that the radular morphology of *Turris amicta*, the other species assigned to the subgenus, was different from that of other species in the genus; most *Turris* species do not have the broad central tooth reported to be present in *T. amicta*. This was apparently the major rationale for separating the *T. annulata*/*T. amicta* clade into a subgenus. The radula of *T. annulata* has not yet been described.

In this author's best judgment, *T. annulata* is probably only distantly related to other Philippine species included in the genus *Turris*. The tendency towards a weakly gemmulate sinus cord, and the fact that the sinus and peripheral cord are essentially equivalent in size in Philippine specimens (instead of being distinctly smaller and displaced at a position clearly posterior to the periphery of each whorl) are characteristics consistent with this suggestion. In the following sections, we present possible links between some specific *Gemmula*/*Lophiotoma* species and the

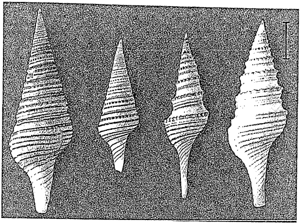

Plate IX. *Gemmula lululimi*, new species. The two specimens on the left are *Gemmula lululimi*, which are compared to *Gemmula speciosa*, the two specimens on the right. Far left, holotype, Balut Island, southern Philippines (gill nets, 50 to 150 m); second from left, paratype 1, Pamilacan Is., off Panglao, Bohol, Philippines (gill nets, 50 to 150 m). Note the generally similar organization of the spiral ribs, and the striking difference in the shell outline of the two species. The size bar is 1 cm.

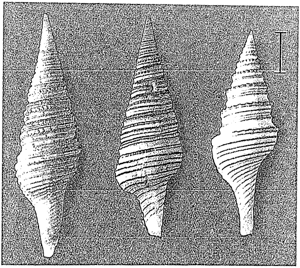

Plate X. A comparison of *Turris annulata* (far left), *Gemmula lululimi* (middle) and *Gemmula speciosa* (right). Note the similar shell outline of *Turris annulata* and *Gemmula lululimi* - in both cases, the sinus cord is noticeably gemmulate (while other spinal cords are not), a feature particularly obvious in the earlier whorls of the spire. The size bar is 1 cm.

three *Turris* species clades. Clearly, the taxonomy of other Turrinae will need to be more carefully examined by a variety of criteria before an informed decision with regard to the correct taxonomic assignment of *T. annulata* and other clades in *Turris* can be made.

From shell morphology, the Clades I and II *Turris* species appear more closely related to each other than to *T. annulata*. It is possible that all species in the two clades evolved from a common ancestor sometime before the Pliocene (no fossils related to Clades I and II species appear earlier than the Pliocene - from Powell's 1964 comments, the Miocene fossils assigned to *Turris* from Australia are likely related to *T. annulata*). In contrast, other Turrinae (such as *Gemmula*) have a robust fossil record much further back in the Tertiary. The biogeography is also consistent with a relatively recent origin for Clade I and II species. These groups are strictly Indo-Pacific, with the greatest density of species present in the Indo-Pacific arc from the Philippines to New Guinea. In contrast, there are *Gemmula* species in the Atlantic and Eastern Pacific, where *Turris* is absent.

What are the closest relatives of Clade I and Clade II *Turris* species? There are two hypotheses that can be considered *a priori*. The two clades (I and II) may have diverged from all other Turrinae, an implication of including them in the same genus. However, it is possible that even after excluding the Clade III species from *Turris*, the group may still prove not to be monophyletic.

We compare species from other groups in Turrinae with Clade I and Clade II *Turris* species. These comparisons lead to a useful (and experimentally testable) question: are Clade I and Clade II *Turris* species more closely related to each other than to any other Turrinae? If the answer were affirmative, then *Turris* (with *Annulaturris* removed) would be a monophyletic group, and assignment of both species clades to the genus *Turris* would accurately reflect the evolutionary history of the group. On the other hand, based on shell morphology alone, we present one specific alternative possibility: that Clade I species may be more closely related to certain *Lophiotoma* spp., and Clade II species to one branch of the genus *Gemmula* than they are to each other. If this were borne out by further analysis, it would suggest that the present classification of the Turrinae does not accurately reflect true phylogenetic relationships. It is useful to frame these alternatives since in principle, future molecular, anatomical and biochemical work could provide data relevant to these issues, if such work were focused on the appropriate species in the Turrinae.

Specific evolutionary hypotheses

The purpose of this section is to consider the broader phylogeny of species in the genus *Turris*. As indicated in the Discussion above, the three clades, comprising all species in the genus *Turris* (as defined by Powell) may or may not comprise a monophyletic group. Here, alternative hypotheses, each with its own set of experimental predications, are developed. These hypotheses are based on shell morphology alone, since soft tissues were not generally available for analysis. The specific alternatives based on shell characters are intended to provide an incentive for carrying out further studies on the key species discussed.

We start with two general themes: the first, that the three clades presently assigned to *Turris* arose out of some *Gemmula/Lophiotoma/Polystira*-like ancestor(s), seems a reasonable assumption on the basis of the fossil record, biogeography and shell morphology. A second assumption is that a morphological transformation, which we will call the G-T transformation (for *Gemmula-Turris*), played a role in the morphological conversion of shells of *Turris* species from their ancestral form. We present some compelling evidence that such a morphological transformation can occur, perhaps relatively rapidly.

The basis for postulating the G-T transformation is the discovery of an unusual species, which is problematic to assign at the generic level because of its unique characteristics. This taxon, recently collected in deep waters in the central and southern Philippines is closely allied to *Gemmula speciosa*, a well-known Indo-Pacific species, in every respect except one. Because of the position of the slit and the sinus cord, this form would not seem to be typical of species in the genus *Gemmula*, but could just as easily be assigned to the genus *Turris*. Nevertheless, the gemmulate nature of the sinus cord and all other aspects of shell morphology make this a *Gemmula*. The morphological change that it has undergone, when compared to *G. speciosa*, is the prototypic example of a G-T transformation.

Gemmula lululimi, new species

(Plates IX and X)

Description. The shell is 37-58 mm with 15-17 whorls. Spire angle is 25-27°. The spire is high, cone-shaped with a relatively sharp siphonal canal and the ratio of aperture and canal to total length is 0.39. Each spire whorl has three major spiral cords visible. The sinus cord is placed above the major peripheral cord, and is gemmulate, but continuously colored with a golden-brown as are all spiral cords. The strong cord above the sinus cord borders a region which is perpendicular to the axis of the spire, and which has a different texture from the rest of the shell, looking oily and colored light brown in some of the whorls. In addition to the three primary spiral cords visible on the spire whorls, four additional primary cords are present on the body whorl and five additional cords on the thicker section of the canal. The very tip of the canal is cordless and colored white. The species is entirely unique in the genus in that the sinus cord is neither peripheral nor prominently raised.

Discussion. This species has the same golden spiral cords and whitish background as *G. speciosa*. The number of spiral cords, the continuous coloration of the cords and the presence of gemmules on the sinus cord are all characteristics the two species have in common (see Plate IX). However, they have a dramatically different shell morphology. While the sinus cord is highly prominent on the periphery in *T. speciosa*, it has been transformed into a cord that is much less prominent and located posterior to the periphery in *G. lululimi*. This makes the shell morphology strikingly different. In effect, the shell of *G. lululimi* has changed from that of a typical *Gemmula* to one that is much more similar to *T. annulata* (see Plate X).

The shell morphology of *G. lululimi* is most unusual, and as pointed out above, the position of the sinus cord could have justified assignment to *Turris*. However, the striking similarity to *G. speciosa* is the overriding consideration in concluding that the species is a *Gemmula*. Not only are the nature of the spiral cords similar, but the texture of the white background has an unusual satin-like quality in both species, all suggesting a close relationship. The arrangement of the spiral cords varies between the two specimens of *G. lululimi*, variation well within the range observed for *G. speciosa*. Thus, both *G. lululimi* and *T. annulata* are unusual. Given the generic "rules" specified in Powell's monographs, they are rule-breakers that do not properly fit in either *Gemmula* or *Turris*. In effect, *T. annulata* and *G. lululimi* both have shell characters somewhat intermediate between *Gemmula* and *Turris*.

Types. The holotype was collected by gill nets from Balut Island (100-150 m). The only other known specimen of *G. lululimi* is a smaller specimen collected by gill nets from Pamilacan Island, Bohol, Philippines. The holotype and paratype are figured in Plate IX, and compared to *G. speciosa*.

Nomenclature. This species is named for my wife, Lourdes (Lulu) Lim Olivera.

A hypothesis for the origin of Clade I and Clade III *Turris* species

The G-T transformation described above for *G. speciosa* and *G. lululimi* strongly suggests that both species were derived from a common ancestor, and that the latter had undergone the G-T transformation while *Gemmula speciosa* did not (it seems reasonable to assume that the standard *Gemmula*-like state of *G. speciosa* was ancestral, given the much more ancient fossil record of *Gemmula*-like forms). We suggest that a similar transformation may have given rise to Clade I *Turris* species.

Two potential species to illustrate this hypothesis are shown in Plate XI. We suggest that *L. indica* and *T. pagasa* may have come from a common lineage and *T. pagasa* (or an ancestral species) had undergone a G-T transformation, while for *L. indica* such a morphological transformation did not occur. Thus, this is very similar to the *G. speciosa*/*G. lululimi* pair (although not quite as close). It is interesting to note that in both species, there is some variation in the relative strength of the sinus cord versus the next posterior cord (which is the

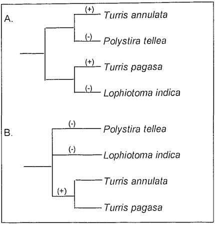

Figure 1. Two hypothetical alternative trees for Clade I and Clade III *Turris* species and other Turrinae. The tree at the bottom shows a scheme consistent with *Turris* being a monophyletic group, and Clade I species (such as *Turris pagasa*) sharing a common ancestor with *Turris annulata* and all other *Turris* species. On top is one specific alternative hypothesis for a polyphyletic origin of species presently assigned to the genus *Turris*. Clade I *Turris* species such as *Turris pagasa* are postulated to be more closely related to other Turrinae such as *Lophiotoma indica* than to *Turris annulata*. (In this specific hypothesis, *Turris annulata* is *Polystira*-like. Other trees consistent with a polyphyletic origin for species in *Turris* are feasible.) The (+) and (-) indicate whether the species is hypothesized to have undergone a G-T transformation (see text since the last common ancestral species.

peripheral cord in *T. pagasa*). In the two specimens of *L. indica* shown in Plate XI, the peripheral cord is definitely the major cord in the smaller specimen, but the next cord anterior to the sinus is relatively stronger in the larger specimen, a characteristic leaning towards *Turris*. We note that the structure of the cords is generally similar in the two species. Thus, a reasonable hypothesis for the origin of Clade I *Turris* species is that an ancestral form, from which *L. indica* may also be derived, had undergone a G-T transformation to give rise to an ancestral Clade I *Turris* species, possibly similar to *T. pagasa*. This scenario is really derived from the discovery of the *G. speciosa*/*G. lululimi* pair, which indicated that such a morphological transformation might occur with little change in other aspects of shell morphology.

If this hypothesis were true, and if *T. annulata* were indeed inappropriately grouped with the majority of *T.* species, then anatomical and molecular studies should show that there is a greater similarity between *L. indica* and Clade I *Turris* species such as *T. pagasa*, than between *T. annulata* and Clade I *Turris* species. This is a strong experimental prediction which is testable as shown in Specimen 1. In contrast, the present phylogeny requires that this experimental prediction be wrong.

If the prediction above is borne out, then the true affinities of *T. annulata* would need to be explored. In the opinion of the author, the shell structure seems more like some species of the American genus *Polystira* (in particular forms like *P. tellea*), and *T. annulata* may be derived from an ancestor like the fossil *Polyliria* (see Figure 1).

Phylogeny of Clade I and Clade II *Turris* species: two alternatives

A similar set of alternatives can also be laid out for Clade I and Clade II *Turris* species. These could all be a monophyletic group, with a common ancestor that diverged from other Turrinae. However, one plausible alternative is presented here.

This is based on the implicit assumption that the purple colored canal and aperture region in an important, conserved genetic character (which may or may not be true). Thus, if we examine other Turrinae for this characteristic, there is a form which was named *Gemmula concinna* (Dunker, 1856) which shows the unusual purplish color so characteristic of Clade II *Turris* species. Thus, an evolutionary scenario in which an ancestor that evolved the purplish coloration in the aperture/canal region underwent a G-T transformation (to yield Clade II *Turris* species such as *T. cryptorrhaphe*), while another descendant lineage did not undergo the morphological transformation, giving rise to the non-Turris *G concinna*. If this were the case, Clade I and Clade II *Turris* species may have arisen independently, both by G-T transformations of *Gemmula*/*Lophiotoma*-like ancestors, but from different lineages. It will be of interest to assess these alternative explanations using a combination of anatomical examination of soft tissues of the relevant

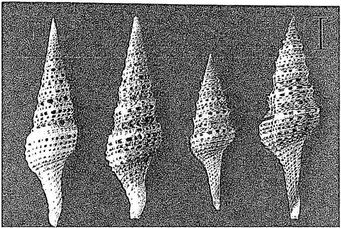

Plate XI. A comparison between *Turris pagasa* (left two specimens) and *Lophiotoma indica* (right two specimens). Note the generally similar maculations on the ribs of both shells, but the very different shape. As is discussed in the text, a G-T transformation would convert *Lophiotoma indica* into a form that looked similar to *Turris pagasa*. (It should be noted that the particular specimens of *Lophiotoma indica* shown in the figure are somewhat atypical, and some workers have assigned this form to *Lophiotoma accuta* instead of *Lophiotoma indica*.) The size bar is 1 cm.

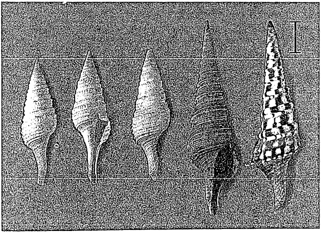

Plate XII. *Gemmula lisajoni*, renamed homony. The three specimens on the left are *Gemmula lisajoni*, followed by *Turris cryptorrhaphe* (second from right) and *Turris undosa* (far right). The characteristic purplish color of the canal and aperture is compared between these three forms. The three specimens of *Gemmula lisajoni*, numbered left to right specimens 1, 2 and 3, are all from Mactan Island, Cebu, Philippines, collected by gill nets (50 to 150 m). The size bar is 1 cm.

species, as well as by collecting the appropriate molecular data. We believe that this type of phylogenetic prediction is useful since the differentiating molecular experiments can be carried out given modern molecular methodology, and definitive judgements made between alternative hypotheses of the types proposed above.

The *Gemmula* with the purple canal shown in Plate XII (where it is compared to Clade II *Turris* species) has long been known by the name *G. concinna*. It has also been recognized that this name is preoccupied, which both Powell (1964) and Springsteen and Leobrera (1986) commented on. As Powell stated, "Nothing exactly matching Dunker's *concinna* is known to the writer, so this preoccupied species is left unnamed until it is rediscovered from a definite locality. A specimen from the Andaman Islands in the United States National Museum, attributed to *concinna* lacks the overall brown and violet-stained anterior end and is in fact inseparable from the South African *gilchristi*." A definite locality for the species was rediscovered when specimens were found using gill nets off Mactan Island in the Philippines, and one such specimen was in fact figured by Springsteen and Leobrera (1986) (who noted that their assignment of *G. concinna* to this form was not valid).

Since this very distinctive species is apparently without a valid name, it is illustrated and named here.

Gemmula lisajoni, new name
(Plate XII)

Discussion. This species is unmistakable, since it is the only known turrid with a typical gemmulate sinus cord on a golden-brown shell, but with a pinkish-violet-stained anterior end, including the entire canal. The canal is slightly curved, and the contrast between the golden-brown shell and the pinkish-purple canal is most striking and instantly identifiable as was clear from the comments of Powell (1964). Although he apparently never saw a specimen of this species, he was able to match Dunker's description with a figure on a tablet.

Types. One of the specimens shown in Plate XII has been deposited in the Philippine National Museum. All three specimens were collected off Mactan Island, by gill nets between 50 to 150 m.

Nomenclature. This species is named for my children, Felicia Marie (Lisa), and Juan Ariston (Jon). The name *lisajoni*, with its contrasting colors, is a momento of their contrasting personalities as children, which added spice to the joys of parenthood.

An obvious question is whether the color of the anterior canal of *Gemmula lisajoni* is homologous or analogous to the violet-colored canal of Clade II *Turris* species. Clearly, the two groups seem otherwise considerably diverged from each other, but if indeed this is a homology, a molecular analysis may reveal an unexpected link between these forms. If it is an analogy, *Gemmula lisajoni* should be just as divergent from any *Turris* as other *Gemmula* species. Additional anatomical and molecular data should permit a clearcut choice between these two alternatives.

Prospects

Table 2 lists the measurements and locality data for specimens of new and renamed *Turris* and *Gemula* species in the Olivera collection, which provided the basis for the descriptions and comparisons presented in this article. We expect that when a larger suite of specimens of some of the new species described here are available from localities outside the Philippines, an even greater range of variation for each species will be recognized. Thus, the few specimens of *T. dollyae* the author has seen from New Guinea and Australia are distinctive from Philippine shells, but are still clearly assignable to this species [one is illustrated in the recent book on Australian shells by Wilson (Wilson et al. 1994), and identified as *T. crispa*].

The availability of many more Philippine *Turris* specimens has been indispensable for clarifying the distinct forms of this genus. One source of taxonomic confusion is that the differences in shell morphology between species is often subtle. In addition, some species are quite variable (i.e., *T. babylonia*, *T. normandavidsoni*, *T. nadaensis*). Thus, in the past, when only an occasional specimen became available, it was very difficult to assign. For several centuries, miscellaneous forms were identified

Table 2. Locality and dimensions of the new Turrinae species.

Species	Measurement (mm)		Locality
	Height	Width	
Turris dollyae			
Holotype	119.0	25.6	Tabaco Bay, Albay, Luzon
Paratype # 1	79.5	16.9	Sogod Cebu
Paratype # 2	104.9	22.7	Bogo, Cebu
Paratype # 3	111.6	24.2	Panglao, Bohol
Paratype # 4	122.9	24.5	Panglao, Bohol
Paratype # 5	103.0	22.0	Panglao, Bohol
Paratype # 6	88.7	20.3	Panglao, Bohol
Paratype # 7	114.3	24.9	Tabaco Bay, Albay Luzon
Paratype # 8	85.0	17.7	Northern Cebu
Paratype # 9	86.3	18.9	Northern Cebu
Paratype # 10	90.2	19.5	Northern Cebu
Paratype # 11	80.4	17.5	Northern Cebu
Paratype # 12	118.1	25.0	"Philippines" (old collection)
Paratype # 13	101.7	21.3	Bogo, Cebu
Paratype # 14	94.4	18.0	Bogo, Cebu
Paratype # 15	87.5	18.2	Bogo, Cebu
Paratype # 16	90.9	18.2	Mactan Is., Cebu
Turris normandavidsoni			
Holotype	66.3	15.2	Sogod, Cebu
Paratype # 1	72.1	17.1	Sogod, Cebu
Paratype # 2	73.4	16.3	Sogod, Cebu
Paratype # 3	55.6	14.6	Olango Is., Cebu
Paratype # 4	82.5	18.6	Batangas Bay, Luzon
Paratype # 5	84.2	19.8	Not specified (old collection)
Paratype # 6	70.3	15.6	Sogod, Cebu
Paratype # 7	78.8	15.7	Sogod, Cebu
Paratype # 8	67.5	15.5	Sogod, Cebu
Paratype # 9	66.8	15.2	Sogod, Cebu
Paratype # 10	62.0	14.8	Olango Is., Cebu
Paratype # 11	58.8	15.7	Olango Is., Cebu
Paratype # 12	64.2	15.6	Olango Is., Cebu
Paratype # 13	64.4	14.1	Sogod, Cebu
Paratype # 14	62.6	14.5	Sogod, Cebu
Paratype # 15	79.0	17.0	Sogod, Cebu
Turris pagasa			
Holotype	63.5	16.2	Pamilacan Is., Bohol
Paratype # 1	61.3	17.3	Dipolog, Northern Mindinao
Paratype # 2	98.4	24.3	Bogo, Cebu
Turris totiphyllis			
Holotype	75.7	21.2	Olango Is., Cebu
Paratype # 1	90.2	24.5	Olango Is., Cebu
Paratype # 2	67.2	18.9	Balicasag, Bohol
Paratype # 3	75.7	21.1	Balicasag, Bohol
Paratype # 4	85.6	22.8	Balicasag, Bohol
Paratype # 5	66.8	20.6	Balicasag, Bohol
Paratype # 6	70.3	19.8	Olango Is., Cebu
Paratype # 7	79.0	22.6	"Philippines" (old collection)
Gemmula lululimi			
Holotype	58.1	17.9	Balut Is
Paratype # 1	36.7	11.5	Pamilican Is., Bohol
Gemmula lisajoni			
Specimen # 1	41.5	11.2	Mactan Is., Cebu
Specimen # 2	43.7	12.7	Mactan Is., Cebu
Specimen # 3	43.3	13.6	Mactan Is., Cebu

as either *T. babylonia* or *T. crispa* (= *Turris grandis*, Gray 1834). Although this article is very much a "work in progress," it is intended to provide an updated taxonomic framework for future studies on this genus. The Powell monographs (Powell 1964, 1966, 1967), though over 30 years old, still serve as a definitive resource, in that these remain the only comprehensive treatment of the Turrinae. The update we have provided has necessarily focused only on Philippine forms, and only the genus *Turris* (s.s.).

One general impression gained from this survey is that the genus is enjoying a species radiation in the Philippines and the Indo-Pacific arc which is relatively recent, resulting in forms that are far larger than is the norm for tropical Turridae. The underlying biological adaptations that are the basis for this relatively recent (in geological terms) radiation of *Turris* species remains completely unknown, and this remains the major scientific question to be addressed in the future.

Acknowledgements

This work was indirectly supported by the Venom Core of NIH grant GM 48677; materials collected for that Program were used in this study. I also thank the University of Utah Distinguished Professor Fund from the Dean, College of Science, which supported this study. I thank Nancy Kurtzeborn for her good cheer and patience during the endless revisions in preparing this manuscript. The figures for this paper were done by Kerry Matz.

References

Bratcher T & Cernohorsky W. 1987. Living Terebras of the World. A Monograph of the Recent Terebridae of the World. American Malacologists, Inc., Melbourne, FL.

Dia-Monje V. 1994. Elucidation of the Precursor Structures of w-Toxins and Mitochondrial DNA Evolution of *Conus* Snails. Doctoral Dissertation, Molecular Biology and Biotechnology Program, College of Science, University of the Philippines, Diliman, Quezon City, Philipp.

Griffith and Pidgeon (1834) Cuvier's Animal Kingdom, Vol. 12, Mollusca.

Hinton AG. 1972. Shells of New Guinea and the Central Indo-Pacific. Robert Brown and Assoc., Port Moresby, P.N.G.

Lamarck JBPADeM. 1816. Tableau encyclopédique et méthodique des trois règnes de la nature. Paris.

Linnaeus C. 1758. Systema Naturae per Regna Tria Naturae. Editio Decima, Reformata. Vol. 1 Regnum Animale. Stockholm.

Monje VD, Ward R, Olivera BM & Cruz LJ. 1999. 16S mitochondrial ribosomal RNA gene sequences: a comparison of seven *Conus* species. Philipp.. J. Sci. 128:225-237.

Olivera BM, Rivier J, Clark C, Ramilo CA, Corpuz GP, Abogadie FC, Mena EE, Woodward SR, Hillyard DR & Cruz LJ. 1990. Diversity of *Conus* neuropeptides. Science 249:257-263.

Olivera BM, Walker C, Cartier GE, Hooper D, Santos AD, Schoenfeld R, Shetty R, Watkins M, Bandyopadhyay P & Hillyard DR. 1999. Speciation of cone snails and interspecific hyperdivergence of their venom peptides: potential evolutionary significance of introns. Ann. N.Y. Acad. Sci. 870:223-237.

Powell AWB. 1964. The family Turridae in the Indo-Pacific. Part 1. The subfamily Turrinae. Indo-Pacific Mollusca 1:227-346.

Powell AWB. 1966. The molluscan families Speightiidae and Turridae. Bulletin of the Auckland Institute and Museum 5:1-184 + 23 plates.

Powell AWB. 1967. The family Turridae in the Indo-Pacific. Part 1a. The subfamily Turrinae concluded. Indo-Pacific Mollusca 1:409-456.

Reeve LA. 1843-46. Monograph of the genus Pleurotoma. Conchologia Iconica 1:1-369.

Röckel D, Korn W & Kohn AJ. 1995. Manual of the Living Conidae. Verlag Christa Hemmen, Wiesbaden, Germany.

Röding PF. 1798. Museum Boltenianum...: pars secunda continens Conchylia. Hamburg.

Sowerby GB. 1825. A Catalogue of the Shells Contained in the Collection of the Late Earl of Tankerville. London.

Springsteen FJ & Leobrera FM. 1986. Shells of the Philippines. Carfel Shell Museum, Manila, Philippines.

Tapparone-Canefri C. 1878. Catalogue des coquilles. Rapportées de la Nouvelle-Guinée par M. Raffray. Bul. Société Zoologique de France 3:244-277.

Taylor JD, Kantor YI & Sysoev AV. 1993. Foregut anatomy, feeding mechanisms, relationships and classification of the Conoidea (= Toxoglossa) (Gastropoda). Bull. nat. Hist. Mus. Lond. (Zool.) 59:125-170.

Tryon, W. (1884) Manual of Conchology.

Wilson B, Wilson C & Baker P. 1994. Australian Marine Shells. Prosobranch Gastropods. Part Two (Neograstropods). Odyssey, Kallaroo, West Australia.

Philippine Journal of Science
128 (4): 331 - 337, December 1999
ISSN 0031 - 7683

RESEARCH

Varietal Effects on Properties of Molded Puffed Brown-Rice Cakes

Bienvenido O. Juliano[1]*, Leslie T. Roferos[1] and Michael Pels[2]

[1]Philippine Rice Research Institute Los Baños, 4031 College, Laguna, Philippines
[2]Real Foods Pty Ltd, 47 Campbell Road, St. Peters, NSW 2044, Australia

Ten types of brown rice differing in amylose content (AC) and gelatinization temperature (GT) were converted in a Lite Energy rice cake machine into molded rice cake at specific volumes of 7 and 11 mL/g. Color, Instron hardness, Rapid Visco Analyser (RVA) viscosity and differential scanning calorimetry (DSC) of the puffed cake were determined. Waxy rice types burned and failed to expand. It was determined from Instron three-point bending and puncture tests that PSB Rc 14 cake (high-intermediate GT, intermediate AC) was hardest and IR24 cake (low GT, low AC) was softest at a specific volume of 7 mL/g. PSB Rc 14, PSB Rc 6 (low GT, high AC) and IR64 (high-intermediate GT, intermediate AC) cakes were hardest and PRJ 5 (low GT-low AC) cake was softest at a specific volume of 11 mL/g. Cake hardness was not always similar for rice types of the same GT-AC type. Most samples were completely gelatinized as indicated by the absence of a gelatinization endotherm in DSC and very low viscosity in the RVA profiles of the rice cakes. RVA viscosity was highest for starting cold paste.

Key words: amylose content effect, gelatinization temperature effect, Instron hardness, RVA viscosity

Molded puffed rice (*ampaw*) is a popular snack in the Philippines (Juliano & Sakurai 1985, Villareal & Juliano 1987, Carpio et al. 1990). It is prepared from non-waxy milled rice by gun-puffing at 210°C at a gauge pressure of 12-13 kg/cm^2 and by molding the puffed rice using caramel solution as binder and sweetener. Partially flaked parboiled waxy brown rice (*pinipig*) is also gun-puffed or puffed by roasting in hot oil, mixed with cooked caramel and molded. Protein content correlates negatively with expansion ratio of puffed rice (Villareal & Juliano 1987).

Rice cakes are a relatively new ethnic snack in the United States and are derived from Australia (Hsieh et al. 1989, USA Rice Council 1992). The US retail market was US$57 million in 1987 (Hsieh et al. 1989) and close to US$300 million in 1996 (Real Foods Pty Ltd data). They are marketed as disc-shaped, puffed products that are low in energy (calories) due to their low serving weight. The main ingredient is long-grain or medium-grain US brown rice. Other minor ingredients such as sesame seed, millet, salt and flavoring may be added. They are consumed in the US mainly as plain-flavored low-calorie snacks, (USA Rice Council 1992).

Puffed rice cakes are produced by a Lite Energy rice cake machine based on pressure-drop method with no added binder. The machine consists of two separate sets of electrically-heated molds into which, using pneumatic air cylinders, the rice is deposited, crushed, heated (e.g. 214°C for 7 s [Hsieh et al. 1990]) and then forced to expand rapidly into a small chamber. The rice grains fuse together to form a cake.

---

*Corresponding author: bjuliano@laguna.net

Better cakes are produced from brown rice than from milled rice as the bran layer helps control the expansion and produces a better-formed cake (Real Foods Pty Ltd data). Quality factors of concern are appearance and/or volume, color, texture and integrity of the rice cakes (Huff et al. 1992).

Because of the potential market for these rice cakes in the Philippines and Asia, the effect of rice variety on the properties of the product was studied in collaboration with Real Foods Pty Ltd. Ten aged brown rice samples (2 kg each) representing the various amylose content (AC) and gelatinization temperature (GT) types were airshipped to Australia for puffing under identical conditions and then returned to PhilRice Los Baños for assessment.

MATERIALS AND METHODS

Source and Analysis of Brown Rice

Aged rough rice samples were obtained from the 1995 crops and 1996 dry season crops of the seed production and seed health units of PhilRice. RD4 waxy brown rice was obtained from Ngamchuen Kongseree, Pathumthani Rice Research Center, Thanyaburi, Pathumthani, Thailand. Rough rice was dehulled in a Satake THU-35 type dehusker. Brown rice length and width were determined on duplicate 10 grains using a photoenlarger (10x). Brown rice was milled in a McGill miller no. 2. The milled rice was analyzed in duplicate for alkali spreading value of six grains (Little et al. 1958) and Instron cooked rice hardness using a water-rice weight ratio of 1.2 for cooking (Juliano & Villareal 1993). Milled rice was ground into a flour in a Udy cyclone mill and analyzed in duplicate for crude protein (N x 5.95) and apparent amylose content (Juliano et al. 1981) and for unreplicated Amylograph and Rapid Visco Analyzer (RVA) pasting viscosity values (Juliano et al. 1985, Juliano 1996). Both Amylograph and RVA runs started at 50°C, heating to 95°C and cooling to 50°C (Juliano 1996). Mean standard deviation of duplicate Amylograph runs was 45 BU for peak, 25 BU for breakdown, 30 BU for consistency and 40 BU for setback, whereas mean standard deviation for duplicate RVA runs was 3 RVU for peak, 2 RVU for breakdown, 6 RVU for consistency and 3 RVU for setback (Roferos & Juliano 1997).

Preparation of rice cakes

Each brown rice sample (2 kg) was frozen for 4 days before phytosanitary certification. They were airshipped to St. Peters, Australia for rice cake processing in a Grain Popper (Lite Energy) twin-head model rice cake machine (Hsieh et al. 1989) under identical conditions. The standard 102 x 16 mm (diameter x thickness) cake (11 mL/g specific volume, 0.09 g/mL bulk density) and the denser and crunchier 95 x 13.5 mm (diameter x thickness) cake (7 mL/g specific volume, 0.14 g/mL bulk density) were prepared from the brown rice samples adjusted to 14.0-16.5% moisture content with moisture tempering for at least 6 h. The 20 batches of 20-30 rice cakes were packed in sealed plastic bags and airshipped to PhilRice Los Baños for evaluation.

Analysis of rice cakes

The rice cakes or rice cake powders were analyzed in duplicate for color using a Minolta Chromameter CR-110 in L*a*b* mode and for hardness (3-6 cakes) by a modified breaking test (Hsieh et al. 1990) using a 9.62-cm^2 plunger with a 47-mm diam opening. A three-point bending cell 44 mm apart and 62 mm wide was also used (Davis 1921) on triplicate whole cake without trimming. The broken samples from the Instron measurement were ground in a Udy cyclone mill with 40-mesh sieve. From the ground sample, 3.00 g flour samples (dry-weight basis) with total water adjusted to 25 g were analyzed in duplicate for RVA-3D pasting viscosity (Whalen 1996, Whalen et al. 1997). The program measured cold viscosity (peak viscosity in 0-2 min at 30°C), peak (during 2-6 min ramp to 95°C), trough (lowest viscosity at 6-10 min at 95°C) and final viscosity on cooling at 30°C (10-11 min cooling on [set at 30°C] and hold at 30°C to 22 min). Breakdown (peak minus trough at 95°C), consistency (highest value at 30°C cool down minus final viscosity at 95°C) and setback (highest value at 30°C cool down minus

Table 1. Physicochemical properties of brown and milled rices used for brown-rice cakes.

Variety or Line Name	Brown Rice					Milled Rice				
						amylograph viscosity (BU)				
	length (mm)	width (mm)	crude protein (% wb)	amylose content (% db)	alkali spreading value	peak	break-down	consis-tency	set-back	Instron cooked rice hardness[a] (kg/cm²)
IR65	6.8	2.0	12.3	2.2	7.0	485	135	10	-125	0.6±0.1
RD4	7.4	2.3	13.4	5.5	2.1	920	415	140	-275	0.8±0.1
PRJ 5	4.7	2.7	9.2	11.7	7.0	685	330	165	-165	0.8±0.0
IR24	6.8	2.2	9.4	13.8	6.9	825	320	195	-125	0.9±0.0
Sinandomeng	*6.8*	*2.0*	*9.4*	12.7	6.0	815	415	170	-245	0.9±0.0
PSB Rc 12	6.9	2.1	11.4	20.8	7.0	595	175	325	150	1.5±0.1
PSB Rc 14	6.4	2.1	8.6	19.6	5.0	665	180	245	65	1.3±0.1
IR64	6.8	2.2	8.8	19.8	4.7	715	250	290	40	1.1±0.2
PSB Rc 6	6.3	2.1	11.3	22.0	7.0	630	70	505	435	1.7±0.1
PSB Rc 2	6.9	2.2	12.0	23.6	5.0	485	125	420	295	1.8±0.3
Mean	6.6	2.2	10.6	15.2	5.8	680	240	245	-5	1.1±0.1
± SD	0.2	0.1	0.2	0.3	0.1					

[a]Mean ± standard deviation.

peak at 95°C) were calculated (Whalen et al. 1997).

Rice cake flour was used in duplicate to check for residual gelatinization enthalpy using a Shimadzu DSC-50 differential scanning calorimeter (DSC) using 2 mg rice with 10 mL water in a low pressure cell at a heating rate of 10°C/min from ambient temperature to 100°C.

RESULTS AND DISCUSSION

Raw rice properties

Only PRJ 5 was short-grained since it is a japonica type from the Philippines (Table 1). Protein content of brown rice was high in most samples except for PSB Rc 14 and IR64. All AC-GT combinations were represented except high-GT, low-AC rice. Amylograph viscosity showed highest peak viscosities for low-AC rice types and high-GT waxy rice RD4 and lowest peak viscosity for low-GT waxy IR65 and intermediate-GT, high-AC rice PSB Rc 2. Breakdown was highest for low-AC rice types and RD4 and least for waxy IR65 and high-AC rice types. Consistency and setback were lowest for waxy and low-AC rice types and highest for high-AC rice types, particularly the low-GT PSB Rc 6.

Instron cooked rice hardness at constant water-rice ratio of 1.2 increased progressively with AC (Table 1). Cooked IR64 was softer than cooked PSB Rc 12 among the intermediate-AC samples.

RVA peak viscosity was highest for Sinandomeng and lowest for PSB Rc 2 (Table 2). Breakdown was also highest for Sinandomeng. Consistency was lowest for waxy rice and highest for intermediate-high-AC rice types except for PSB Rc 2. Breakdown was also highest in intermediate-high-AC samples. RVA and Amylograph viscosity did not give identical curves probably because of the greater shear in the RVA.

Properties of rice cakes

Rice cakes were prepared from all, except for the two waxy rice types, IR65 and RD4, that burned and stuck on the mold at both specific volumes. Runs with waxy rice at 19% water also burned, particularly IR65. Their cake would not hold together, in contrast to nonwaxy cakes. Thus under the conditions of rice cake making, the presence of amylose seems important for proper puffing and adhesion of rice cakes.

Brown rice cakes puffed at specific volume of 11 mL/g were slightly whiter (higher L* value) than those at specific volume of 7 mL/g probably because of the lower density of the cakes. They, however, had similar a* (greenness) and b* (yellowness) values (Tables 3 and 4). PSB Rc 2 cake was the least white and

Table 2. RVA viscosity of raw rices.

Variety/Line Name	RVA viscosity (RVU)			
	Peak	Breakdown	Consistency	Setback
IR65	210	31	49	18
RD4	256	110	13	-97
PRJ 5	249	117	124	7
IR24	240	85	187	102
Sinandomeng	294	141	154	13
PSB Rc 12	178	46	277	231
PSB Rc 14	169	46	218	182
IR64	189	57	224	167
PSB Rc 6	225	18	229	211
PSB Rc 2	113	26	152	126
Mean	212	68	163	96

greenest at specific volume of 7 mL/g and PSB Rc 6, the least white at specific volume of 11 mL/g. Both PSB Rc 2 and PSB Rc 6 were greenest at specific volume of 11 mL/g, whereas Sinandomeng cake was whitest and least yellow at both specific volumes. Huff et al. (1992) obtained similar b* values but lower L* and a* values for rice cakes from US medium and long grain brown rice types.

Instron hardness of the rice cake at specific volume of 7 mL/g by a three-point bending system was highest for PSB Rc 14, followed by IR64 and lowest for PRJ 5 (Table 3). PSB Rc 14 cake was harder than PSB Rc 12 cake and high-AC and low-AC cakes. Using a modified puncture test (Hsieh et al. 1990), cakes at specific volume of 7 mL/g were evaluated. PSB Rc 14 cake was the hardest and PRJ 5 cake was the softest for both peak and work (Table 3). Sinandomeng cake was as soft as PRJ 5 cake based on work. PSB Rc 14 cake was also harder than PSB Rc 12 cake and the high-AC and low-AC cakes. The first peak force or crispness peak was not observed, signifying that the cakes already had water activity greater than 0.44 (Hsieh et al. 1990).

With cakes at specific volume of 11 mL/g, Instron three-point hardness was lowest for low-AC rice types and highest in IR64 and PSB Rc 6 (Table 4). Among intermediate-AC cakes, PSB Rc 12 was softer than IR64. Among low-AC cakes, PRJ 5 was harder than IR24. With the puncture method, IR24 had the softest cake and PSB Rc 6, PSB Rc 14 and IR64 had the hardest cake (Table 3). Similar results were obtained from work (area under the curve). PRJ 5 cake was harder than IR24 cake among the low-AC cakes. Among high-AC rice cakes, PSB Rc 6 was harder than PSB Rc 2.

Similar mean three-point bending hardness values were observed for cakes at specific volumes of 7 and 11 mL/g, but PSB Rc 6 cake was harder for the denser cake (7 mL/g) (Tables 3 and 4). Higher puncture hardness values were observed at the lower specific volume for IR24, PSB Rc 14, IR64 and PSB Rc 2 cakes. On the other hand, PRJ 5 cake showed the opposite effect. Highest hardness values were observed for PSB Rc 14 cake at a specific volume of 7 mL/g (Table 3). Based on puncture work, IR24 and PSB Rc 14 cakes were harder at a specific volume of 7 mL/g. Huff et al. (1992) also reported much more fragile cakes from US medium grain (low-GT, low-AC) brown rice than from US long grain (intermediate-GT, intermediate-AC) brown rice.

The performance of brown rice types within the same AC-GT type was not always the same, particularly the three low-GT, low-AC rice types (Tables 3 and 4). Among the intermediate-AC rice types, low-GT PSB Rc 12 cake was softer than the two high-intermediate-GT cakes, but IR64 cake was softer at 7 mL/g. Among the high-AC cakes, PSB Rc 6 (low GT) was softer than PSB Rc 2 (intermediate GT) at a specific volume of 7 mL/g, but the reverse was true for cakes at a specific volume of 11 mL/g.

The viscosity profile of rice cakes using the RVA (Whalen et al. 1997) reflected complete gelatinization

Table 3. Properties of molded puffed-brown rice cakes with specific volume of 7 mL/g.

Variety or line name	Specific volume (mL/g)	Cake color			Instron hardness[a]		Instron work[a] (kg.cm)	RVA viscosity[b] (RVU)					
		L*	a*	b*	3-point bending	Puncture (kg/cm2)		Cold 30°C Start	Cold 30°C End	Start at 95°C	Break-down	Consis-tency	Set back
IR65	--	73.9	7.0	15.0	--	---	--	17	14	5	0	2	2
RD4	--	70.0	7.3	18.1	--	---	--	47	52	16	2	11	9
PRJ 5	7.7	72.1	6.3	14.2	2.5±0.1	0.69±0.01	5.3±0.7	50	30	11	6	10	4
IR24	7.4	72.9	6.3	13.0	2.8±0.5	0.86±0.14	6.5±0.6	101	99	125	42	-28	-70
Sinandomeng	7.0	73.1	6.1	12.9	2.7±0.4	0.73±0.14	5.3±1.1	58	55	51	26	28	2
PSB Rc 12	6.9	72.0	6.0	13.5	3.3±0.6	0.87±0.07	6.6±0.3	48	43	43	18	27	9
PSB Rc 14	7.3	72.3	6.6	13.1	4.4±0.4	1.46±0.23	12.1±3.3	65	57	44	30	28	-2
IR64	6.9	72.6	6.5	13.2	4.0±0.6	1.18±0.10	8.1±1.5	59	43	28	16	18	2
PSB Rc 6	7.2	71.9	7.2	14.0	3.0±0.3	0.94±0.04	6.8±1.4	45	40	49	24	29	5
PSB Rc 2	7.0	70.0	6.5	13.9	3.3±0.2	1.14±0.06	7.6±1.2	50	46	60	37	44	7
Mean ± SD	7.2	72.1 ±1.2	6.4 ±0.2	13.5 ±1.0	3.2±0.4	0.98±0.10	7.3±1.3	60	52	51	25	20	-5

[a] Mean ± standard deviation.

[b] No peak of 30°C cold and 95°C heated paste, except peak at 56°C of cold RD4 cake.

Table 4. Properties of molded puffed-brown rice cakes with specific volume of 11 mL/g.

Variety or line name	Specific volume (mL/g)	Cake color			Instron hardness[a]		Instron work[a] (kg.cm)	RVA viscosity[b] (RVU)					
		L*	a*	b*	3-point bending	Puncture (kg/cm2)		Cold 30°C Start	Cold 30°C End	Start at 95°C	Break-down	Consis-tency	Set-back
PRJ 5	11.3	73.0	6.3	13.8	2.9±0.1	0.86±0.15	7.8±1.9	51	4	2	0	29	29
IR24	10.6	75.2	6.4	13.4	2.5±0.2	0.55±0.13	4.6±0.9	49	9	4	0	6	6
Sinandomeng	10.9	75.8	5.9	11.5	2.7±0.4	0.68±0.15	6.1±1.1	55	49	15	6	21	15
PSB Rc 12	11.0	73.2	6.4	13.8	3.0±0.5	0.70±0.19	6.3±1.5	71	62	30	22	19	-3
PSB Rc 14	11.1	74.4	6.4	12.9	3.6±0.5	0.93±0.20	9.4±2.3	59	20	13	3	12	9
IR64	11.9	75.5	6.4	12.4	4.0±0.4	0.90±0.12	9.0±1.9	75	12	12	7	11	4
PSB Rc 6	10.6	72.8	7.0	11.9	4.0±0.2	0.94±0.19	9.0±1.6	72	57	56	43	52	9
PSB Rc 2	11.0	73.7	7.0	11.9	3.6±0.5	0.64±0.04	5.9±1.1	60	50	28	20	26	6
Mean ± SD	10.9	74.7 ±1.2	6.5 ±0.3	12.7 ±1.1	3.3±0.4	0.78±0.15	7.3±1.5	62	33	20	10	22	9

[a] Mean ± standard deviation.

[b] No peak was observed for cold paste at 30°C and for hot paste at 95°C.

and was similar to extrusion of cooked corn product (Whalen 1996) and pasted cooked rice and rice extrudate at 15% moisture (Whalen et al. 1997) with no peak initially at 30°C and upon heating to 95°C and little increase in viscosity on cooling at 30°C (Tables 3 and 4). The raw flour had much higher viscosity values (Table 2). Waxy IR65 had the lowest viscosity. IR24 had the lowest RVA pattern among the nonwaxy rice cakes. Villareal & Juliano (1987) also reported a much reduced gel viscosity of gun-puffed milled rice as compared with starting raw rice. The DSC thermograms of rice cakes confirmed that all cake samples were essentially gelatinized by the absence of endotherms in the GT range, except for PSB Rc 12 and PSB Rc 14 cakes at 11 mL/g and for PSB Rc 2, Sinandomeng and PRJ 5 cakes at 7 mL/g (data not shown). Hence, difference in degree of starch cooking was not a factor in differences in hardness and adhesion of the rice cakes. Hsieh et al. (1989) also reported complete starch gelatinization of US long grain brown rice in puffed rice cake.

Simple correlation coefficients showed better correlation between the two hardness methods for cakes at specific volume of 7 mL/g than for cakes at 11 mL/g (Table 5). Puncture hardness and work were highly correlated for both sets of cakes. Brown rice dimensions and protein content were not significantly correlated with cake hardness and work. Amylose

Table 5. Simple correlation coefficients (r) between Instron hardness of puffed brown rice cake and grain properties.

Property	r[a] with Instron hardness/work at specific volume					
	3-point bending		*Puncture (kg/cm2)*		Puncture work (kg.cm)	
	7 ml/g	11 ml/g	7 ml/g	11 ml/g	7 ml/g	11 ml/g
Instron hardness						
Three-point bending 7 ml/g	1.00	0.62	**0.94	0.45	**0.92	0.57
Three-point bending 11 ml/g		1.00	0.66	0.71	0.51	*0.76
Puncture (kg/cm2) 7 ml/g			1.00	0.39	**0.96	0.51
Puncture (kg/cm2) 11 ml/g				1.00	0.43	**0.99
Puncture work (kg.cm) 7 ml/g					1.00	0.53
Brown rice length	0.37	0.11	0.34	-0.44	0.22	-0.33
Brown rice width	-0.37	-0.17	-0.33	0.16	-0.29	0.08
Brown rice protein content	-0.33	-0.22	-0.27	0.15	-0.17	-0.21
Milled rice amylose content	0.58	*0.77	0.63	0.22	0.48	0.30
Alkali spreading value	*-0.74	-0.52	*-0.77	-0.19	-0.04	-0.32
Amylograph peak viscosity	-0.26	-0.54	-0.36	-0.16	-0.24	-0.18
Amylograph breakdown viscosity	-0.44	*-0.71	-0.50	-0.33	-0.41	-0.36
Amylograph consistency	0.19	*0.72	0.29	0.24	0.14	0.26
Amylograph setback viscosity	0.32	*0.74	0.42	0.29	0.30	0.32
RVA peak viscosity	-0.63	-0.55	*-0.71	-0.04	-0.58	-0.13
RVA breakdown viscosity	-0.54	*-0.74	-0.62	-0.27	-0.52	-0.33
RVA consistency	0.52	0.35	0.34	0.23	0.36	0.27
RVA setback viscosity	0.62	0.60	0.56	0.29	0.52	0.35
Instron cooked rice hardness	0.32	0.62	0.42	0.11	0.30	0.15
Cake RVA 7 or 11 ml/g						
Starting 30°C viscosity	-0.03	*0.75	0.03	0.48	0.10	0.52
End 30°C viscosity	-0.05	0.16	0.03	-0.15	0.09	-0.15
Starting 95°C viscosity	-0.18	0.55	-0.05	0.25	-0.04	0.24
"Breakdown" viscosity	0.10	0.54	0.31	0.22	0.27	0.20
"Consistency"	0.32	0.39	0.33	0.40	0.23	0.32
"Setback" viscosity	0.22	-0.26	0.13	0.25	0.07	0.16

[a] *Correlations marked by * are significant at* 0.05 > P > 0.01 and those marked by ** at P < 0.01. Unmarked values are not significant.

content only correlated with three-point bending hardness of 11 mL/g cakes, but alkali spreading value correlated negatively with hardness by both methods only for 7 mL/g cakes. Three-point bending hardness of 11 mL/g cakes correlated with Amylograph breakdown, consistency and setback, raw-rice RVA breakdown and rice-cake RVA *starting* viscosity at 30°C, but not in 7 mL/g cakes. Puncture hardness of 7 mL/g cakes correlated with raw-rice RVA peak viscosity, but not in 11 mL/g cakes. Thus, no rice property correlated consistently with hardness for both sets of cakes.

Thus, intermediate-AC rice types with intermediate-high GT provides the best raw brown rice for molded cakes, although high-AC, low-GT brown rice was also satisfactory at high cake specific volume. Waxy rice types burned and failed to adhere together and expand, whereas the low-AC, low-GT rice types were softer. The presence of intermediate to high AC was needed for optimum texture and integrity (grain adhesion) of the rice cake. Complete starch gelatinization was confirmed by both DSC and RVA analyses.

Follow-up pilot plant studies should be undertaken on more Philippine varieties to verify the above results.

Acknowledgment

The authors wish to thank Tess Rola for manuscript editing.

References

Carpio EV, Gonzalez AM, Aco EV & Robles JS . 1990. Survey and documentation of traditional food processing equipment. Project report to Philippine Rice Research Institute, Maligaya, Muñoz, Nueva Ecija. Institute of Food Science and Technology, University of the Philippines Los Baños, College, Laguna (Philippines).

Davis CE. 1921. Shortening: its definition and measurement. Indus. Eng. Chem. 13: 797-799.

Hsieh F, Hu L, Huff HE & Peng IC. 1990. Effects of water activity on textural characteristics of puffed rice cake. Lebensmittel-Wissenschaft und-Technologie 23: 471-473.

Hsieh F, Huff HE, Peng IC & Marek SW. 1989. Puffing of rice cakes as influenced by tempering and heating conditions. J Food Sci. 54: 1310-1312.

Huff HE, Hsieh F & Peng IC. 1992. Rice cake production using long-grain and medium-grain brown rice. J Food Sci. 57: 1164-1167.

Juliano BO. 1996. Rice quality screening with the Rapid Visco Analyser. In: Applications of the Rapid Visco Analyser (eds CE Walker & JL Hazelton). Presented in part at American Association of Cereal Chemists annual meeting/RVA symposium, 23-27 Oct 1994, Nashville, TN (USA) pp. 18-24. Newport Scientific Pty Ltd, Warriewood, NSW (Australia).

Juliano BO, Perez CM, Alyoshin EP, Romanov VB, Bean MM, Nishita KD, Blakeney AB, Welsh LA, Delgado LL, El Baya AW, Fossati G, Kongseree N, Mendes FP, Brilhante S, Suzuki H, Tada AM & Webb BD. 1985. Cooperative study on amylography of milled rice flour for pasting viscosity and starch gelatinization temperature. Starch/Die Stärke 37: 40-50.

Juliano BO, Perez CM, Blakeney AB, Castillo DT, Kongseree N, Laignelet B, Lapis ET, Murty VVS, Paule CM & Webb BD. 1981. International cooperative testing on the amylose content of milled rice. Starch/Die Stärke 33: 157-163.

Juliano BO & Sakurai J. 1985. Miscellaneous rice products. In: Rice chemistry and technology, 2nd ed. (Ed BO Juliano) pp. 569-618. American Association of Cereal Chemists, St Paul, MN (USA).

Juliano BO & Villareal CP. 1993. Grain quality evaluation of world rice types. International Rice Research Institute, Manila.

Little RR, Hilder GB & Dawson EH. 1958. Differential effect of dilute alkali on 25 varieties of milled white rice. Cereal Chem. 35: 111-126.

Roferos LT & Juliano BO. 1997. Chemometrics of grain quality of raw and cooked Philippine milled rice. Phil. Agriculturist 80:211-236.

USA Rice Council. 1992. Rice: consumer attitudes and consumption patterns. Houston, TX (USA).

Villareal CP & Juliano BO. 1987. Varietal differences in quality characteristics of puffed rice types. Cereal Chem. 64: 337-342.

Whalen PJ. 1996. Fingerprinting cereal products. In: Applications of the Rapid Visco Analyser (eds CE Walker & JL Hazelton). Presented in part at the American Association of Cereal Chemists annual meeting/RVA symposium, 23-27 Oct 1994, Nashville, TN (USA) pp. 73-75. Newport Scientific Pty Ltd., Warriewood, NSW (Australia).

Whalen PJ, Bason ML, Booth RI, Walker CE & Williams PJ. 1997. Measurement of extrusion effects by viscosity profile using the Rapid ViscoAnalyser. Cereal Foods World 42: 469-475.

Philippine Journal of Science
128 (4): 339 - 345, December 1999
ISSN 0031 - 7683

Preparation of End-functionalized Polymers by Allylic Sulfide Chain Transfer and Subsequent Synthesis of Block Copolymers

W. Ken Busfield[1], Clovia Isabel Z. Holdsworth[2]*, Dorotea T. Ouano[3], San H. Thang[4]

[1] School of Science, Griffith University, Nathan, Qld 4111, Australia
[2]Chemistry Department, De La Salle University, 2401 Taft Avenue, Manila, Philippines
[3] Chemistry Department, Adamson University, San Marcelino St., Ermita, Manila, Philippines
[4] CSIRO Division of Molecular Science, Private Bag 10, Clayton South, Victoria 3169, Australia

Carboxy-terminated end-functional polymers have been prepared by addition-fragmentation chain transfer employing a novel chain transfer agent, α-(Carboxymethylthiomethyl)acrylic acid. Chain transfer constants for styrene, methyl methacrylate, methacrylonitrile and vinyl acetate single and mixed systems ranged from 0.28 to 41.4. α-(Carboxymethylthiomethyl)acrylic acid has been evaluated to preferentially react with styrene over methacrylonitrile and methyl methacrylate propagating radicals in copolymer systems. Poly(styrene)-*block*-poly(methacrylonitrile) and poly(styrene)-*block*-poly(methyl methacrylate) were successfully obtained by the condensation reaction between hydroxy- and carboxy-terminated end-functional oligomers.

Key words: free radical, addition-fragmentation, end-functional polymers, oligomers, co-oligomers

The process of free radical chain transfer has been shown to be a versatile method of synthesizing end-reactive polymers. This has the advantage over the other methods in that a greater number of monomers can be utilized, and with the proper choice of functional additives, both mono- and di- end-functional polymers may be prepared. The development of new classes of chain transfer agents by the CSIRO Division of Molecular Science (Rizzardo et al. 1988, 1990, 1992, 1995) and elsewhere (Bailey et al. 1986, Colombani & Chaumont 1996, Yamada et al. 1992) has provided a wider choice of more specific functional additives for the preparation of end-reactive oligomers and polymers by the free radical method. These compounds with the general formula $H_2C{=}CXY$, which include the allylic sulfides, act via a two-step radical addition-fragmentation mechanism. They are more versatile than other chain transfer agents because their chain transfer efficiency may be improved by modifying substituent X. Further, it is possible to prepare a mono, di-, or tri- end-functional polymer simply by functionalizing either or both X and Y.

This paper reports on the preparation of end-functional polymers and oligomers by using allylic sulfide α-(Carboxymethylthiomethyl)acrylic acid (CMTMAA) as chain transfer agent. The focus is on the efficiency of CMTMAA in providing functionality to, and controlling the molecular weights of the polymers in pure and mixed systems. Previous work has shown CMTMAA to be an efficient chain transfer agent towards styrene (S) and methyl methacrylate (MMA) in single feed systems (Rizzardo et al. 1988). This is the first reported study on S / MMA copolymers and methacrylonitrile (MAN) single and mixed feed systems. Successful coupling between carboxy-terminated oligomers prepared in this study and hydroxy-terminated oligomers previously synthesized is also described.

---

*Corresponding author: coscizh@mail.dlsu.edu.ph

Methods

Materials and Reagents

2,2'-Azobisisobutyronitrile (AIBN) **(1)**, generously provided by R.I. Chemical Corporation was recrystallized twice from ethanol. Methacrylonitrile (MAN) (Sigma) **(2)**, methyl methacrylate (MMA) (Aldrich) **(3)**, styrene (S) (Aldrich) **(4)**, and vinyl acetate (VAc) (Aldrich) **(5)**, were distilled under nitrogen at pressures <50 mm Hg and stored in the refrigerator over calcium hydride. α-Carboxy-methylthiomethylacrylic acid **(6)**, generously provided by the Division of Polymers, CSIRO, Australia, was recrystallized twice from hot toluene. AR grade acetone, chloroform, methanol and xylene were used as received.

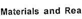

(1)

(2)

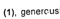

(3)

(4)

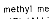

(5)

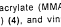

(6)

Polymerization and Characterization of End-functional Polymers

A typical polymerization procedure is as follows: 20.0 mg of AIBN were mixed with 5.0 ml of the monomer in an ampule. The required amount of the chain transfer agent was added to the reaction mixture which was then degassed by three freeze-evacuate-thaw cycles at ≤ 10^{-2} mm Hg. The ampule was sealed in vacuo and the mixture polymerized at 60°C. Polymerization was stopped at conversion ≤ 20% by quenching in liquid nitrogen. This is to ensure that the steady-state assumption for kinetic studies is still valid (i.e. radicals are formed and destroyed at identical rates). After thawing, the reacted mixture was poured slowly into excess methanol while stirring.

The precipitated polymer was collected, dried, redissolved in an appropriate solvent, then reprecipitated in methanol. The process was repeated at least three times and the purified polymer was dried under vacuum for at least 48 hours.

Molecular weights of the polymers were determined on a Millipore-Waters Gel Permeation Chromatograph using PS standards and THF as solvent. NMR experiments were performed on JEOL Lambda 400 at room temperature or higher (40°) in deuterated chloroform ($CDCl_3$).

Preparation of Block Copolymers

Equal weights of a carboxyl-terminated oligomer and a hydroxy-terminated oligomer were mixed in xylene. The mixture was refluxed for about eight hours under nitrogen. After evaporating the solvent, the product residue was dissolved in chloroform and precipitated in excess methanol. Unreacted oligomers were separated from the block copolymer product by fractional precipitation in methanol. The first precipitate obtained, expected to be the block copolymer, was collected, dried and reprecipitated in methanol. Final drying was done under vacuum for about eight hours.

Results and Discussion

Mechanism of Chain Transfer and End-functionalization

Polyvinyl acetate (PVAc), homo-, and copolymers of S, MMA and MAN from several feed compositions were prepared with varying amounts of CMTMAA as chain transfer agent under identical conditions of initiator (AIBN) concentration and temperature of 60°C. The mechanism, illustrated in Scheme 1, showed chain transfer to CMTMAA to be the main termination reaction.

Addition of the allylic sulfide to the propagating radical is rapidly followed by fragmentation of the thiyl radical which then initiates a new chain, thus, producing polymers with endstructure **(7)**. The resulting end-functionalized polymer may be described as tri-end-functional with carboxy groups at the α and ω ends, as well as a double bond at the ω end.

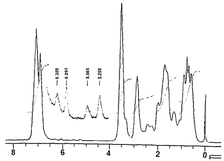

Figure 1. ¹H NMR double bond region of S / MMA (25% / 75% feed) copolymer prepared with 0.2720 M CMTMAA, MW = 4,360.

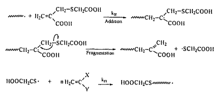

Scheme 1

Efficient end-functionalization of the polymers by CMTMAA was ascertained by ¹H NMR experiments. The ¹H NMR spectrum of PS prepared in the presence of CMTMAA showed signals at 5.3 and 6.1 ppm attributable to the olefinic endgroup derived from CMTMAA directly attached to a S propagating chain. The PMMA ¹H NMR spectrum, on the other hand, contained signals at 5.6 and 6.3 ppm due to CMTMAA-derived olefinic end-groups. These two sets of olefinic end-groups were evident in the S/ MMA copolymer (e.g. Fig. 1) suggesting that CMTMAA reacted with both S and MMA propagating chains. The olefinic peak assignments were consistent with the ¹H NMR results obtained in a previous study in which PS and PMMA were also end-functionalized with an allylic sulfide (Busfield et al. 1999). The olefinic endgroup was observed in all other polymers prepared with CMTMAA.

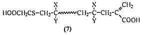

$$HOOCH_2CS-CH_2-\underset{Y}{\overset{X}{C}}\sim\sim\sim CH_2-\underset{Y}{\overset{X}{C}}-CH_2-C(=CH_2)COOH$$

(7)

Control of Molecular Weight

The presence of a chain transfer agent in the polymerization mixture causes premature termination. Thus, a functional chain transfer agent, like CMTMAA, not only provides the reactive end-groups but also regulates the molecular weights of the polymers. As shown in Table 1, the molecular weights (all PS equivalents) of the polymers markedly decreased with increasing concentration of CMTMAA. Further, the polymers exhibited a narrow MW distribution consistent with efficient reinitiation following chain transfer (i.e. M_w / $M_n \leq 2.3$). With PVAc, a large reduction in MW and polymer yields were observed with the addition of increasing amounts of chain transfer agent suggesting a degradative chain transfer.

Evaluation of Chain Transfer Constants

The concomitant decrease in MW and (hence) degree of polymerization, with increasing concentration of chain transfer agent is related to the efficiency of the additive in controlling the MW of polymers and can be summarized by the kinetic expression

$$\frac{1}{\overline{DP}} = \frac{1}{\overline{DP}_0} + C_x \frac{[CTA]}{[M]} \qquad (1)$$

Known as the Mayo equation, the relation considers that the degree of polymerization, $\overline{DP}$, is affected by any reaction that stops the growth of the chain. C_x, called the chain transfer constant, which is the ratio of the rate constant for the reaction of the propagating radical with the chain transfer agent (k_{tr}) to that of propagation (k_p), describes the efficiency of the chain transfer agent in controlling the polymer MW. It is normally evaluated from the slope of the plot of 1 / $\overline{DP}$ against the ratio of the concentrations of the chain transfer agent, [CTA] to the monomer(s) ([M] in homopolymerization or $[M_1]$ + $[M_2]$ in copolymerization) in the feed of a series of reactions in which the ratio of [CTA] to [M] is successively increased. $\overline{DP}_0$ is the degree of polymerization in the absence of transfer. $\overline{DP}$ was calculated using the number average molecular weights, M_n, according to the equation = M_n / M_F where M_F is the molecular weight of the monomer unit. For copolymers, M_F = $MW_{(M1)} \times F_1 + MW_{(M2)} \times (1 - F_1)$ where F is the monomer fraction in the polymer. F was obtained using the copolymer equation:

Table 1. Molecular weights of polymers prepared in the presence of CMTMAA at 60°C.

Monomer Feed (mol %)		[CMTMAA]	% Yield	M_n^a	M_w^a	M_w/M_n
MMA		0.0	32.0	103,020	223,820	2.2
		0.0170	10.3	57,810	101,140	1.7
		0.0341	7.5	33,070	49,450	1.5
		0.0682	7.0	21,190	26,210	1.2
		0.1360	5.8	11,630	15,120	1.3
S/MMA	25/75	0.0	3.6	86,980	201,150	2.3
		0.0341	3.7	34,010	44,260	1.3
		0.0682	3.6	11,900	19,440	1.6
		0.1360	3.0	8,350	9,180	1.1
		0.2720	4.9	4,360	6,100	1.4
	50/50	0.0	2.5	101,930	160,460	1.6
		0.0170	2.9	39,620	63,680	1.6
		0.0341	2.6	17,980	32,310	1.8
		0.0682	2.5	12,750	18,800	1.5
Styrene		0.0	2.4	77,760	114,950	1.5
		0.0170	1.2	45,510	76,210	1.7
		0.0341	2.3	32,710	51,960	1.6
		0.0682	1.5	16,240	27,610	1.7
		0.1360	2.0	5,660	9,060	1.6
		0.2720	2.1	2,710	4,560	1.7
S/MAN	50/50	0.0	2.8	56,280	78,790	1.4
		0.0170	2.3	35,110	57,470	1.6
		0.0341	2.4	29,800	61,770	2.1
		0.0682	1.8	23,660	37,830	1.6
MAN		0.0	0.20	32,990	56,510	1.7
		0.0170	0.18	25,840	36,000	1.4
		0.0341	0.18	23,370	42,060	1.8
		0.0682	0.14	15,480	20,020	1.3
VAc		0.0	17.4	503,300	907,100	1.8
		0.0115	2.0	2,200	4,200	1.9
		0.0236	2.9	900	1,900	2.0
		0.0457	0.87	500	900	1.8

^{a} PS equivalents

$$\frac{F_1}{F_2} = \frac{f_1}{f_2}\,\frac{[r_1 f_1 + f_2]}{[f_1 + r_2 f_2]} \qquad (2)$$

where r_1 and r_2 are literature values (Brandrup & Immergut 1989) of the reactivity ratios of the monomer pair and f is the mole fraction of the monomer in the reaction feed. An ideal chain transfer agent is one with $C_x = 1$, that is, the ratio of the rates at which monomer and transfer agent are consumed by growing polymer radicals is constant. A very high C_x indicates degradative chain transfer, a very low C_x suggests an inefficient chain transfer and MW control. In the preparation of end-reactive polymers and oligomers, chain transfer agents with C_x in the range 0.1 to ten, at most to twenty, have been utilized though the preferred range is between 0.5-2.0 (two) (Corner 1984, Rizzardo et al. 1995).

The C_x's for CMTMAA determined from the Mayo plots are listed in Table 2. Values obtained range from 0.28 in the MAN system to 41.4 in the VAc system. The C_x values obtained for pure S (1.23) and pure MMA (0.53) are in close agreement with the results obtained by Rizzardo and co-workers (1988) (i.e. 1.27 and 0.74, respectively). The very high C_x for CMTMAA in the VAc system is consistent with degradative chain transfer. C_x values obtained for the other polymer systems suggest an efficient end-functionalization and MW control.

Since C_x gives the ratio of k_{tr} to k_p, it is possible to determine k_{tr} using literature values of k_p (Brandrup & Immergut 1989, Moad & Solomon 1995). The results summarized in Table 2, showed the k_{tr} for MMA to be 1.2 larger than that for S which, in turn, is 4.5 times larger than that for MAN. The rate of addition of CMTMAA towards the propagating radicals in the order MMA > S > MAN is consistent with the expected (i.e. least stable radical is the most reactive).

It is noteworthy that in copolymer systems, the efficiency of a chain transfer agent is affected by the reactivity ratios (ratio of rate of self-propagation to cross-propagation) and the monomer feed (Tsuchida 1972). For a mixed monomer feed of M_1 and M_2 copolymerized in the presence of chain transfer agent T and described by the following competing terminal reactions,

$$\sim\!\sim M_1\cdot + M_1 \xrightarrow{k_{11}} \sim\!\sim M_1\cdot \qquad (3a)$$

$$\sim\!\sim M_1\cdot + M_2 \xrightarrow{k_{12}} \sim\!\sim M_2\cdot \qquad (3b)$$

$$\sim\!\sim M_2\cdot + M_1 \xrightarrow{k_{21}} \sim\!\sim M_1\cdot \qquad (3c)$$

$$\sim\!\sim M_2\cdot + M_2 \xrightarrow{k_{22}} \sim\!\sim M_2\cdot \qquad (3d)$$

$$\sim\!\sim M_1\cdot + T \xrightarrow{k_{1T}} \sim\!\sim T\cdot \qquad (3e)$$

$$\sim\!\sim M_2\cdot + T \xrightarrow{k_{2T}} \sim\!\sim T\cdot \qquad (3f)$$

the transfer reactivity ratios k_{1T} / k_{12} and k_{2T} / k_{21} can be inferred from the C_x's of the corresponding homopolymers and the propagation reactivity ratios. Thus, if $C_{x1} = k_{1T} / k_{11}$ and $C_{x2} = k_{2T} / k_{22}$, and the propagation reactivity ratios are $r_1 = k_{11} / k_{12}$ and $r_2 = k_{22} / k_{21}$, then the transfer reactivity ratios are $t_1 = k_{1T} / k_{12} = C_{x1}\, r_1$ and $t_2 = k_{2T} / k_{21} = C_{x2}\, r_2$.

Table 2. Chain transfer constants for CMTMAA at 60°C and reactivity ratios for S / MMA and S / MAN copolymer systems.

Monomer Feed (mol %)		C_x (Corr. coeff)	k_p^* (L/mol.s)	k_{tr} (L/mol.s)	Propagation reactivity ratios*	Transfer reactivity ratios
MMA		0.53 ± 0.01 (0.996)	759	402	0.46	0.24
S/MMA	25/75	0.78 ± 0.01 (0.974)				
	50/50	0.96 ± 0.03 (0.981)				
Styrene		1.23 ± 0.28 (0.994)	279	343	0.52 0.30	0.64 0.37
S/MAN	50/50	0.28 ± 0.01 (0.994)				
MAN		0.37 ± 0.01 (0.987)	206	76	0.16	0.06
Vac		41.4 (0.998)	~1000	~41000		

*literature values

Transfer reactivity ratios given in Table 2 for S / MMA (0.64 and 0.24, respectively) and S / MAN (0.37 and 0.06, respectively) suggest a higher rate of CMTMAA addition to an S-propagating radical in both copolymer systems. The preference of S for self-propagation and that of MAN and MMA for cross-propagation (i.e. $r_S > r_{MMA}$ and $r_S > r_{MAN}$), indicate that more S-propagating radicals are generated, hence, a higher probability of S-CMTMAA reaction producing more S-derived end-groups. For instance, even in a 25% S / 75% MMA feed (see Fig. 1), the number of S-derived olefinic end-groups, obtained by proton integration, was calculated to be 1.4 times the number of MMA-derived olefinic end-functionality. In the case of S / MAN where the propagation reactivity ratios are far from comparable (0.30 and 0.16, respectively), the competition between cross-propagation and transfer reactions is evident. The rate of the reaction between the MAN propagating radical and the S monomer is 17 times faster than that between the MAN propagating radical and CMTMAA (1 / t = 1 / 0.06). Conversely, the rate of the reaction between the S propagating radical and the MAN monomer is 2.7 times faster than that between the S propagating radical and CMTMAA (1 / 0.37). Hence, in a 50% / 50% monomer feed, the cross-propagation reactions prevail over transfer to CMTMAA resulting in a C_x value (0.28) which is lower than those obtained for the homopolymers.

Block Copolymerization

The carboxy-terminated oligomeric products were copolymerized with selected samples of hydroxy-and carboxy-terminated polymers prepared from a previous study. The latter were also prepared by the addition-fragmentation chain transfer using the following allylic sulfides: 2-hydroxyethyl-a-(((2-hydroxyethyl)thio)-methyl)acrylate **(8)**, and a-(((2-hydroxyethyl)thio)-methyl) acrylic acid **(9)**,

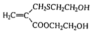

$H_2C{=}C(CH_2SCH_2CH_2OH)(COOCH_2CH_2OH)$

(8)

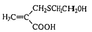

$H_2C{=}C(CH_2SCH_2CH_2OH)(COOH)$

(9)

and were proven by NMR experiments to possess the following endstructures **(10)** and **(11)**, respectively (Zayas 1995):

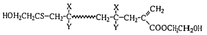

$HOH_2CH_2CS{-}CH_2{-}C(X)(Y){\sim\sim\sim}CH_2{-}C(X)(Y){-}CH_2{-}C({=}CH_2)(COOCH_2CH_2OH)$

(10)

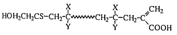

$HOH_2CH_2CS{-}CH_2{-}C(X)(Y){\sim\sim\sim}CH_2{-}C(X)(Y){-}CH_2{-}C({=}CH_2)(COOH)$

(11)

The hydroxy and carboxy end-groups are susceptible to esterification, thus, an oligomer of endstructure **(7)** could easily react with an oligomer of endstructure **(10)** to yield an AB-block copolymer linkage **(12)**. The block copolymer still has the potential to undergo grafting on the remaining double bond functionality.

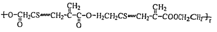

$\left[O{-}C({=}O)CH_2CS{\sim\sim}CH_2{-}C({=}CH_2){-}C({=}O){-}O{-}H_2CH_2CS{\sim\sim}CH_2{-}C({=}CH_2){-}COOCH_2CH_2\right]_r$

(12)

PS-*block*-PMAN and PS-*block*-PMMA copolymers were prepared using the end-functional oligomers described in Table 3. The molecular weights of the copolymerization product were observed to be significantly higher than the molecular weights of the starting oligomers and corresponded to a range of 1 to 3 repeating block units. These indicate successful coupling between the oligomers. Further, the MW distribution of the block copolymers were narrow which suggests that the copolymers were efficiently

Table 3. Block copolymerization results.

Block	End-functionality of oligomers	M_n of starting oligomers			Copolymer		
		PS	PMAN^b	PMMA^a	M_n^{b}	M_w/M_n	% Yield
Block 1	α,ω-carboxy^a	1,500^a			24,800	1.6	74
	α,ω-hydroxy^b		6,400				
Block 2	α,ω-carboxy^a			2,000	16,100	1.4	75
	α,ω-hydroxy^b	12,800^b					
Block 3	α,ω-carboxy^a			7,500	31,600	1.6	62
	α-hydroxy, ω-carboxy^b	11,700^b					

^{a} by endgroup analysis (titration). ^{b}by GPC, PS equivalents

separated from the unreacted oligomers by fractional precipitation.

Figure 2 is the overlayed IR spectra of the starting oligomers and the copolymer PS-*block*-PMAN (Block 1). The spectrum indicated a significant loss of the -OH peak (3200-3600 cm^{-1}) which is very evident in the starting oligomers. Peaks between 1750-2000 cm^{-1}, characteristic of PS, and the -CN peak at 2250 cm^{-1} attributable to PMAN, were observed confirming successful block copolymerization between PS and PMAN. The IR spectra of PS-*block*-PMMA corresponding to Blocks 2 and 3 also showed attributes of the starting oligomers, notably between 1750-2000 cm^{-1}, characteristic of PS, and the carbonyl peak of PMMA at about 1700 cm^{-1}. An appreciable reduction in the intensity of the -OH peak (3200-3600 cm^{-1}) was also observed after the reaction.

CMTMAA as novel transfer reagent

Carboxy-terminated end-functional polymers can be obtained by addition-fragmentation chain transfer in the presence of CMTMAA. The C_x values in homo- and copolymer systems, determined using the Mayo relation, range from 0.28 to 41.4. These values are acceptable for the end-functional polymers to be used for the synthesis of more complex structures. CMTMAA has a preference for S over MAN and MMA propagating radicals in copolymer systems.

PS-*block*-MAN and PS-*block*-PMMA are obtained by esterification reaction between hydroxy- and carboxy-terminated oligomers.

Acknowledgments

Financial support from De La Salle University through the University Research Coordinating Office (URCO) and the College of Science Research Council, and technical assistance provided by Ms. Annette Neuendorff of Griffith University and the staff of the National Chemistry Instrumentation Center are gratefully acknowledged.

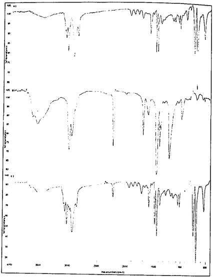

Figure 2. IR spectra of a.) α,ω-carboxy-terminated PS; b.) α,ω-hydroxy-terminated PMAN; c.) PS-*block*-PMAN copolymer (Block 1).

References

Bailey WJ, Chen PY, Chen SC, Chiao WB, Endo T, Gapud B, Kuruganti V, Lin YN, Ni Z, Pan CY, Shaffer SE, Sydney L, Wu SR, Yamamoto N, Yamazake N, Yonezawa K & Zhou LL. 1986. Free radical ring-opening polymerization and its use to make biodegradable polymers and functionally terminated oligomers. Makromolekular Chemie, Macromolecular Symposium 6:81.

Brandrup J & Immergut EH. 1989. Polymer handbook. John Wiley & Sons, New York.

Busfield WK, Zayas-Holdsworth CI & Thang SH. 1999. End-functionalised copolymers prepared by the addition-fragmentation chain transfer method. Styrene/ methyl methacrylate system. Polymer. 40:389-396.

Colombani D & Chaumont P. 1996. Addition fragmentation processes in free radical polymerization. Prog. Polymer Sci. 21:439-503.

Corner T. 1984. The synthesis of graft copolymers. In: Free radical polymerisation (ed T. Corner) 62:95-142. Springer-Verlag, Berlin.

Moad G & Solomon DH. 1995. The chemistry of free radical polymerization. Pergamon, London.

Rizzardo E, Meijs, GF & Thang SH. 1988. PCT Int. Appl. WO 88 / 4304 A1. Patent. CSIRO, Australia.

Rizzardo E, Meijs, GF & Thang SH. 1990. PCT/AU90/ 00523. Patent. CSIRO, Australia.

Rizzardo E & Meijs GF. 1992. PCT / AU92 / 00029. Patent. CSIRO, Australia.

Rizzardo E, Meijs GF & Thang SH. 1995. Chain transfer by radical addition-fragmentation mechanisms: Synthesis of macromonomers and end-functional oligomers. Macromolecular Symposium 98:101-123.

Tsuchida E, Kitamura K & Shinohara I. 1972. Simplified treatment of cooligomerization kinetics. J. Polymer Sci.: Polymer Chem. Ed. 10:3639-3650.

Yamada B, Kobatake S & Otsu T. 1992. Control of molecular weight and end group of polymers by addition fragmentation reaction with alpha-(bromomethyl)acrylate and allyl bromide. Polymer J. 24:281-290.

Zayas CIS. 1995. End-functionalized copolymers by allylic sulfide chain transfer. PhD Thesis, Griffith University.

Philippine Journal of Science
128 (4): 347 - 351, December 1999
ISSN 0031 - 7683

Antimicrobial Flavones from *Coleus amboinicus*

Consolacion Y. Ragasa[1*], Zeus Pendon[1], Veronica Sangalang[1]
and John A. Rideout[2]

[1]Chemistry Department, De La Salle University, 2401 Taft Avenue, Manila, 1004, Philippines,
[2]Chemistry Department, Central Queensland University, Rockhampton, Queensland, 4702, Australia

The air dried leaves of *Coleus amboinicus* Lour. afforded three flavones: salvigenin, cirsimaritin and chrysoeriol by silica gel chromatography. Their structures were elucidated by extensive 1D and 2D NMR and UV spectroscopy. Antimicrobial assay on salvigenin and cirsimaritin indicated that they have low antimicrobial activities against *P. aeruginosa, B. subtilis, E. coli, S. aureus, C. albicans, T. mentagrophytes* and *A. niger.*

Key words: *Coleus amboinicus* Lour., *Coleus aromaticus* Benth., Labiatae, cirsimaritin, salvigenin, chrysoeriol, antimicrobial

Coleus amboinicus Lour., also known as *Coleus aromaticus* Benth, common name, oregano is a common medicinal plant found throughout the Philippines. It was investigated because of its wide range of medicinal applications and availability. The leaves are externally applied to burns and bites of centipedes and scorpions. A poultice of the leaves is applied to temples and forehead for headache. An infusion of the leaves is used as an aromatic carminative, administered in cases of dyspepsia and as cure for asthma (Quisumbing 1978). An earlier study on *Coleus aromaticus* reported on the identification of the essential oil constituents: α-pinene, β-pinene, myrcene, limonene, γ-terpinene, γ-cymene, β-caryophyllene, β-selinene, ethyl salicylate, thymol, carvacrol, eugenol and unidentified phenolic fraction (Malik *et. al.* 1985). In another study, thymol, γ-cymene, terpinen-4-ol, caryophyllene, verbenone, tert-butyl anisole and a sesquiterpene (Hague 1988) were reported. Furthermore, the isolation of cirsimaritin and β-sitosterol-β-D-glucoside (Misra *et. al.* 1977), (Z)-1,3-hexadiene, (Z)-3-hexenol, (E,Z)-α-farnesene, (E,E)-α-farnesene and α-murolene (Prudent 1995) have been reported. The leaf oil was found to be active against *Vibrio cholera* (Prudent et al. 1995).

We now report the isolation and structure elucidation of salvigenin **1**, cirsimaritin **2** and chrysoeriol **3** (Figure 1) from the leaves of *Coleus amboinicus* and the antimicrobial test results of **1** and **2**. This is the first report on the isolation of **1** and **3** from *C. amboinicus* and on the antimicrobial properties of **1** and **2**.

---

[*]Corresponding author: COSCYR@mail.DLSU.edu.ph

Abbreviations used: Fourier-Transform-Infrared (FT-IR), Nuclear magnetic resonance (NMR).

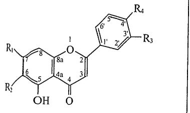

1 $R_1 = R_2 = R_4 = OCH_3$, $R_3 = H$

2 $R_1 = R_2 = OCH_3$, $R_3 = H$, $R_4 = OH$

3 $R_1 = R_4 = OH$, $R_2 = H$, $R_3 = OCH_3$

Figure 1. The three flavones isolated from *Coleus amboinicus*: salvigenin (1), cirsimaritin (2) and chrysoeriol (3).

Methods

General Experimental Procedures

NMR spectra were recorded in deuterated chloroform ($CDCl_3$) solutions on a Bruker AMX NMR spectrometer with $CDCl_3$ (d 7.26, 77.0 ppm) as reference. The FT-IR spectrum was recorded on a Perkin Elmer 1600 spectrometer. The UV spectrum was obtained on an HP 8452A diode array spectrometer. Silica gel type 60 (Merck) was used for column chromatography and plastic-backed plates coated with silica gel F_{254} (Merck) for thin layer chromatography. Fractions were monitored by TLC and spots were visualized by spraying with vanillin:sulfuric acid (H_2SO_4) followed by warming. All reagents used were analytical grade reagents (AR).

Sample Collection

The sample was obtained from Lukban, Quezon in August 1998. It was identified as *Coleus amboinicus* at the Philippine National Museum and a voucher specimen (#034) is kept at the Chemistry Department of De La Salle University, Manila, Philippines.

Isolation

Air-dried leaves (650 grams) of *Coleus amboinicus* were ground in an osterizer and then soaked in chloroform ($CHCl_3$, 2.5 L) for three days. The mixture was filtered and the filtrate was concentrated *in vacuo* to afford the crude extract (50 g). The crude extract was dissolved in ethanol (EtOH, 1.25 L), then treated with 4% aqueous lead acetate [$Pb(OAc)_2$, 1.25 L] to precipitate the more polar components (Padolina *et al* 1974). The mixture was then filtered and the filtrate was concentrated *in vacuo* until a mixture of water and an oily residue remained. The concentrate was extracted with $CHCl_3$. The extract was dried with anhydrous sodium sulfate (Na_2SO_4), then filtered. The filtrate was concentrated *in vacuo* to afford the treated extract (10 g) which was fractionated by gravity column chromatography using increasing proportions of acetone (Me_2CO) in $CHCl_3$ (10% increment) up to pure Me_2CO as eluents. The 10% and 20% Me_2CO in $CHCl_3$ fractions were combined and the mixture was rechromatographed twice in dicloromethane: cyanomethane:diethylether (CH_2Cl_2:CH_3CN:Et_2O, 95:2.5:2.5) to afford **1** (50 mg, yellowish crystals) after recrystallization from Et_2O. The 30%-40% Me_2CO in $CHCl_3$ fractions were rechromatographed thrice in CH_2Cl_2:CH_3CN:Et_2O (90:5.0:5.0) to afford **2** (25 mg, yellowish crystals) and **3** (10 mg, yellowish crystals) after recrystallization from Et_2O.

Antimicrobial tests

The antimicrobial tests were conducted at the Natural Sciences Research Institute, University of the Philippines Diliman, Quezon City. The microorganisms used were: *Pseudomonas aeruginosa* UPCC 1244, *Bacillus subtilis* UPCC 1149, *Escherichia coli* UPCC 1195, *Staphylococcus aureus* UPCC 1143, *Candida albicans* UPCC 2168, *Tricophyton mentagrophytes* UPCC 4193, and *Aspergillus niger* UPCC 3701.

The antimicrobial assay procedure reported in the literature (Guevara & Recio 1985) was employed.

Results and Discussion

Three flavones were isolated from the chloroform extract of the air-dried leaves of *Coleus amboinicus*. The structures of flavones **1-3** were elucidated by extensive 1D and 2D NMR spectroscopy as follows.

The ^1H NMR spectral data of 1 (Table 1) indicated resonances for three methoxy groups at δ 3.89 (3H, s), 3.93 (3H, s) and 3.97 (3H, s) and six aromatic protons at δ 7.02 (2H, d, J = 8 Hz), 7.85 (2H, d, J =

Table 1. 400 MHz ^{1}H NMR spectra of 1-3 in $CDCl_3$

Proton No.	1 (δ, ppm)	2 (δ, ppm)	3 (δ, ppm)
H-3	6.59 (1H, s)	6.72 (1H, s)	6.74 (1H, s)
H-6	-	-	6.31 (1H, s, br)
H-8	6.55 (1H, s)	6.90 (1H, s)	6.60 (1H, s, br)
H-2', H-6'	7.02 (2H, d, J = 8.4 Hz)	7.09 (2H, d, J = 8.8 Hz)	7.06 (H-6', 1H, d, J = 8.4 Hz)
H-3', H-5'	7.85 (2H, d, J = 8.6 Hz)	8.02 (2H, d, J = 8.8 Hz)	7.68 (H-3', 1H, d, J = 2.0 Hz), 7.65 (H-5', 1H, dd, 2.0, 8.3 Hz)
C-5 (OH)	12.8 (1H, s)	13.0 (1H, s)	13.1 (1H, s, br)
C-6 (OCH_3)	3.93 (3H, s)	3.85 (3H, s)	-
C-7 (OCH_3)	3.97 (3H, s)	4.04 (3H, s)	-
C-2' (OCH_3)	-	-	4.05 (3H, s)
C-4' (OCH_3)	3.89 (3H, s)	-	-
C-4' (OH)	-	9.3 (1H, s, br)	-

12 Hz), 6.59 (1H, s) and 6.55 (1H, s) characteristic of flavones. The resonance at δ 12.8 (1H, br, s) was attributed to an OH attached to C-5 which was deshielded due to chelation with the carbonyl oxygen at C-4 (Roitman & James 1985). The presence of an OH is supported by the IR absorption at 3421 cm^{-1}.

The ^{13}C NMR spectrum of **1** (Table 2) indicated resonances for six protonated aromatic carbons, four of which were equivalent [δ 114.5 (2C) and 128.0 (2C)]; eight non-protonated aromatic carbons, six of which were oxygenated (δ 132.6, 153.1, 153.2, 158.7, 162.6, 164.0); and three methoxy carbons (δ 55.5, 56.3, 60.8). The ^{1}H and ^{13}C assignments were verified by HMQC and connectivities were verified by heteronuclear long-range correlations, HMBC, optimized for J = 10 Hz (Table 3). The NMR data for **1** were almost identical to that reported (Harie *et. al.* 1998) for salvigenin in dimethylsulfoxide (DMSO). The UV spectrum of **1** indicated λ_{max} (EtOH) = 326 nm (Band I) and 278 nm (Band II) which are similar to those reported for salvigenin (Voirin 1983).

The ^{1}H NMR spectrum of **2** (Table 1) showed resonances for *ortho* aromatic protons at δ 7.09 (2H, d, J = 8.8 Hz) and 8.02 (2H, d, J = 8.8 Hz). Except for the slight shielding and deshielding of some proton and carbon (Table 2) resonances and the non-appearance of one of the methoxy groups, the spectral data of **1** and **2** are similar. The chelated OH (δ 13.0) at C-5 remained. Since there is no additional aromatic proton, it was deduced that instead of a methoxy in **1**, a hydroxy was found in **2**. Another OH resonance was found at δ 9.3. The position of this OH remains to be determined by HMBC.

The second OH of **2** was attached to C-4'. This was deduced from the long-range correlation of C-6 with the OH on C-5, H-8 and OCH_3 attached to C-6 and the long-range correlation of C-7 with the OCH_3 attached to C-7 and H-8. Thus, the OH in **2** was attached to C-4'. All long-range correlations (Table 3) observed are consistent with the structure of **2**. Literature search revealed that **2** is cirsimaritin (Ramachandran & Sivakumar 1992). The UV spectrum of **2** indicated λ_{max} (EtOH) = 321.5 nm (Band I) and 277.5 nm (Band II) which are similar to

Table 2. 100 MHz ^{13}C NMR *Spectra of 1-3 in* $CDCl_3$

Carbon No.	1 (δ, ppm)	2 (δ, ppm)	3 (δ, ppm)
C-2	164.0	165.5	164.3
C-3	90.6	91.9	103.8
C-4	182.7	183.5	182.2
C-4a	106.1	106.7	104.4
C-5	153.2	153.8	162.6
C-6	132.6	133.7	98.8
C-7	158.7	160.2	164.4
C-8	104.1	103.9	93.9
C-8a	153.1	154.3	158.2
C-1'	123.6	123.2	122.6
C-2', C-6'	114.5	116.9	148.2 (C-2'), 106.1 (C-6')
C-3', C-5'	128.0	129.3	109.6 (C-3'), 120.5 (C-5')
C-4'	162.6	162.3	150.9
C-6 (OCH_3)	60.8	60.5	-
C-7 (OCH_3)	56.3	56.8	-
C-2' (OCH_3)	-	-	55.7
C-4' (OCH_3)	55.5	-	-

Table 3. 400 MHz HMBC spectral data of 1-3 in $CDCl_3$

Carbon No.	Salvigenin	Cirsimaritin	Chrysoeriol
C-2	H-3	H-3	H-3
C-4	H-3	-	-
C-4a	C-5 (OH), H-3, H-8	C-5(OH), H-3, H-8	H-3, H-6, H-8
C-5	C-5 (OH)	C-5(OH)	C-5 (OH), H-6
C-6	C-5 (OH), 3.93 (OCH_3), H-8	C-5 (OH), 3.85 (OCH_3), H-8	C-5 (OH), H-8
C-7	H-8, 3.97 (OCH_3)	H-8, 4.04 (OCH_3)	H-8
C-8a	H-8	H-8	H-6
C-1'	H-2', H-3	H-2', H-6'	H-2', H-3
C-2'	H-2', H-6'	H-6'	H-3, H-6'
C-3'	H-2', H-5'	H-5'	H-5'
C-4'	H-3', H-5', 3.89 (OCH_3)	H-3', H-5'	H-3', H-5'
C-5'	H-3', H-6'	H-3'	H-3'
C-6'	H-2'	H-2'	-

those reported for cirsimaritin (Voirin 1983).

The ¹H NMR spectrum of **3** (Table 1) indicated the resonance of only one methoxy group. Comparison of the ¹H NMR spectral data of **3** with **2** indicated that **3** did not just result from the loss of a methoxy group in **2**; signals for a para disubstituted aromatic ring are no longer found in **3**. Instead, an aromatic proton doublet at δ 7.68 (J = 2.0 Hz) indicating meta coupling; another doublet at δ 7.06 (J = 8.4 Hz) indicating ortho coupling; and a doublet of doublets at δ 7.65 (J = 2.0, 8.3 Hz) indicating ortho and meta coupling, are observed, along with two aromatic proton broadened singlets (meta coupled) at δ 6.31 and 6.60, and the H-3 singlet at δ 6.74. This was supported by the COSY spectrum which indicated that the proton at δ 7.06 is coupled to the proton at δ 7.65, which was in turn coupled to the proton at δ 7.68; while a small coupling is observed between the protons at δ 6.60 and 6.31. Since the chelated OH at δ 13.0 remained, the three aromatic protons should be found in ring C. The presence of six aromatic protons leaves one methoxy and three hydroxy groups in the flavone.

The ¹³C NMR spectrum of **3** (Table 2) indicated six oxygenated aromatic carbons (δ 148.2, 150.9, 158.2, 162.6, 164.3, 164.4). The ¹H and ¹³C assignments were verified by HMQC and connectivities were verified by heteronuclear long-range correlation HMBC optimized for J = 10 Hz (Table 3). The positions of the three hydroxys and methoxy were determined by HMBC. C-6 was long-range correlated to H-8 and the OH at C-5. C-7 was long-range correlated to H-8, while C-8 was correlated to H-6. C-7 thus bears the second OH. The third hydroxy and the single methoxy group, were assigned to C3' and C-4' of ring C, on the basis of carbon chemical shifts and proton coupling. The third OH was assigned to C-4' since this carbon was long-range correlated to H-2' and H-6'. The OCH_3 was attached to C-3' since this carbon was long-range correlated to H-2', H-5' and OCH_3. The structure of **3** was supported by the NOESY spectrum which indicated that the methoxy at δ 4.05

Table 4. Antimicrobial test results of **1** and **2**.

Test Organism	Sample	Sample (μg)	Clearing Zone (mm)	AI
P. aeruginosa	1	40	12	0.2
	2	40	13	0.3
	Tetracycline	30	20	1.0
B. subtilis	1	40	-	0
	2	40	-	0
	Chloramphenicol	30	40	3.0
E. coli	1	40	-	0
	2	40	-	0
	Tetracycline	30	20	2.0
S. aureus	1	40	11	0.1
	2	40	11	0.1
	Chloramphenicol	30	18	0.8
C. albicans	1	40	13	0.3
	2	40	12	0.2
	Chlotrimazole	30	25	1.5
T. mentagrophytes	1	40	15	0.5
	2	40	14	0.4
	Chlotrimazole	30	40	3.0
A. niger	1	40	12	0.2
	2	40	13	0.3
	Cycloheximide	30	28	1.8

is close in space to the aromatic proton at δ 7.68 (H-2'). The NMR data of **3** are similar to those reported for chrysoeriol in DMSO (Harborne 1994). The UV spectrum of **3** indicated λ_{max} (EtOH) = 340 nm (Band I) and 270 253 and 247.5 nm (Band II) which are similar to those reported for chrysoeriol (Voirin 1983).

Compounds **1** and **2** were tested for antimicrobial activity against seven microorganisms, namely: *S. aureus, E. coli, P. aeroginosa, B. subtilis, C. albicans, T. mentagrophytes* and *A. niger.* Results of the study (Table 4) indicated that **1**, at a concentration of 40 mg, is active against *P. aeruginosa* with an activity index (AI) of 0.2, while **2** gave an AI of 0.3. Compound **1** was found active against the fungi, *C. albicans* (AI = 0.2), *T. mentagrophytes* (AI = 0.4) and *A. niger* (AI = 0.2), while **2** was found active against the fungi, *C. albicans* (AI = 0.3), *T. mentagrophytes* (AI = 0.4) and *A. niger* (AI = 0.3). Thus, **1** and **2** have low antimicrobial activities. They were found inactive against *B. subtilis* and *E. coli* and *S. aureus.*

Acknowledgments

The antimicrobial tests were conducted at the Natural Sciences Research Institute, University of the Philippines. A research grant from the Science Foundation through the University Research Coordination Office (URCO) of De La Salle University is gratefully acknowledged.

References

Guevara BQ & Recio BV. 1985. Phytochemical, microbiological and pharmacological screening of medicinal plants. Acta Manilana Supplements. UST Research Center, Manila.

Hague I. 1988. Analysis of volatile constituents of Pakistani *coleus aromalicus* plant oil by capillary gas chromatography/mass spectrometry. J. Chem. Soc. Pakistan 10(3):369–371.

Harborne JB. 1994. The flavonoids. pp. 450-451. Chapman and Hall, NY.

Harie T, Ohtsuru Y, Shibata K, Yamashita K, Tsukayama M & Kawamura Y. 1998. ^{13}C NMR spectral assignment of the a-ring of polyoxygenated flavones. Phytochem. 47(5):865-874.

Malik MS, Ahmad R, Khan SA & Bhatty MK. 1985. Studies on the essential oil of the *Coleus aromalicus* plant. Chem. Abstr. 103:345.

Misra TN, Singh RS, Sharma SC & Tandon JS. 1976. Chemical investigation of *Coleus aromaticus* Benth. Part II. J. Indian Chem. Soc. 53(10):1064-1065

Padolina WG, Yoshioka H, Nakatani N, Mabry TJ, Monti SA, Davis RE, Cox PJ, Sim GA, Watson WH & Wu IB. 1974. Glaucolide -A and -B, new germacranolide-type sesquiterpene lactones from *Vernonia cinerea.* Tetrahedron 30:1161-1170.

Prudent D, F Perineau, JM Bessiere, GM Michel & JC Baccou. 1995. Analysis of the essential oil of wild oregano from Martinique (*Coleus aromaticus* Benth)-evaluation of its bacteriostatic and fungistic properties. J. Essential Oil Res. 7(2):165-173.

Quisumbing, E. 1978. Medicinal plants Pt. 2. pp. 813-815. Bureau of Printing, Manila.

Ramachandran Nair AG & Sivakumar R. 1992. Non-identity of hortensin from *Millingtonia hortensin* with 3,4-dihydroxy-6,7-dimethoxyflavone. Phytochem. 31(2):671-677.

Roitman JN & James LF. 1985. Chemistry of toxic range plants. Highly oxygenated flavonol methyl ethers from *Gutierrezia microcephala.* Phytochem. 24(4):835-848.

Voirin B. 1983. UV spectral differentiation of 5-hydroxy- and 5-hydroxy-3-methoxyflavones with mono-4', di-(3', 4', 5')-substituted b rings. Phytochem. 22: 2108-2112.

Philippine Journal of Science
128 (4): 319 - 330, December 1999
ISSN 0031 - 7683

RESEARCH

The Morphology and Identity of Two Species of *Balanophora* in Bukidnon, Philippines

Victor B. Amoroso* and Andrade C. Semitara

College of Arts and Sciences
Central Mindanao University
Musuan, Bukidnon, Philippines

Morphological studies of *Balanophora* revealed the presence of two distinct species: *B. papuana* Schltr. and *B. fungosa* ssp. *fungosa* J.R. and S. Forster. Although previously reported in Luzon and Palawan, *B. fungosa* is a new record in Mindanao. Morphological comparisons revealed that *B. papuana* is dioecious, has pale yellow to reddish brown and scabrous tuber, opposite-decussate phyllotaxy and red leaves. On the other hand, *B. fungosa* ssp. *fungosa* is monoecious, has pale yellow to yellow-brown and granulated tuber, spiral or rarely subopposite phyllotaxy and pale yellow leaves.

Key words: *Balanophora papuana*, *Balanophora fungosa ssp. fungosa*, holoparasitic plant, root parasite

One of the very few families of holoparasitic plants is Balanophoraceae. This family is represented in the Philippines by the lone genus *Balanophora*. With 15 species worldwide, this genus is distributed in the subtropics to tropical Asia, Melanesia, Pacific Islands, Australia, Madagascar, and Africa (Hansen, 1976).

According to Brown (1973), the development of *Balanophora* starts when the germinating seedling of the parasite reaches the host. It develops a large tubercle, which, on contact, destroys the cortex of the root. Hsiao et al. (1995) and Gedalovich-Shedletzky & Kuijt (1990) have proven that *Balanophora* is completely dependent on its host throughout its entire life. They anatomically established that vascular tissues of the host are extensively ramified to the vegetative bodies known as tubers.

Merrill (1967) identified five species of *Balanophora* in the Philippines: *B. decurrens* Fawcet, *B. fungosa* Forst., *B. incarnatha* Elm., *B. micrantha* Warb. and *B. subglobosa* Elm. However, Hansen (1976) and Pancho (1983) listed only three Philippine species with two subspecies, namely, *B. abbreviata (B. micrantha), B. papuana* Schltr. *(B. incarnantha)* and *B. fungosa* Forst. with subspecies *indica (B. decurrens)* and *B. fungosa* ssp. *fungosa.*

In 1995 and 1996, Amoroso collected unidentified specimens of the genus *Balanophora* in two different localities in Bukidnon. Preliminary observations of these plants indicate that their characteristics differ from one another. They were thought to be distinct and different species of *Balanophora*. Since Merrill (1967) and Hansen (1976) reported only two species of *Balanophora* in Mindanao, *B. abbreviata* Bl. and *B. papuana* Schltr., the morphology of these newly collected plants of *Balanophora* was compared to determine their taxonomic status and identity.

---

*Corresponding author: v.amoroso@eudoramail.com

Materials and Methods

Collection and Identification of Specimens

Fresh specimens of *Balanophora* were collected in Bukidnon from Mt. Kinasalapi and Mt. Musuan, in the municipality of Lantapan and Maramag, respectively. The specimens were identified using the key of Hansen (1976).

Preparation of Pickled Specimens

Collected specimens were pickled in 70% ethyl alcohol for morphological observations. Other samples were preserved by poisoning and deposited in the Herbarium of the Department of Biology, Central Mindanao University, Musuan, Bukidnon.

Morphological observations

Morphological studies on the two species of *Balanophora* were conducted by measuring plant height, stem height as well as width and length of tuber and leaf. Descriptions of different organs were done by taking note of the texture of tuber; the color of tuber, stem, leaf, and bract; the shape of tuber, bract, anther, spadicle and pollen; the presence or absence of warts in tubers; the number of leaves, floral parts and anthers; the arrangement of leaves; the position and symmetry of male flower; and the type of inflorescence.

Photographs were made from suitable materials using light and stereo microscopes.

Results and Discussion

Plants suspected to be *B. papuana* Schltr. were observed in dense primary and secondary forest of Mt. Kinasalapi, Lantapan, Bukidnon at an elevation of 1,695 m above sea level (masl) while plants suspected to be *B. fungosa* ssp. *fungosa* J.R. and S. Forst. were found in secondary forest of Mt. Musuan, Bukidnon at an elevation of 335 masl. Both species are parasitic on the roots of *Ficus* spp., consistent with Merrill's (1967) report.

Although previously reported by Hansen (1976) and Huang and Tseng-Chieng (1996) in Upper Burma, Ryu Kyu Island, East Java, Celebes, New Guinea, Micronesia, Australia and Philippines (Luzon and Palawan only), *B. fungosa* ssp. *fungosa* is a new record in Mindanao Island.

A. Morphological Descriptions

1. *Balanophora papuana* Schltr.

Habit and Habitat. Root parasites, annual, herbaceous, and dioecious. Average height of 4.5-11.5 cm from fusion with host root to top of inflorescence (Figs. 1-A and B).

Tubers. Tubers subterranean, occurring as a mass, about 4-18 cm wide, branching from the base. Single tuber usually subspherical or depressed, 1.0-4.5 cm, pale yellow to reddish-brown and surface scabrous with scattered stellate warts (Fig. 2).

Aerial Stems. Aerial stems bearing male inflorescence, slightly erect, soft, fleshy, waxy, yellow which appear from a cup-rimmed pit at the apical part of each single tuber about 8-9 cm long and 1.2 cm wide (Figs. 2 & 3).

Leaves. Leaves of male plant persistent, simple, smooth, waxy, appressed, opposite, decussate, occurring in pairs of three or four; margin entire; apex obtuse; base broad, spatulate or slightly cucullate; red especially during anthesis, 3.0 x 1.5 cm (at least two nerves forked) conspicuous, longitudinal nerves (Figs. 1-B and 3-A).

Inflorescence. Female inflorescence head-like in appearance, obovoid, 1.5-2.5 x 1-2 cm with flowers densely arranged along the surface of main axis. Pistillate flowers sessile, 395-451 mm wide, about 846 mm long. Style 677 mm long and ovary naked, and without a cavity (Figs. 4-A & B). Bracts absent but replaced by club-shaped spadicles. Spadicles 1.240-1.297 mm long with a cylindrical lower part about 282-338 mm wide. Usually, pistillate flowers have no perianth, pale yellow and situated at the lower part of spadicles.

Male inflorescence racemose (Fig. 3) and bisymmetric or zygomorphic on account of lateral elongation; consists of red flowers bearing two narrow, acute, 5 x 3 mm, lateral tepals and 2 mm wide, truncate, 5 x 4 mm, median tepals. Male flowers imperfect, incomplete, often in vertical rows, 4-merous with pedicels that vary from 2-7 mm in length (Figs. 5 and 7) and subtended by short (at most 2 mm), rudimentary, truncate, red bracts. Stamens fused to

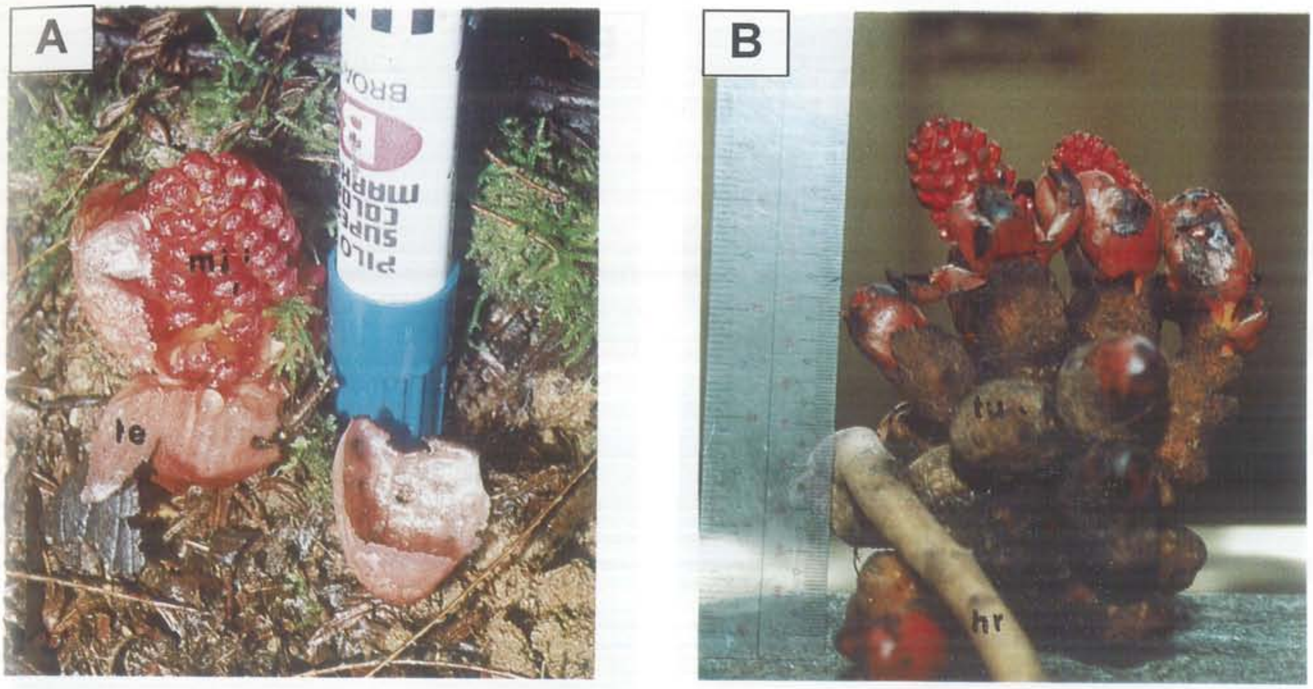

Figure 1. *Balanophora papuana* Schltr. in its natural habitat (A) and habit (B) showing tuber (tu), host root (hr), male inflorescence (mi) and leaf (le).

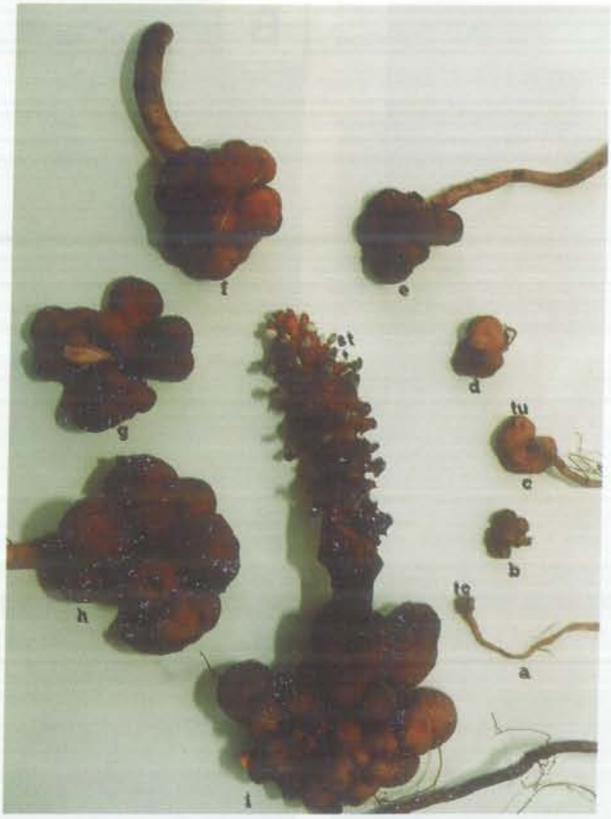

Figure 2. Gross morphological development of the sporophyte of *B. papuana* from vegetative (a-h) to reproductive stages (tc = tubercle, tu = tuber, st = staminate flowers).

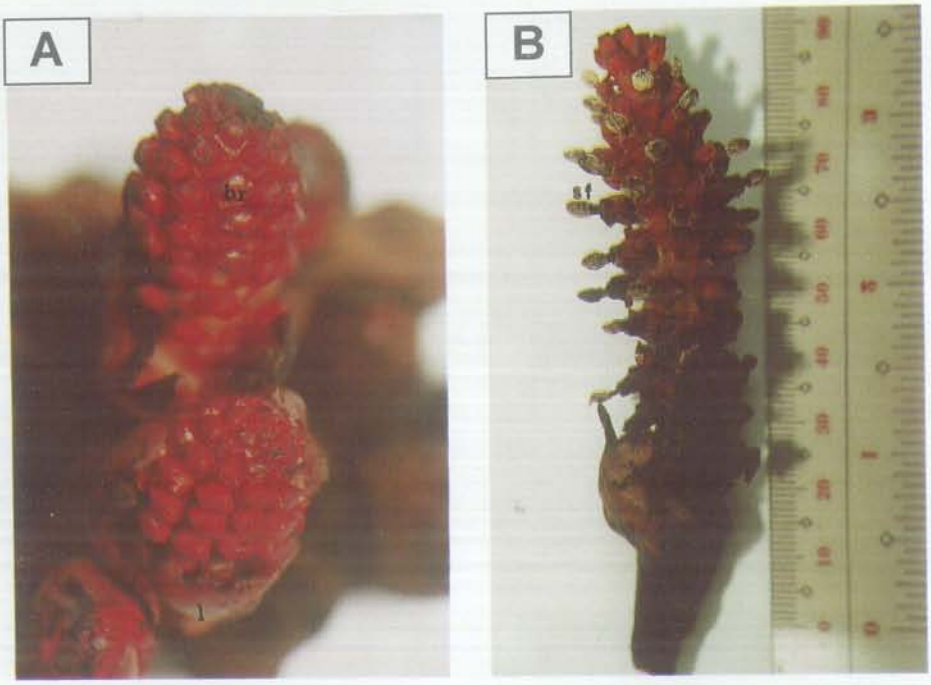

Figure 3. Unopened (A) and opened (B) racemose type of inflorescence of *B. papuana* showing staminate flowers (sf), bracts (br) and leaves (l).

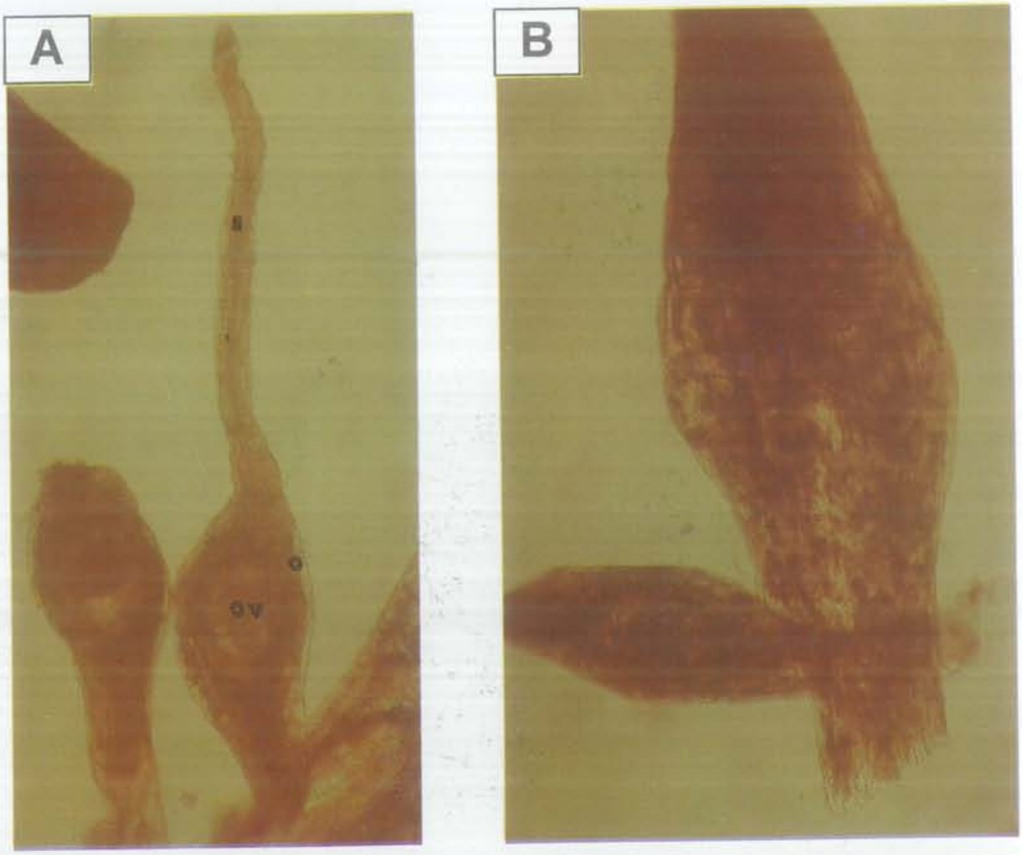

Figure 4. Pistillate flower (A) and spadicle (B) of *B. papuana* showing ovary (o), style (s) and ovule (ov) (x 100).

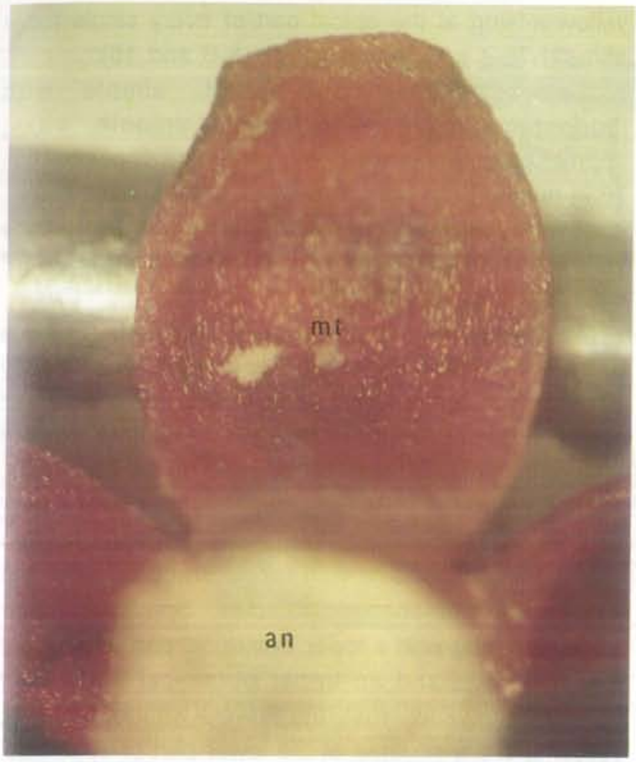

Figure 5. Enlarged view of staminate flower of *B. papuana* showing median tepals (mt) and anther (an) (x40).

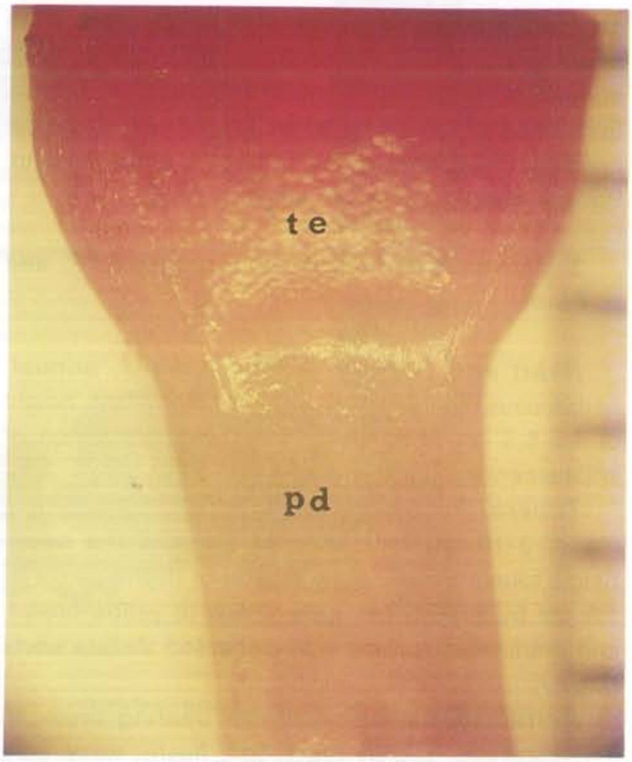

Figure 6. Unopened staminate flower of *B. papuana* showing its pedicel (pd) and fused tepals (te) (x40).

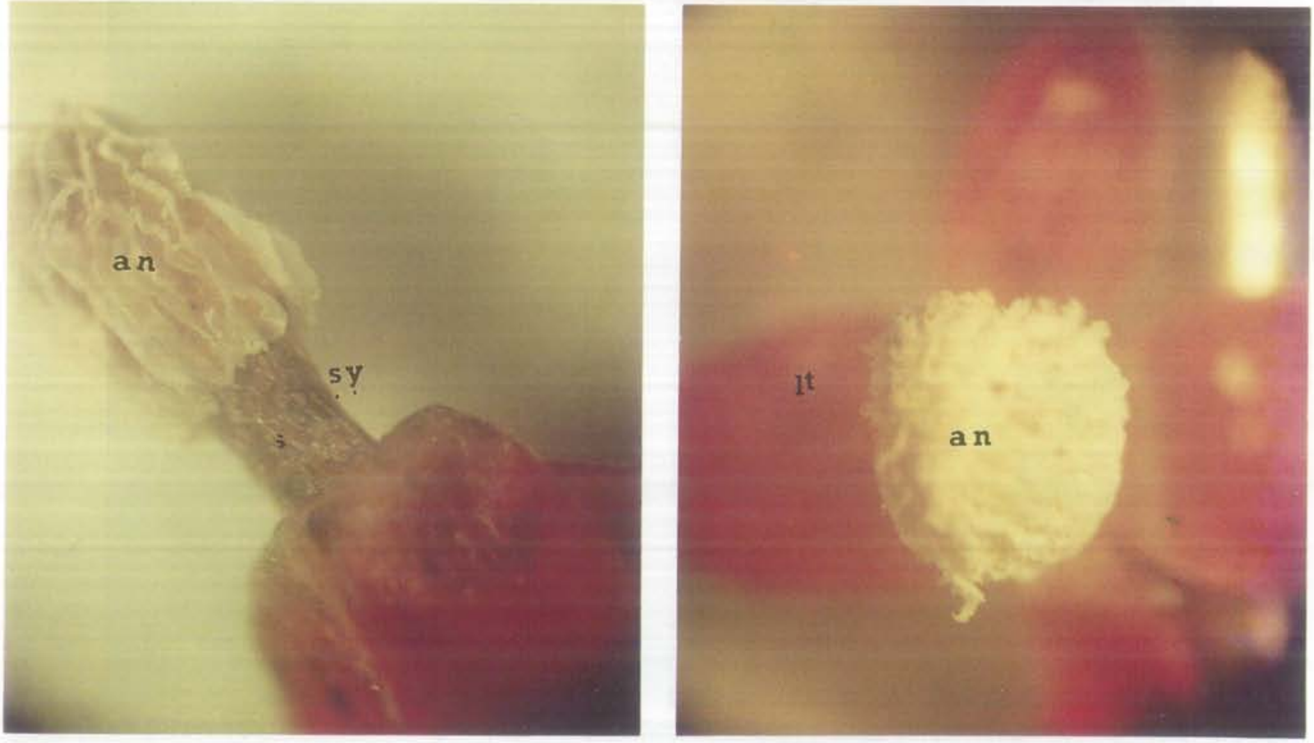

Figure 7. Opened staminate flower of *B. papuana* showing an elongated synandrium (sy), also showing anther (an) and lateral tepal (lt) (x 40).

an elongated synandrium with fertile part often slightly obconical, 4 x 3 mm. Anther cells numerous, white during anthesis, parallel, running from base to top of synandrium with a longitudinal opening. Filaments united to form a single column. Pollens slightly triangular with two wings.

2. *Balanophora fungosa* ssp. *fungosa* J.R. and S. Forst.

Habit and Habitat. Root parasites, annual, herbaceous, monoecious, and in colony with height of 4.5-8.5 cm from fusion with host root to top of inflorescence (Fig. 8).

Tubers. Tubers subterranean, single or in a mass, 3-10 cm wide, branching from the base. Single tubers usually subspherical or depressed, 1.3-1.5 cm by 2.0-2.5 cm, pale yellow to yellow-brown, and granulated surface with dispersed stellate warts (Fig. 9).

Aerial Stems. Aerial stems bearing bisexual inflorescences, slightly erect, soft, fleshy, waxy, pale yellow arising at the apical part of every single tuber about 1.75-4 x 0.5-1 cm (Figs. 8-B and 10).

Leaves. Leaves persistent, simple with inconspicuous venation pattern, smooth, waxy, appressed, spirally arranged, rarely subopposite, 12-26 in number; margin entire, apex obtuse, base broad, spatulate, slightly cucullate (hood-shaped); pale yellow in anthesis, and 1.9-2.3 cm long and 0.8-1.2 cm wide (Figs. 8 and 10).

Inflorescence. Inflorescence bisexual. Female part of the inflorescence head type, obovate to elliptic, 1-2.4 cm in length and 0.8-2.2 cm in diameter during anthesis (Figs. 8 and 10). Pistillate flowers arranged densely along the surface of the main axis, sessile with style 564-896 mm long and ovary 395-451 mm by 169-226 mm (Fig. 12). Pistillate flowers measure about 1.579 mm long. Bracts absent but replaced by club-shaped spadicles. Spadicles 1.240-1.564 mm long with a lower cylindrical part about 169-226 mm wide and an upper obconical part about 282-395 mm wide. Pistillate flowers without perianth, yellow and are situated at the lower part of spadicles.

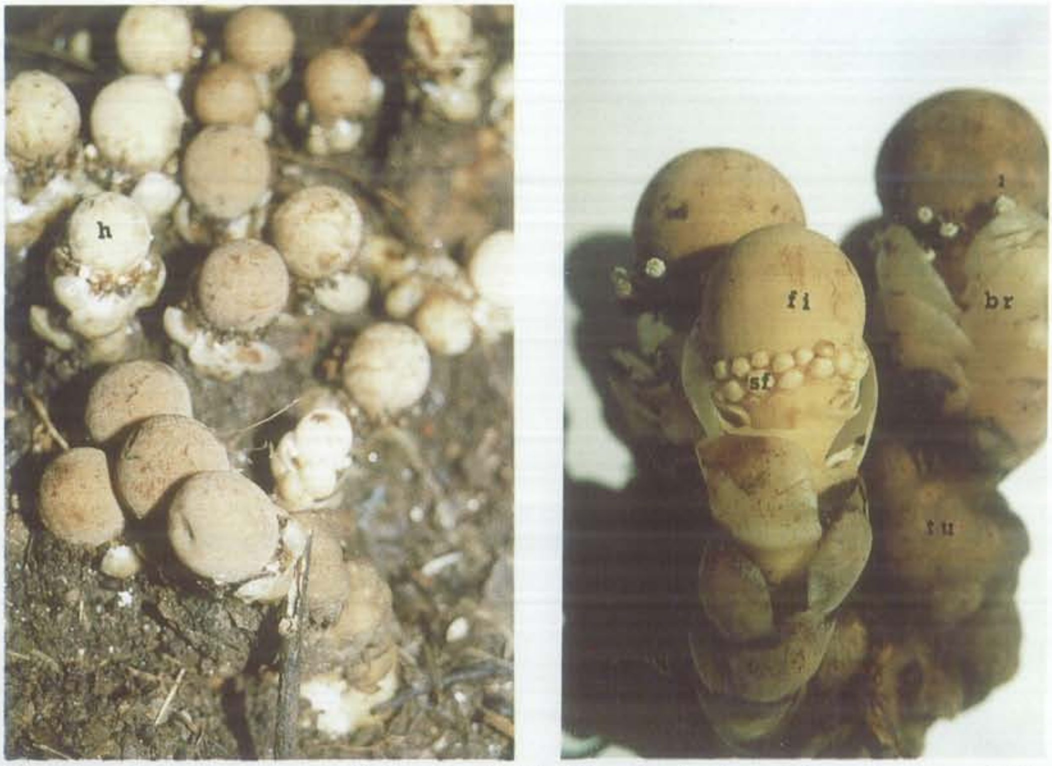

Figure 8. *Balanophora fungosa* ssp. *fungosa* in its natural habitat (A) and early stage of flower development (B) showing head inflorescence (h), female inflorescence (fi), staminate flower (sf), bract (br), tuber (tu), leaf (le).

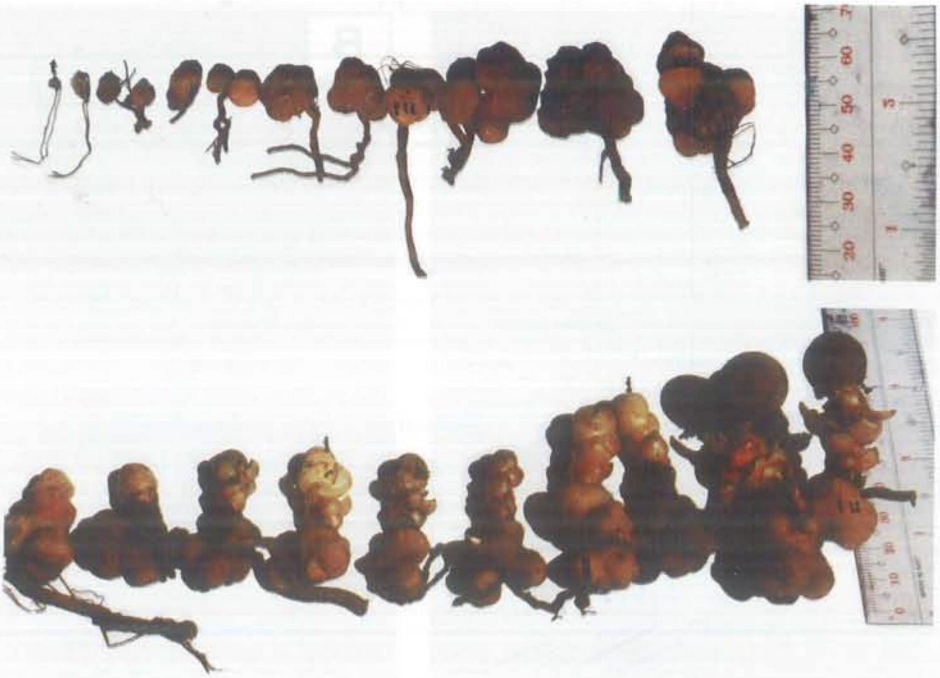

Figure 9. Gross morphological development of *Balanophora fungosa* ssp. *fungosa* from tubercle (upper left side) to inflorescence stage (bottom) showing tubercle (t), tuber (tu) and inflorescence (i).

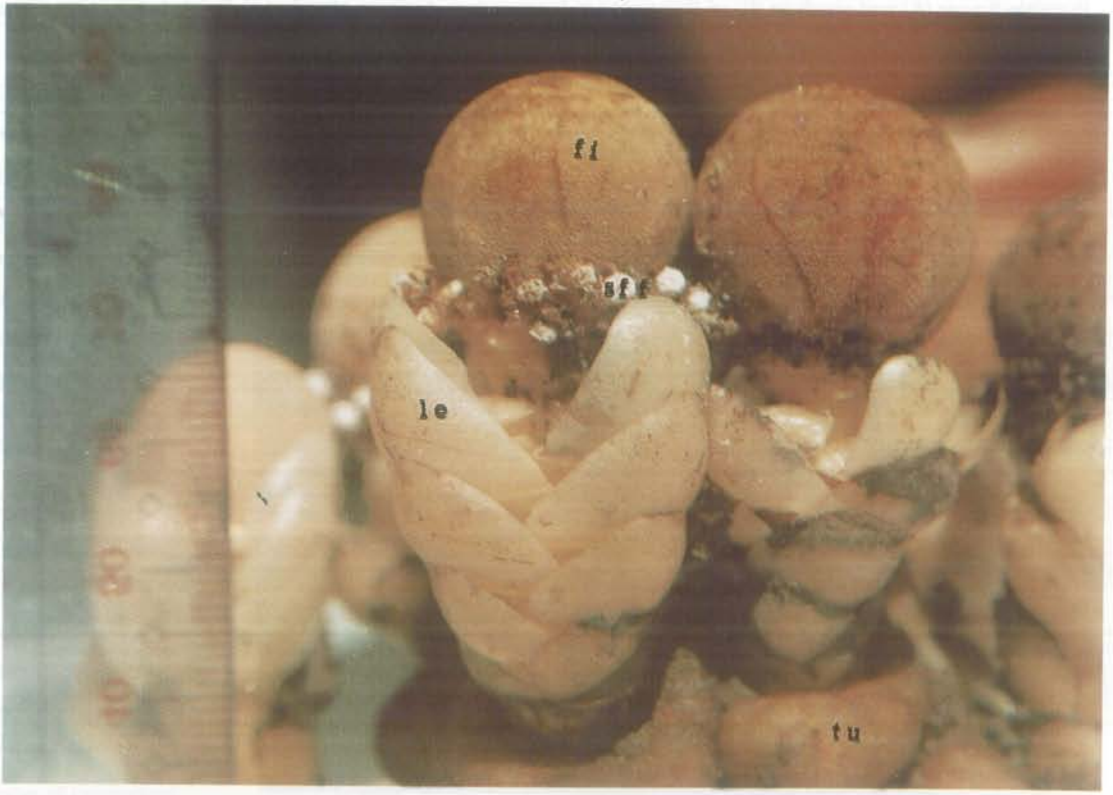

Figure 10. *B. fungosa* ssp. *fungosa* showing subopposite phyllotaxy and advanced stage of flower development. Also shown are the female inflorescence (fi), staminate flower (sf), tuber (tu) and leaf (le).

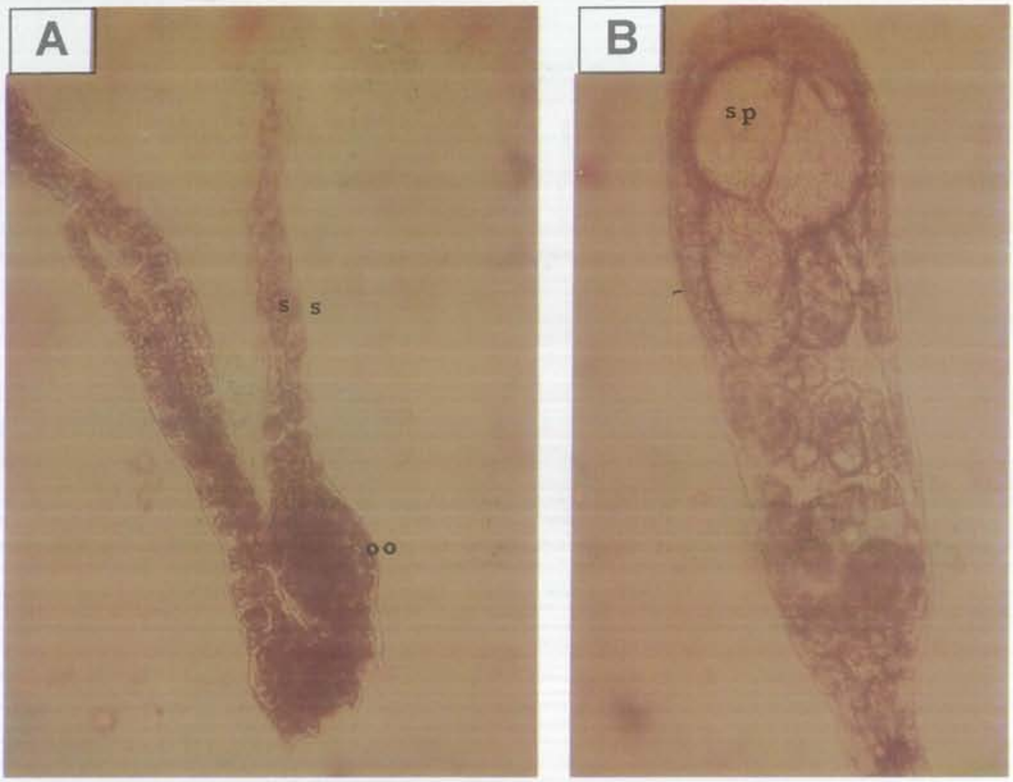

Figure 11. Pistillate flower (A) and spadicle (B) of *Balanophora fungosa* ssp. *fungosa* showing style (s), ovary (o) and spadicle (sp) (x100).

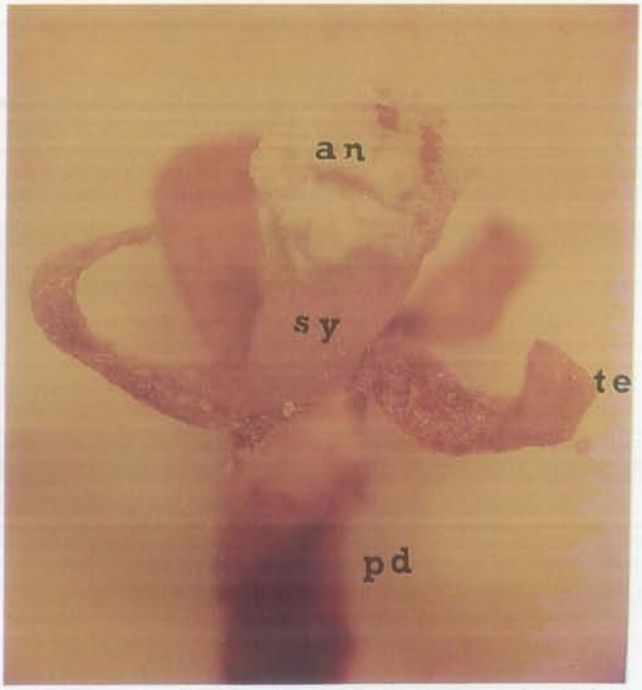

Figure 12. Enlarged view of staminate flower of *B. fungosa* ssp. *fungosa* showing anther (an), synandrium (sy), tepal (te) and pedicel (pd) (x20).

Table 1. Comparative gross morphological* comparisons of *Balanophora papuana* Schltr. and *Balanophora fungosa* ssp. *fungosa* J.R. and S. Forst. and their original descriptions**

Features	***B. papuana Schltr.***		***B. fungosa ssp. fungosa*** **J.R. and S. Forst**	
	Author's description	**Original description**	**Author's description**	**Original description**
HABIT	annual herbaceous phytoparasite		annual herbaceous phytoparasite	
PLANT HEIGHT, cm	4.5 - 11.5 from fusion with host, root to top of inflorescence		4.5 - 8.5 from fusion with host root to top of inflorescence	
TUBER				
color	***pale yellow to reddish brown***		***pale yellow to yellow brown***	
tuber	***scabrous***	***tesellate***	***granular***	***granular***
warts	stellate, scattered	stellate	stellate, scattered	stellate
distribution	single or in a mass	in a mass	single or in a mass	single or in a mass
massive tuber diameter, cm	4 - 18	14 - 24	3 - 10	10 - 15
SINGLE TUBER				
shape	subspherical or depressed		subspherical or depressed	subspherical or depressed
height, cm	1.4	1 - 6	1.3 - 1.5	1.5 x 2.5
width, cm	1 - 4.5	1 - 4	2.0 - 2.5	
AERIAL STEM				
height, cm	***8-9 (male plant only)***		***1.7 - 4***	***2.5 - 11***
diameter, cm	***1.2 (male plant only)***		***0.5 - 1***	
color	yellow		pale yellow	
surface	waxy		waxy	
LEAVES				
attachment	sessile		sessile	
texture	smooth and waxy		smooth and waxy	
type	simple		simple	
venation	parallel		parallel	
phyllotaxy	***opposite, decussate***	***opposite, decussate***	***spiral, rarely sub-opposite***	***spiral, rarely sub-opposite***
outline	spatulate or slightly cucullate		spatulate or slightly cucullate	slightly cucullate
margin	entire		entire	
apex	obtuse		obtuse	obtuse
base	broad		broad	
number	***6 - 8***	***2 - 5***	***12 - 26***	***15 - 30***
color	***red***	***red***	***pale yellow***	
length, cm	3	3 1/4	1.9 - 2.3	2 - 3
width, cm	1.5	2.5	0.8 - 1.2	1.5 x 2
number of longitudinal nerves	7 - 12 (at least 2 nerves are forking)	7 - 11	apparently 7 nerves	

* marked differences are in ***bold italics***

** based on Hansen (1976)

Table 2. Morphological comparisons of the inflorescence of the *Balanophora* spp.

Features	*B. papuana Schltr.*		*A. fungosa ssp. fungosa* J.R. and S. Forst	
	Author's description	**Original description**	**Author's description**	**Original description**
SEXUALITY	***dioecious, unisexual***	***dioecious***	***monoecious, bisexual***	***monoecious, bisexual***
MALE INFLORESCENCE	racemose		none	
STAMINATE FLOWERS				
distribution	***densely distributed along the main axis of the stem***		***sparsely distributed in a zone about 0.5 cm high below the female part of inflorescence***	
number	numerous	4-5 - merous	1 - 26	2 - 20
symmetry	***bisymmetric or zygomorphic***	***bisymmetric or zygomorphic***	***actinomorphic***	***actinomorphic***
arrangement	***usually in vertical rows***		***usually in 2 horizontal rows***	
tepal				
• number	4 (2 median & 2 lateral)		4 - 5	4 - 5
• outline	median-elliptical; lateral-obovate	median-truncate; lateral-ovate	lanceolate	ovate-elliptic
• apex	median- truncate; lateral-acute	truncate	acute	acute
• length, mm	5 (median & lateral)	4 - 5	4	
width, mm	3 lateral; 4 median	0.5	2	
pedicel length, mm	2 - 7	2 - 7	2 - 3	3 - 7
bracts				
• length, mm	short (at most 2)		short (1 - 2)	short (1 - 2)
• apex	truncate		truncate	truncate
• development	rudimentary	rudimentary	rudimentary	rudimentary
• ***color***	***red***	***yellow to orange-yellow or red***	***yellowish***	***yellow to orange-yellow or yellowish brown sometimes with pinkish tinges***
synandrium				
• shape	slightly obconical	slightly obconical	sightly obovoid-ellipsoid	ovoid-ellipsoid
• ***length***	***4 mm in anthesis***	***3 mm***	***3 - 4 mm in anthesis***	
• ***diameter***	***3 mm in anthesis***		***2 - 3 mm in anthesis***	
anther cells				
• ***arrangement***	***parallel***	***parallel***	***convoluted***	
• ***opening***	***longitudinal***		***somewhat convoluted***	
• color in anthesis	white		white	
• type	head		head	
• ***shape***	***obovoid***		***obovate to subspherical***	
size				
• length, cm	1.5 - 2.5	2.5	1 - 2.4	
• width, cm	1 - 2	1.5	0.8 - 2.2	
color			pale yellow when young and yellow brown to brown when matured	

Table 2. Morphological comparisons of the inflorescence of the *Balanophora* spp., continued...

Features	*B. papuana Schltr.*		*A. fungosa ssp. fungosa* J.R. and S. Forst	
	Author's description	**Original description**	**Author's description**	**Original description**
PISTILLATE FLOWERS				
length, µm	846 in unopened flower	1150	at most 1579 in opened flower	1250
attachment	sessile		sessile	
color	light brown		brown	
location, µm	lower part of spadicles		lower part of spadicles	
style length, µm	677		564 - 896	
ovary	naked		naked	
• length, µm	395 - 451	180	395 - 451	400
• width, µm	169 - 226	140	169 - 226	
spadicles				
• length, µm	1240 - 1297	900 - 1200	1240 - 1564	1110 - 1150
• lower part				
width, µm	113 - 282	100	169 - 226	
shape	cylindrical		cylindrical	
• upper part				
width, µm	282 - 338	200 - 300	282 - 395	
shape	obconical		obconical	
perianth	absent		absent	

* marked differences are in italics
** based on Hansen (1976)

In general, inflorescences pale yellow when young and yellow brown when matured.

Staminate flowers arranged in a zone, 0.5 cm high below female part of inflorescence, often in 2 horizontal rows, 4-5 merous, actinomorphic, numbers 1-26. Pedicels 2-3 mm long, tepals ovate-elliptic and acute apex. Bracts short (1-2 mm long), rudimentary, truncate and yellow (Fig. 13). Synandrium with subspherical fertile part 3-4 x 2-3 mm. Anthers, white in anthesis, horseshoe-shaped 4-5 with convoluted opening. Filaments united to form a single column. Pollens spherical with 2 wings.

B. Morphological Comparisons

Comparative morphological descriptions of *Balanophora papuana* Schltr. and *B. fungosa* ssp. *fungosa* J.R. and S. Forst. showed distinct similarities and differences on both vegetative and reproductive features (Table 1 & Table 2). The similarities can be attributed to their genus characters and the differences may be due to adaptability and parasitic nature of the plants.

Morphological similarities observed in the two taxa are the following: tubers are usually in a mass, subspherical or depressed and surface with scattered stellate warts; aerial stem slightly erect, soft, fleshy and waxy; leaves persistent, sessile, appressed, smooth, waxy, margin entire, apex obtuse, base broad and spatulate or slightly cucullate; male flowers subtended by short, truncate rudimentary bracts and anthers white during anthesis; and female inflorescence head type with sessile pistillate flowers situated at the lower part of spadicles, ovary naked, style and ovule solitary, perianth absent and spadicles club-shaped.

Although the two taxa showed similarities in the aforementioned morphological characters, differences could also be observed on their vegetative features such as the color and texture of tuber; the length and width of aerial stem; the number, phyllotaxy, color and size of leaves, as well as on their reproductive characters such as the type of inflorescence, symmetry, sexuality and presence or absence of floral parts.

In *B. papuana*, the tuber is pale yellow to reddish brown and scabrous whereas pale yellow to yellow-brown and granulated in *B. fungosa* ssp. *fungosa*.

Another morphological difference between the two taxa is the length and width of aerial stems. Aerial stems of *B. papuana* range from 8-9 cm long and 1.2 cm wide while the aerial stems of *B. fungosa* ssp. *fungosa* range from 1.7-4 cm long and 0.5-1 cm wide.

Comparison of leaf characters also reveals striking differences. The leaves of *B. papuana* are 3-4 pairs, opposite, decussate, parallel veined with 7-12 conspicuous veins, red and about 3 cm long and 1.5 cm wide. In *B. fungosa* ssp. *fungosa*, the leaves ranging form 12 to 26, spirally arranged or rarely subopposite with inconspicuous parallel veins, pale yellow in anthesis and about 1.9-2.3 cm long and 0.8-1.2 cm wide.

Morphological differences of the flower have also been observed. *B. papuana* is dioecious with racemose type of unisexual inflorescences whereas *B. fungosa* ssp. *fungosa* is monoecious with staminate flowers arranged in a zone about 0.5 cm high below the female part of bisexual inflorescences. Staminate flowers of *B. papuana* are numerous, bisymmetrical or zygomorphic and usually arranged in horizontal rows.

As to the tepal, *B. papuana* consists of two narrow, acute, 5 x 3 mm lateral tepals and 2 mm wide, truncate, 5 x 4 mm, median tepals whereas *B. fungosa* ssp. *fungosa* consists of 4 - 5 narrow, acute, 4.0 x 2 mm tepals.

They also differed in the length of pedicels. Pedicels of *B. papuana* range from 2-7 mm in length and 2-3 mm in *B. fungosa* ssp. *fungosa*.

The difference also lies on the shape and size of the upper part of synandrium. *B. papuana* has slightly obconical upper part of synandrium and measures about 4 x 3 mm in size. In *B. fungosa* ssp. *fungosa*, its synandrium has obovoid upper part and measures 3 - 4 x 2 - 3 mm.

The anther cells of *Balanophora* are also variable between species. Anther cells of *B. papuana* are divided into parallel loculi running from the base to top of synandrium with longitudinal opening. In *B. fungosa ssp. fungosa*, the anther cells are horseshoe-shaped running also from base to top of synandrium with somewhat convoluted opening.

Balanophora in Bukidnon

Morphological studies of *Balanophora* were conducted to determine the taxonomic status of the *Balanophora* collected in Bukidnon.

Balanophora papuana Schltr. and *B. fungosa ssp. fungosa* J.R. and S. Forst. are annual, herbaceous plants that parasitize on the roots of *Ficus* species. Both taxa have similar shape of tubers with stellate warts but differ with respect to color and texture of the said organ.

Morphological differences in sexuality, symmetry, number of male flowers and tepals, length of pedicels and shape of anther cells support the presence of two distinct species of *Balanophora*: *Balanophora papuana* Schltr. and *Balanophora fungosa ssp. fungosa* J.R. and S. Forster. The determination of the taxonomic status of the latter adds to the new record of *Balanophora* species in the island of Mindanao.

Acknowledgement

The authors are grateful to Ms. Jonna A. Timada for encoding the manuscript.

References

Brown W. 1973. The plant kingdom. Ginn and Company. Lexington, Massachusetts, USA. 69 p.

Hansen C. 1976. Balanophoraceae. In: Flora malesiana (ed. V Steenis). 7(1): 783-805.

Gedalovich-Shedletzky E & Kuijt J. 1990. An ultrastructural study of the tuber strands of *Balanophora* (Balanophoraceae). Can. J. Bot. 68:1271-1279.

Hsiao SC, Mauseth JD & Peng CI. 1995. Composite bundles, the host/parasite interface in the holoparasitic angiosperms *Langsdorffia* and *Balanophora* (Balanophoraceae). Am. J. Bot. 82:81-90.

Huang SF & Huang TC. 1996. Balanophoraceae. In: Flora of Taiwan (ed. TC Huang). 2:287-293.

Merrill ED. 1967. An enumeration of Philippine flowering plants. A. Asher & Co. Amsterdam. 2:118-119.

Pancho JV. 1983. The vascular flora of Mt. Makiling and vicinity. Kalikasan: Philipp. J. Biol. pp. 105.